Pharmacological Induction of Molecular Chaperones Restores Mitochondrial Function in Hyperglycemically Stressed Sensory Neurons

By
Liang Zhang

Submitted to the graduate degree program in Pharmacology & Toxicology and the Graduate Faculty of the University of Kansas in partial fulfillment of the requirements for the degree of Doctor of Philosophy

Chairperson Dr. Rick Dobrowsky

Dr. Jeffrey Staudinger

Dr. Honglian Shi

Dr. Brian Blagg

Dr. Mark Richter

Date Defended: August 16, 2012

The Dissertation Committee for Liang Zhang
certifies that this is the approved version of the following dissertation:

Pharmacological Induction of Molecular Chaperones Restores Mitochondrial Function in Hyperglycemically Stressed Sensory Neurons

_____
Chairperson Dr. Rick Dobrowsky

Date approved: August 16, 2012

Abstract

Distal diabetic peripheral polyneuropathy (DPN) is a prevalent complication resulting from chronic hyperglycemia in diabetic patients. It is associated with incapacitating pain, foot ulceration, and lower-limb amputations and brings about physical and psychological burdens to a patient's quality of life and a large economic burden to the health care system. Despite the prevalence and severity of DPN, the development of therapies that have focused on "diabetes specific" targets has met with limited translational success. This is due, at least in part, to the fact that disease progression among individuals does not occur with temporal and/or biochemical uniformity. Thus, our innovative approach has explored the premise that it is not necessary to target a specific pathogenic mechanism to reverse DPN and that pharmacologic induction of cytoprotective molecular chaperones affords a novel mechanism to improve myelinated and unmyelinated fiber function in DPN. To this end, we established that KU-32, a novel, non-toxic small molecule inhibitor of the molecular chaperone heat shock protein 90 (Hsp90) was able to protect sensory neurons from glucotoxicity and decrease the symptoms of DPN in diabetic mice. However, despite KU-32's efficacy in improving the sensory deficits of DPN in diabetic mice, specific mechanisms of neuroprotection remain unidentified. Thus, this dissertation utilized variations of stable isotope labeling with amino acids in cell culture (SILAC) as a novel, unbiased and systematic approach to quantitatively study the effect of hyperglycemia and KU-32 on the mitochondrial proteomes from dorsal root ganglia (DRG) neurons and Schwann cells (SCs) as *in vitro* models of DPN.

This dissertation provides the first quantitative characterization of the temporal effect of hyperglycemia on the SC proteome using SILAC. Specifically, hyperglycemia increased the expression of numerous mitochondrial proteins in SCs that regulate oxidative phosphorylation and anti-oxidant responses. Consistent with these observations, hyperglycemia did not induce superoxide production in SCs and this correlated with an increase in MnSOD and the extent of proton leak, which may function in reducing oxidative stress. Although hyperglycemia increased mitochondrial respiration, the increase in proton leak suggests that respiration is less efficient at producing ATP. However, this deficiency may be offset by the ability of hyperglycemia to increase glycolysis in SCs. In contrast, hyperglycemia decreased mitochondrial respiratory capacity in DRG sensory neurons and promoted a robust induction in superoxide production. Treatment of KU-32 antagonized the effect of hyperglycemia by decreasing mitochondrial superoxide levels and improving organellar bioenergetics in DRG neurons. These functional improvements correlated with the translational induction of MnSOD and mitochondrial chaperones by KU-32. Overall, studies in this dissertation provide evidence that sensory neurons and SCs have rather distinct energetic responses to hyperglycemia and that SCs can more effectively decrease glucose-induced oxidative stress. These studies also provide proof-of-principle that pharmacological induction of molecular chaperones may ameliorate DPN by helping sensory neurons to decrease oxidative stress and improve mitochondrial bioenergetics in response to glucotoxicity.

Acknowledgements

Avec de la patience on arrives a tout – with patience reach to all.

The completion and success of this project would not have been possible without the guidance, support and advice from people who have helped me during my study.

I would like to express my deepest gratitude to my advisor, Dr. Rick Dobrowsky. Rick's diligence and enthusiasm in science has been my constant inspiration throughout my graduate career. Without his patient, guidance, support and trust in my ability, I would never have achieved the success in this project. I would like to thank Dr. Brian Blagg for serving on my committee and kindly provide KU-32 for my studies, without it, this project would not have been possible. I would like to thank Dr. Jeff Staudinger, Dr. Honglian Shi and Dr. Mark Richter for serving on my committee. Additionally, I would like to thank Dr. Nadezhda Galeva for analyzing the proteomic samples, Dr. David Moore and Ms. Heather Shinogle for help with imaging and image quantification.

Finally, I would like to thank my parents for their invaluable understanding and support. To my father, Dr. Qide Zhang, you have always been my role model and my driving force for my pursuit in the field of science. To my mother, Dr. Shangbing Yu, your advice "*avec de la patience on arrives a tout*" has constantly encouraged me whenever I met with setbacks, without your advices and support, I would not have achieved this far.

The research presented in this dissertation was funded by the JDR Foundation and NIH grant (NS054847, DK073594 to R.T.D.) and (CA120458, CA109265 to B.S.J.B.).

List of Abbreviations

ALA	Alpha-lipoic acid
ANT1	Adenine nucleotide transporter 1 protein
AGEs	Advanced glycation end products
RAGEs	AGE receptor
AR	Aldose reductase
ARIs	Aldose reductase inhibitors
ADA	American Diabetes Association
Aps	Amplitude of compound action potentials
B-H FDR	Benjamini and Hochberg False Discovery Rate
BinGO	Biological Networks Gene Ontology
CREB	cAMP responsive element-binding protein
3-DG	3-Deoxyglucosone
DAPIT	Diabetes-associated protein in insulin sensitive tissues
DCCT	Diabetic Control and Complications Trial
DKA	Diabetic ketoacidosis
DPN	Diabetic peripheral neuropathy
DAG	Diacylglycerol
dFCS	Dialyzed fetal calf serum
DPN	Distal peripheral polyneuropathy
DRG	Dorsal root ganglia
Drp1	Dynamin related protein 1
eNOS	Endothelial nitric oxide synthase
ECAR	Extracellular acidification
FCCP	carbonylcyanide-4-trifluoromethoxy-phenylhydrazone
FPG	Fasting plasma glucose
GLA	γ-linoleic acid
GM	Geldanamycin
GeLC-LTQ-FT MS/MS	Gel electrophoresis and liquid chromatography linear quadrupole ion trap Fourier transform ion cyclotron resonance tandem mass spectrometry
GO	Gene Ontology
GDM	Gestational diabetes mellitus
GLUT	Glucose transporter
GSH	Glutathione
GSSG	Oxidized glutathione
HbA1C	Glycated hemoglobin
HSF-1	Heat shock factor-1
Hsp	Heat shock protein

HSR	Heat shock response
Hsc	Heat-shock cognate
HM	Heavy mitochondria
H_2O_2	Hydrogen peroxide
HNC	Hyperosmolar non-ketotic coma
IGT	Impaired glucose tolerance
IAAs	Insulin autoantibodies
IGF-1	Insulin-like growth factor-1
IDF	International Diabetes Federation
MnSOD	Manganese superoxide dismutase
MRC	Maximal respiratory capacity
MGO	Methylglyoxal
mtHsp70	Mitochondrial Hsp70
TIM44	Mitochondrial import inner membrane translocase subunit 44
MIBA	Mitochondrial isolation buffer
$\Delta\Psi m$	Mitochondrial membrane potential
MOI	Multiplicity of infection
MI	Myo-inositol
NDDG	National Diabetes Data Group
NIDDK	National Institute of Diabetes and Digestive and Kidney Diseases
NCV	Nerve conduction velocity
NADPH	Nicotinamide adenine dinucleotide phosphate
NRF	Nuclear respiratory factor
NF- κB	Nuclear factor kappa B
O-GlcNAC	O-linked N-acetyl glucosamine
OGTT	Oral glucose tolerances test
OxPhos	Oxidative phosphorylation
OCR	Oxygen consumption rate
PBS	Phosphate buffered saline
PI	Phosphoinositol
PAI-1	Plasminogen activator inhibitor-1
PKC	Protein kinase C
ROS	Reactive oxygen species
rhNGF	Recombinant human nerve growth factor
RNAi	RNA interference
RDNS	Rochester Diabetic Neuropathy Study
SCs	Schwann cells
SSRIs	Selective serontonin reuptake inhibitors
SILAC	stable-isotope labeling with amino acids in cell culture
pSILAC	Pulse stable-isotope labeling with amino acids in cell culture

SOD	Superoxide dismutase
TGF-β1	Transforming growth factor-β1
TCAs	Tricyclic antidepressant
T1DM	Type 1 diabetes mellitus
T2DM	Type 2 diabetes mellitus
UCP	Uncoupling proteins
UKPDS	United Kingdom Prospective Diabetes Study
UDP-GlcNAc	Uridine diphosphate-N-acetyl glucosamine
VEGF	Vascular endothelial growth factor
WHO	World Health Organization

Table of Contents

List of Tables & Figures

Chapter 1: Introduction

1.1 Overview of Diabetes Mellitus

Diabetes mellitus is a heterogeneous group of chronic metabolic disorders characterized by hyperglycemia and insulin deficiency or insulin resistance[1]. Even as a non-communicable disease, the incidence of diabetes is rising at an epidemic rate due to pronounced changes in human environment, behavior, and lifestyle[2]. Statistics from the International Diabetes Federation (IDF) projects that 9.9% or one adult in 10 of the global population will be diabetic by 2030[3]. India, China, and the United States (U.S.) are currently the countries with the largest diabetic populations[3]. As of 2010, roughly 8.3% of the U.S. population was diagnosed with diabetes[4]. Thus, diabetes and its association with an increased rate of premature morbidity and mortality has become a major challenge for public health in the 21st century[3].

The National Diabetes Data Group (NDDG) and the World Health Organization (WHO) categorized diabetes mellitus into three major groups: Type 1 diabetes mellitus (T1DM), Type 2 diabetes mellitus (T2DM), and gestational diabetes mellitus (GDM)[1,5]. All forms of diabetes can be diagnosed by the presence of classic diabetic symptoms along with the gross and unequivocal elevation of blood glucose with repeated testing[6-7].

Types of diabetes mellitus, risk factors and prevalence

Type 1 diabetes mellitus (T1DM), formerly known as insulin-dependent diabetes is the consequence of chronic autoimmune disorder which selectively eliminates pancreatic β-cells, producing insulinopenia. The absolute deficiency in insulin leads to

extreme hyperglycemia and classical diabetic symptoms such as polyuria, polydipsia (increased thirst), polyphagia (increased hunger), fatigue, and rapid weight loss[3]. T1DM accounts for approximately 10% of all diabetic cases in North America and Europe[6]. Even though the onset of T1DM can occur in any age group, more than 80% of T1DM occurs in children and young adults with no prior family history of the disease[6]. Current management of T1DM emphasizes glycemic control with mandatory insulin administration to maintain a patient's life and prevent acute complications that can be fatal with negligence[3,8-9].

The clinical manifestation of T1DM is preceded by an asymptomatic period of highly variable duration. During this period, four classic disease-associated autoantibodies can be detected as the first sign of emerging β-cell autoimmunity. These include islet cell antibodies, insulin autoantibodies (IAAs), autoantibodies to the 65-kDa isoform of GAD and the tyrosine phosphatase-related IA-2 molecule[9]. Both genetic predisposition and environmental factors have been proposed as triggers and potentiators of pancreatic β-cell destruction[8-9]. The most important genes contributing to disease susceptibility are located in the HLA region of chromosome 6 where it also controls immune responses[6,9]. Yet, less than 10% of individuals with genetically predisposed susceptibility progress to clinical disease[9]. Early introduction of supplementary milk feeding during infancy, appearance of autoantibodies subsequent to enterovirus infections or increased immune response to foreign antigens have been proposed as environmental events that leads to HLA-mediated T1DM[9]. Nevertheless, further studies are needed to provide concrete evidence to the cause(s) of T1DM and approaches to disease prevention.

Type 2 diabetes mellitus (T2DM), accounts for over 90% of the total diagnosed cases in diabetes and is the leading cause of the diabetes epidemic[1-3]. T2DM is a heterogeneous metabolic disorder that precipitates from an array of factors but is characterized by insulin resistance and relative insulin deficiency[3]. The prevalence of this disorder increases with age and obesity, with incident rates peaking at 40-59 years of age[4,10]. Patients with T2DM are often asymptomatic and can remain undiagnosed for decades. About 50% of the T2DM patients are diagnosed during routine exams, diabetes screening, or while being treated for another condition[3,8,10]. Thus, the total prevalence of T2DM is estimated to be twice the number of diagnosed cases[3,6]. Chronic secondary complications include both macrovascular diseases and microvascular abnormality of the eyes, kidneys and peripheral nerves[1,3,5,10]. Initial management of T2DM includes self-monitoring and lifestyle changes[3,5]. When patients fail to keep their glycemic level at bay, medications such as metformin and/or insulin are introduced[4].

Unlike T1DM, which is an autoimmune disease, the etiology of T2DM is polygenic. The clinical course of T2DM progresses as muscles, liver and fat tissues fail to respond adequately to normal levels of insulin. The ensuing, hyperglycemia initiates a continuous overstimulation of insulin secretion and produces hyperinsulinemia coincident with insulin resistance[10-11]. Insulin deficiency eventually follows with deteriorated β-cell function as a result of the hyperglycemia[11]. Strong genetic predispositions are often associated with T2DM[10]. Multiple genes that control β-cell development or function have been associated with an increased risk of developing T2DM[12]. Conditions such as obesity, hypertension and/or dyslipidemia are also considered as independent risk factors contributing to the pathogenesis of T2DM[10].

Gestational diabetes mellitus (GDM) is defined as carbohydrate intolerance diagnosed during pregnancy and occurs in 2%-10% of all pregnancies[4,13]. Most cases of GDM resolve with delivery, but infants born to mothers with GDM are often at risk of delivery complications due to macrosomia, low blood sugar and jaundice[4-5]. In addition, about 5%-10% of women with GDM are diagnosed with T2DM immediately or within 5 years after pregnancy. GDM resembles T2DM as they share many of the same risk factors and genetic susceptibilities[13]. A combination of relatively inadequate insulin secretion and responsiveness are involved in both T2DM and GDM[1,4]. Hence, these two diseases are considered as etiologically indistinct with one preceding the other[13]. Even with recovery, women with GDM are more susceptible to the onset T2DM in the future[4-5,10].

A number of other types of diabetes also exist and include conditions developed from specific genetic mutations, surgery, medications, infections, pancreatic disease and other illnesses[4]. One can also be diagnosed as pre-diabetic when the blood glucose levels are intermediate between normal (99 mg/dl) and diabetic (126 mg/dl), impaired glucose tolerance (IGT)[4]. Individuals with IGT have an increased risk of heart disease, stroke and T2DM[10]. With change of lifestyle and adequate control of blood glucose, individuals with IGT can delay or prevent the onset of T2DM[3,5].

Diagnosis & Screening Criteria for Diabetes

The WHO, the IDF and the National Institute of Diabetes and Digestive and Kidney Diseases (NIDDK), recommend fasting plasma glucose (FPG) tests, oral glucose tolerances tests (OGTT) or glycated hemoglobin (HbA_{1C}) tests as diagnostic criteria for diabetes (Table 1)[5,7]. The FPG test is the preferred method for diagnosing diabetes

because of its convenience and low cost[5,7]. Blood glucose is measured in a patient who has fasted for at least 8 hours[5]. The OGTT is a more sensitive method for diagnosing those with ambiguous FPG and individuals with IGT but without apparent symptoms[5-6]. After an 8 hr fast, plasma glucose level is measured immediately before and 2 hours after a 75-gram oral glucose challenge[5]. Despite the accuracy of FPG or the OGTT test in diagnosing diabetes, single measures of glucose concentration are incapable of predicting the prevalence of diabetes-specific complications[14]. Thus, the level of HbA_{1C} is recommended as a long-term measure of glycemic control.

Diagnosis	**FPG Test Plasma Glucose Result (mg/dL)**	**OGTT 2-hour Plasma Glucose Result (mg/dL)**	**HbA1c %**
Normal	≤ 99	≤ 139	≤ 6.0
Prediabetes (Impaired glucose tolerance)	100 – 125	140 – 199	6.0 – 6.4
Diabetes*	≥ 126	≥ 200	≥ 6.5

Table 1. Diagnostic Criteria for Diabetes. * Confirmed by repeating the test on a different day.

Glycated hemoglobin (hemoglobin A1c, HbA_{1C}) is the product of non-enzymatic glycation when exposed to plasma glucose[14]. HbA_{1C} serves as an accurate and precise measure of blood glucose levels that are associated with an increased risk for developing diabetic complications[14]. Hence, an International Expert Committee that includes representatives of the American Diabetes Association (ADA), IDF, and the European Association for the Study of Diabetes (EASD) recommended HbA_{1c} be used as part of the diagnosis for diabetes[14]. Several advantages of the HbA_{1C} assay surpass the FPG test, including greater convenience as fasting is not required, greater pre-analytical stability, and less day-to-day perturbations during periods of stress and illness[10]. However, in some parts of the world the cost of HbA_{1C} assay may preclude its availability[10].

Mortality & Economic Impact of Diabetes

Diabetes substantially cripples society and its citizens via a direct burden to national healthcare systems and an indirect loss of productivity from diabetes-related morbidity and premature mortality. According to IDF, the estimated healthcare expenditures due to diabetes, in 2011, account for $465 billion or 11% of the total healthcare expenditures in the world[3]. Approximately 20% of the health care in the U.S. is spent by individuals diagnosed with diabetes[15]. Although diabetes-induced death is likely under reported or under estimated, diabetes has been recognized as being responsible for a large portion of premature deaths in most countries[3]. Diabetes was the 7th leading cause of death in the U.S. in 2007, individuals with diabetes along with secondary complications are twice as likely to die prematurely than their counterparts[3-4].

1.2 Complications of Diabetes

Without proper glycemic management, both acute and chronic complications may arise, leading to life-threatening events. Patients with T1DM are vulnerable to both acute and chronic complications whereas individuals diagnosed with T2DM suffer more often from chronic complications.

Acute Metabolic Complications

Acute metabolic complications of diabetes consist of diabetic ketoacidosis (DKA), hyperosmolar non-ketotic coma (HNC), and hypoglycemia. Both DKA and HNC are related to insulin deficiency and require hospitalization for treatments[16]. Hypoglycemia is a consequence of improper diabetes treatments with either oral agents or insulin therapy and can usually be treated in an ambulatory care setting[16].

DKA is clinically defined by an absolute insulin deficiency with hyperglycemia (>200 mg/dL) that leads to increased lipolysis, hyperketonemia (beta hydroxybutyrate >0.5 mmol/L) and acidosis (pH $\leq$7.3)[16]. It is diagnosed predominately in T1DM patients as an initial manifestation of previously undiagnosed diabetes; under certain circumstances those with advanced T2DM may also experience DKA[16]. Precipitating factors for DKA in known diabetic patients include infection, illnesses or poor compliance with insulin therapy[16]. DKA is life-threatening and always requires professional medical attention. The most important aspects in preventing DKA remain self-compliance and monitoring in diagnosed diabetic patients[16].

HNC is a type of diabetic coma associated with high mortality mostly in older T2DM patients[16]. HNC precipitates from relative insulin deficiency and extreme hyperglycemia (>600 mg/dL) associated with elevated serum osmolality (>320

mosm/kg), polyuria and dehydration[16]. HNC is distinct from DKA with the absence of lipolysis and ketoacidosis formation. Patients will progress into stupor and coma if the condition is uncorrected. Precipitating factors of HNC include infection, myocardial infarction, stroke or another acute illness and is almost always a sign of poor management from patients. Hydration and small dose of insulin can be used to correct hyperglycemia[16].

Chronic Complications of Diabetes

Chronic diabetic complications are the major source of morbidity and mortality in diabetic patients. Despite the differences in pathogenesis, both T1DM and T2DM patients are vulnerable to chronic complications[17]. Chronic hyperglycemia together with other risk factors induce physiological changes and abnormalities that are categorized as macrovascular and microvascular diseases[17]. Landmark studies from the Diabetic Control and Complications Trial (DCCT) and the United Kingdom Prospective Diabetes Study (UKPDS), showed that intensive control of blood glucose may attenuate, delay or prevent the progression of diabetic complications, but reversal of the complications does not occur[18-19].

Vascular Diseases

The rapidly escalating population of patients with T2DM contributes to the growing epidemic of macrovascular complications that includes diseases of coronary arteries, peripheral arteries, carotid vessels and ischemic stroke[20]. Diabetes mellitus has been considered as an independent risk factor and predictor for the development of

arterial dysfunctions, which accounts for over 50% of all morbidity and mortality in diabetes[5,17].

The vast majority of diabetic patients with vascular disease died of causes related to atherosclerosis[21]. It is the product of chronic hyperglycemia, dyslipidemia and insulin resistance[20]. Biochemical studies support that chronic hyperglycemia can contribute to atherogenesis and endothelium dysfunction through the induction of oxidative stress and inflammation[20-21]. Thus, aggressive glycemic control and management of abnormal metabolic states are required to achieve primary or secondary prevention of the disease. Indeed, multiple clinical observations have demonstrated a linear correlation between intensive glycemic control and decreased risk and progression of macrovascular events in T1DM and T2DM patients[18-19,22-25].

Retinopathy

Retinopathy is a common microvascular complication of diabetes. Almost all patients with T1DM and over 60% of patients with T2DM will suffer from some degree of retinopathy within twenty years after of diagnosis[26]. The damage in retinopathy originates from microvascular leakage and occlusion of the retinal capillaries[26]. The duration and severity of hyperglycemia is the major factor dictating the morbidity of diabetic retinopathy[18-19,22]. Hyperglycemia is thought to modulate disease progression through several biochemical processes including polyol accumulation, formation of advanced glycation end products (AGEs), oxidative stress and activation of protein kinase C (PKC)[27]. Severe vision loss or even blindness as a consequence of diabetic retinopathy can be prevented in patients with proper glycemic control and with treatments such as photocoagulation and vitrectomy[26].

Nephropathy

Diabetic nephropathy is the leading cause of renal failure and kidney transplant in North America and Europe[28]. It affects around 40% of all the diabetic patients with progression toward albuminuria followed by persistently elevated plasma creatinine that eventually leads to death[28]. The cumulative incidence of albuminuria (urine albumin > 300 mg/day) has also been considered as a powerful independent predictor of cardiovascular morbidity and mortality in T2DM diabetic patients[29]. Like retinopathy, the main potentiator of this disease in susceptible individuals is chronic hyperglycemia[30]. Other putative risk factors include hypertension, dyslipidemia and glomerular hyperfiltration[30]. Thus, intensive blood glucose control remains as the main method for preventing the onset of nephropathy[30].

Neuropathy

Diabetic neuropathy refers to the degeneration of the peripheral nerves which affects 60%-70% individuals within twenty years of diabetes and gives rise to significant morbidity and mortality[31]. Unfortunately, the true prevalence of this complication is unknown as epidemiologic studies of diabetic neuropathy are limited to clinically diagnosed individuals that receive continuous medical care[32]. Diagnosing diabetic neuropathy is performed by clinical examinations that quantitatively measure electrophysiologic, sensory and autonomic function[33].

Diabetic neuropathy is a heterogeneous group of nerve disorders. The type of nerve fibers and unique pathophysiologic and prognostic features of various neuropathy syndromes are summarized in Figure 1-1[34]. Sensory and autonomic neuropathy generally progress gradually with the increasing duration of diabetes and are often asymptomatic[34].

Mononeuropathies, radiculopathies or acute painful neuropathies, however, usually present with severe symptoms but remit completely[34].

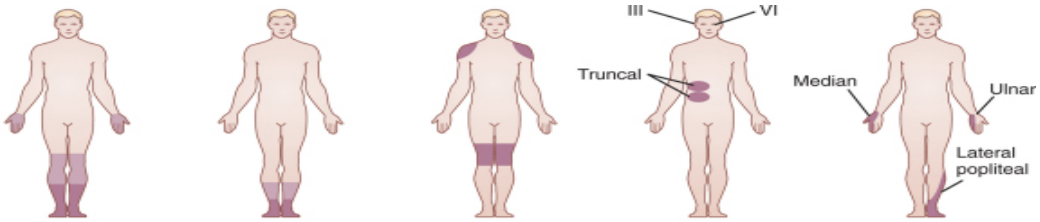

Large-fiber Neuropathy	Small-fiber Neuropathy	Proximal motor neuropathy	Acute mononeuropathies	Entrapments
Sensory loss: 0→+++ (Touch, vibration) Pain: +→ +++ Tendon reflex: N→ ↓↓↓ Motor deficit 0→ +++	Sensory loss: 0→ + (thermal, allodynia) Pain: +→ +++ Tendon reflex: N→ ↓ Motor deficit: 0	Sensory loss: 0→ + Pain: +→ +++ Tendon reflex: ↓↓ Proximal motor deficit: +→ +++	Sensory loss: 0→ + Pain: +→ +++ Tendon reflex: N Motor deficit: +→ +++	Sensory loss in Nerve distribution: +→ +++ Pain: +→ + Tendon reflex: N Motor deficit: +→ +++

Figure 1-1 Different clinical presentation of diabetic neuropathy[34].

Among all diabetic peripheral neuropathies, distal peripheral polyneuropathy (DPN) is the most common chronic syndrome. DPN may be asymptomatic in over 50% of patients and is responsible for >80% of amputations following foot ulceration or injury[33]. Progression of DPN is closely related to the duration and severity of hyperglycemia in both T1DM and T2DM patients[18-19]. Multiple etiologies including metabolic abnormalities, oxidative stress and neurohormonal growth-factor deficiency have been proposed to contribute to the development of DPN[34].

1.3 Distal Peripheral Polyneuropathy

One of the most frequent and troublesome complications of diabetes mellitus is distal peripheral polyneuropathy (DPN). It accounts for over 50% of all diabetic-relate peripheral neuropathies and give rise to incapacitating pain, sensory loss, foot ulceration, infection, gangrene and poor wound healing[35]. In many cases, the end result is lower limb amputation. Progression of this complication along with autonomic neuropathy is a major cause in mortality for diabetic subjects.

Signs & Symptoms

The most common early abnormality indicative of DPN is asymptomatic nerve dysfunction as reflected by decreased nerve conduction velocity (NCV) and amplitude of compound action potentials (APs) in peripheral sensory and motor nerves[33]. These changes are usually followed by a loss of vibratory sensation and ankle reflexes[36]. Clinical indicators of DPN can be divided into negative and positive symptoms[33-34]. The former consist of loss of sensory perception to pain, pressure or temperature; muscle weakness may occur as a sign of motor nerve dysfunction[33]. Positive symptoms include burning, paresthesias, allodynia and hyperalgesia in feet and lower limbs, which are typically worse at night, may be the result of neural hyperexcitability[35]. These symptoms usually begin from the distal end of the hands and feet with proximal progression, reflecting the dying-back nature of DPN.

Pathophysiological Features

The classical manifestations of DPN progress bilaterally in a "glove-and-stocking" distribution beginning from the most distal extremities of the hands and feet[32].

The mixed symptoms and sensory loss are evidence that both large and small afferent nerve fibers are affected[32]. Structural changes of the peripheral nerves during disease progression include axonal atrophy and degeneration, paranodal demyelination, failure of re-innervation, and abnormal microvascular changes[35]. Clinical and animal studies have shown that the progressive nerve degeneration and compromised regenerative plasticity are closely related to the degree of hyperglycemia and the duration of diabetes[37-39]. Skin biopsies from diabetic patients showed significant epidermal denervation, a sign of distal sensory epidermal axon loss and were accompanied by functional impairments[40]. Loss of axonal caliber associated with axonal shrinkage indicates a combined insult on axons and Schwann cells (SCs) as has been reported in teased nerve-fiber studies and diabetic animal models[41-43]. Attempted skin re-innervation and sural nerve regeneration were badly compromised with increased diabetic duration[40,44-45]. In advanced diabetes, evidence for axonal, glial and vascular injuries is detectable in most cases of DPN[46-47].

While the discussions above provide some insights on the morphological changes of peripheral nerves, multiple questions related to the etiology of DPN remain unclear. Additionally, the different clinical presentations of the disease and its symptoms in diabetic patients have made predicting disease progression a challenge. Up-to-date, treatments against DPN remain symptomatic and are limited.

1.4 Current Therapeutic Management & Strategies

Once neuropathy is diagnosed, therapy can be instituted with the goal of reducing symptoms and delaying disease progression. Current available therapies may be classified as symptom management, primary prevention, and causal treatment based on etiology.

Symptomatic Managements

Pain is a severe consequence affecting patients' quality of life and yet remains one of the most difficult issues to manage in DPN. Nevertheless, newly diagnosed patients are often unaware of pain as a symptom of DPN and fail to report it. The prevalence of painful diabetic neuropathy increases with age and duration of diabetes. Hence, symptomatic therapies are often aimed at reducing pain.

The commonly prescribed treatments for painful DPN are antidepressants (TCAs and SSRIs) where combinatorial drug therapies have demonstrated the best efficacy in reducing pain and paresthesias in over 80% of patients[48-49]. However, antidepressants such as TCAs always carry a risk for developing adverse drug reactions in individuals. The nature and chronicity of neuropathic pain also promotes the use of anticonvulsants (carbamazepine and gabapentin) and opioid analgesics (tramadol and NSAIDs)[34]. Nevertheless, these drugs carry a risk of high-dose tolerance, physical dependence and provide only marginal to moderate relief of pain[32]. Topical analgesics such as capsaicin have been reported to exacerbate pain with temporary burning sensation in the initial stage of the treatment but lead to pain relief by decreasing substance P levels in small sensory fibers[32]. Mexiletine is a type of antiarrhythmic medication that is prescribed only as an alternative agent in patients under extreme, refractory symptoms with no cardiac

risk[48]. Clearly, therapies aimed at reducing painful stimuli in neuropathy are polypharmacy nightmares fraught with adverse effects and only moderately efficacious. Hence, more-efficacious and neuropathy-specific medications are needed.

Intensive Glycemic Control

Comprehensive clinical studies have suggested an intimate correlation between hyperglycemia and the severity of DPN. The Rochester Diabetes Project was the first community-based study of neuropathy in a U.S. population[31]. Patients diagnosed with T2DM were followed over 25 years and showed an increase in prevalence of clinically detectable DPN from 4% for diabetes of short duration (<5 years) to 15% after 20 years of diabetes[31]. The follow-up study from the Rochester Diabetic Neuropathy Study (RDNS) showed that DPN was of greatest prevalence among all forms of neuropathy diagnosed in both Type 1 and Type 2 diabetic patients[50].

The Diabetic Control and Complications Trial (DCCT) study reported a statistically significant effect of intensive insulin therapy on reducing cumulative incidence of diabetic neuropathy[18]. The prevalence rates for clinically diagnosed neuropathy in the T1DM were reduced by 60% in those treated by intensive insulin therapy at 5 years compared with conventional treatment, which involved less intensive glycemic control[18]. The United Kingdom Prospective Diabetes Study (UKPDS), which followed a cohort of more than 3,000 patients with T2DM for over 15 years, also showed similar correlation of glycemic control and the reduction in the incidence of neuropathy[19,22-23,28]. Particularly, patients who received intensive glycemic therapy (insulin or sulfonylurea) was associated with improvement in vibration perception compared with those assigned to conventional regimen[19]. The difference between the

two treatment groups was even greater when all microvascular complications were considered. These findings underscore the importance of early, intensive glycemic control in the prevention of diabetic-related complications including neuropathy and point to systemic hyperglycemia as the universal trigger responsible for the onset of diabetic complications. However, despite these favorable results, DPN could not be completely prevented in the above studies, suggesting that additional etiological factors may significantly contribute to disease progression.

Pathogenic Mechanism Specific Management

Several classes of compounds have been developed to counteract specific pathogenic mechanisms involved in DPN. Most of the drugs have demonstrated promising results in preclinical animal prevention studies, but have delivered disappointing results from clinical trials. Some etiological treatment paradigms include: inhibitors of the polyol pathway and advanced glycosylation products, anti-oxidant, drugs that normalize prostanoid metabolism and recombinant human nerve growth factor.

Aldose reductase inhibitors (ARIs) held promise for the treatment and management of DPN. It is argued that since hyperglycemia increases glucose flux through the polyol pathway, inhibition of the pathway using ARIs could prevent tissue accumulation of sorbitol and reduce changes in redox potential. In clinical evaluations of the ARI, Tolerestat, diabetic patients with symmetrical polyneuropathy showed improvement in autonomic function tests and vibration perception with daily administration of the drug whereas placebo-treated patients showed deterioration in most of the variables measured[51-52]. Similarly, a 12-month study with the ARI Zenarestat, showed a dose-dependent improvement in nerve fiber density accompanied by an

increase in NCV[53]. This same response has been noted in experimental ARI trials in diabetic rats[54]. Unfortunately, follow up studies have shown that regenerating nerve fibers following ARI treatment never reach functional or structural maturity[36]. Overall, inhibition of aldose reductase may be efficacious as a preventative measure during the early metabolic phase of DPN, but insufficient to reverse established neuronal deficits.

Another pathogenic-derived drug target is to inhibit the formation of advanced glycation end-products and free radicals with aminoguanidine. Animal studies using aminoguanidine showed improvements in nerve blood flow, vascular permeability, NCV and structural parameters[55-57]. Controlled clinical trials in humans, however, have been abolished due to toxicity[34]. However, inhibiting the effects of advanced glycosylation products by blocking their interaction with the receptor for AGEs (RAGE) may hold promise[58-59].

Linoleic acid is an essential fatty acid constituent of neuronal membranes and is a substrate in prostanoid metabolism. The metabolism of linoleic acid is impaired in diabetes and placebo controlled clinical trials employing γ-linoleic acid (GLA) have reported improvement in clinical measures and electrophysiologic testing[60-61]. Some prostaglandin trials have also reported positive treatment effects following short-term intravenous administration of lipo-PGE[36]. Little adverse effects were noted following administration of these drugs.

Alpha-lipoic acid (ALA) is a thiol replenishing and redox modulating agent. Experimental data has shown that ALA is a potent lipophilic free radical scavenger that is capable of stimulating glucose uptake and pyruvate-dehydrogenase activity, thereby, reducing the level of lactate and pyruvate in serum[62-64]. Short-term studies with

intravenous infusion of ALA have demonstrated increased insulin sensitivity and improvement in clinical symptoms in diabetic patients[65-66]. Nevertheless, long-term followed up studies did not show further improvement of the clinical symptoms or neurological deficits despite the slightly enhanced electrophysiology[67-68].

Impaired neurotrophic support has been associated with peripheral deficits in experimental diabetic models[34]. Treatment with recombinant human nerve growth factor (rhNGF), a selective trophic factor for small-fiber sensory and sympathetic ganglion neurons, has restored neuropeptide levels and prevented sensory neuropathy in diabetic animals[69]. Although early clinical trials of rhNGF appeared to show some beneficial effects on sensory nerve function, regrettably, the improvement was less than significant. In addition, there was challenge in the route of administration as direct injection of neurotrophic factors is associated with hyperalgesia and pressure allodynia at the site of entry[70-71].

In summary, numerous clinical trials have been undertaken to test potential etiology-targeted treatments and with few exceptions, most have been disappointing. This disappointment may be accounted for by the fact that the biochemical progression of DPN in individual patients is never uniform. Thus, the therapeutic approach to DPN has to be reconsidered. It appears that this multi-factorial disease is best treated with multi-drug interventions in order to prevent, block and/or reverse several pathogenic pathways simultaneously. Such approaches however require in-depth knowledge of the natural history of the disease, which is reviewed in the following sections.

1.5 Pathogenesis of Distal Peripheral Neuropathy

Clinical studies and experimental observations of DPN give rise to two plausible etiologies contributing to its pathogenesis that may be operating simultaneously or in parallel. The dying-back of the longest axons may manifest with impairments in growth factor synthesis and axonal transport[45]. Impaired protein synthesis or transport, including vital neurotrophic support may be the source of axonal atrophy and compromise nerve regeneration in DPN[72]. Alternatively, chronic hyperglycemia and inflammatory responses may provoke the accumulation of local injuries and insults that lead to nerve dysfunction[35]. Regardless of whether DPN initiates with distal axons dying back, multiple proximal injuries or both, in most cases, sensory axon degeneration prevails. Sensory neuron loss with replacement by satellite cells (nests of Nageotte), vacuolation of sensory neurons and apoptosis have been reported in both clinical patients and animal studies[38,73]. Hence, studying the molecular changes in sensory neurons, glia and peripheral nerves will provide us with better understanding of the disease.

Regulation of Glucose Transport in Peripheral Nervous System

The majority of the metabolic energy in peripheral nerves is consumed through axolemma repolarization[74]. However, blood-nerve and perineurial diffusion barriers limit the access of free fatty acids as substrates for energy production in peripheral axons and energy from oxidation of ketones plays only a minor role[74-75]. Thus, glucose oxidation becomes the major source of metabolic energy for the peripheral nerves and neurons[74]. Large amounts of glucose are taken up via endoneurial capillaries across the blood-nerve barrier or through the plasma membrane and cytoplasm of myelinated SCs wrapping around the axons[76]. Peripheral nerves require a constant metabolic energy supply but are

not able to uptake glucose in an insulin-dependent manner[77]. Therefore, despite the presence of insulin receptors in dorsal root ganglia (DRG) and peripheral nerve, glucose uptake and utilization in neurons and glial cells depends solely on the extracellular concentration of glucose[75].

Cellular glucose uptake is achieved via plasma membrane carrier proteins that transfer glucose across the lipid bilayer[78]. SCs express two isoforms of insulin insensitive glucose carriers, GLUT1 and GLUT3, which passively transport glucose into peripheral nerves through facilitative diffusion[76,78]. Expression of GLUT1 is predominantly in SCs at the node of Ranvier, whereas GLUT3 is preferentially expressed in the paranodal regions of SC and nodal axons[76,79]. Under conditions operative *in vivo*, SCs that are not part of blood-nerve barrier express low levels of GLUT1 and at steady state, take up a higher proportion of glucose than neurons[76]. Axonal modulation can increase the expression of GLUT1 in SCs, thus affecting glucose uptake and utilization[74]. The delivery of glucose from SCs to the axons and neurons is modulated by axonal-glial interactions which also regulate SC proliferation, differentiation and receptor expressions. Hence, the state of chronic hyperglycemia during diabetes can render peripheral nerves more vulnerable to glucotoxicity due to increased glucose uptake into SCs and neurons.

The Role of Schwann Cells in Diabetic Neuropathy

Schwann cells (SCs) are the principle glial cells in the peripheral nervous system. They are part of the perinurial blood-nerve-barrier and are responsible for proper saltatory conduction along axons, provide trophic support for neurons, and are essential for nerve development and regeneration[80]. Morphological and functional studies indicate

that SCs undergo substantial damage in diabetes and related animal models[73,81-83]. Biochemically, hyperglycemia may induce metabolic damage through the polyol pathway as aldose reductase (AR) is primarily localized to SCs in peripheral nerve. Overexpression of AR through a SC-specific promoter exacerbates NCV deficit in diabetic transgenic mice and implicates the polyol pathway in dysregulation of SCs in diabetes[84].

Additionally, there is evidence indicating that impaired neurotrophic support in glia contributes to neuronal dysfunction in diabetes[36,85]. Hyperglycemia depleted nerve growth factor (NGF) production in cultured SC cells and treating SCs with aldose reductase inhibitors (ARIs), increased NGF secretion/synthesis and prevented hyperglycemia-induced apoptosis[73,86-87]. The loss of trophic support and dysregulation of axonal-glial interaction can also severely compromise myelination and axonal regeneration. A study by Eckersley and co-workers showed that ErbB2, a critical axon-SC signal receptor, was decreased in SCs isolated from diabetic rats whereas expression of p75NTR, which is capable of inducing autocrine apoptosis in SCs, was enhanced[88]. As a result, fewer SCs become available to support nerve regeneration.

Glucose Neurotoxicity

Various neuropathic syndromes seen in patients with diabetes may be the result of multiple etiologies. Nevertheless, the common symptom in diabetes is systemic hyperglycemia and the DCCT has shown that elevated blood glucose clearly plays a central role in the development and progression of diabetic neuropathy[18]. Chronic hyperglycemia increases intracellular glucose metabolism and leads to neuronal and glial cell damage that is often referred to as glucotoxicity[77]. Studies of impaired peripheral

nerve function in DPN hypothesize that the insult from hyperglycemia is likely to be metabolic, vascular or both[89]. Chronic hyperglycemia can increase metabolic insults through activation of alternative glucose metabolic pathways such as the polyol and hexosamine pathways. Under normal conditions, these pathways utilize only a small percent of total glucose but serve as conduits for the shunting of excess glucose under diabetic conditions. However, the enhanced activity of these pathways alone cannot account for the extensive nerve damage that occurs in DPN and the following sections will highlight some of the major pathways that are thought to contribute to DPN.

Polyol (Sorbitol) Pathway

The polyol (sorbitol) pathway converts glucose to fructose via a two-step reduction/oxidation. The rate-limiting step converts glucose to sorbitol by aldose reductase (AR) followed by the formation of fructose through oxidation of sorbitol. Under normoglycemic conditions, glucose is converted to glucose-6-phosphate by hexokinase which has a higher affinity for glucose than AR. Hence, only trace amounts of sorbitol are formed[90]. However, hyperglycemia increases ambient glucose uptake in the peripheral nerve, saturates hexokinase, and shunts the excess glucose to the polyol pathway, leading to intracellular sorbitol accumulation, depletion of organic osmolytes, reducing agents and antioxidants[90].

Polyol pathway activation was the first cogent hypothesis in the search to link altered glucose metabolism with nerve dysfunction[91-92]. In early tissue damage, intracellular sorbitol accumulation induces hyperosmotic swelling. This leads to the compensatory efflux of other organic osmolytes such as taurine and *myo*-inositol (MI)[90,93]. Nevertheless, osmotic pressure from sorbitol accumulation is considered to play a minor

role in tissue damage in neuropathy[92]. Instead, the major mechanism leading to various metabolic disturbances due to increased activity of the polyol pathway are thought to arise from an increased production of ROS and depletion of antioxidants/reducing agents[77,93]. Taurine is an endogenous antioxidant that counteracts oxidative stress and NGF deficit by attenuating nerve blood flow and nerve conduction in diabetic nerves[94]. Thus, taurine depletion compromises antioxidant defense mechanisms and promotes nerve degeneration[94]. Increased activity of AR also disrupts redox balance and increases oxidative stress in the peripheral nerve under diabetic conditions[90]. AR utilizes NADPH as substrate for the reduction of glucose to sorbitol and can alter the cellular ratio of NADPH/NADP. A decrease in NADPH levels can compromise the recycling of glutathione since NAPDH is a co-factor for glutathione reductase, and reduce the clearance of H_2O_2 from mitochondria[95]. Additionally, depletion of NADPH also suppresses nitric oxide production, thereby eliciting microvascular derangements and the slowing of nerve conduction[96-97]. Metabolic damage via the polyol pathway may be highly localized in peripheral nerves since AR is localized primarily in the paranodal cytoplasm of SCs as well as in endoneurial capillaries[98].

Hexosamine Pathway

During normoglycemia, small amounts of the glycolytic intermediate, fructose-6 phosphate are shunted from glycolysis to the hexosamine pathway, which drives the formation of uridine diphosphate-N-acetyl glucosamine (UDP-GlcNAc). As diabetes increases the flux of glucose through glycolysis, the volume of metabolic intermediates increases and can be shunted into the hexosamine pathway. UDP-GlcNAc formation can affect protein function by attaching O-GlcNAC to the serine and threonine residues of

numerous proteins and transcription factors. Studies of O-GlcNAC biology suggest that the hexosamine pathway functions as a cellular "sensor" for energy availability and plays a role in insulin resistance and macrovascular complications[93].

Several gene products including leptin are altered under the hyperglycemia-driven activation of hexosamine pathway. Sp1 is a transcription factor that regulates the expression of tissue type plasminogen activator inhibitor-1 (PAI-1) and transforming growth factor-β1 (TGF-β1) and is modified by UDP-GlcNAc in diabetic complications. Dysregulation of these genes increases nerve ischemia and oxidative stress, which may help contribute to the symptoms of DPN[93]. However, a direct role for the hexosamine pathway in the development of DPN has not been described.

Protein Glycation

Reducing sugars react spontaneously and non-enzymatically with amino groups in proteins forming a reversible Schiff base. Rearrangements of the labile Schiff base product produces irreversible intermediates known as ketoamines or Amadori products[99]. Under normal physiological condition, glucose is in equilibrium with Amadori products and only a small portion of the intermediates undergo further oxidation yielding irreversible cross-linked products termed advanced glycation end products (AGEs)[100]. AGEs accumulate on long-lived proteins and hence the rate of AGE formation is directly proportional to the duration and concentration of glucose, the rate of protein turnover and the permeability of tissue to free glucose[99-100]. Glycolytic intermediates and reactive α-dicarbonyl compounds can glycate proteins at a much faster pace than glucose thus promoting intracellular formation of AGEs in diabetes[100-102]. Some glycating agents include glyceraldehyde-3-phosphate, 3-deoxyglucosone (3-DG) and methylglyoxal

(MGO), which is the most reactive triose. MGO can be produced from glyceraldehyde-3-phosphate, fructose and oxidative decomposition of polyunsaturated fatty acids[99,101,103].

AGEs have been shown to alter enzymatic activity, decrease ligand binding, modify protein half-life and alter immunogenicity[99]. Aggregates of AGE deposition were found in the cytoplasm of endothelial cells, pericytes, axoplasm and SCs of both myelinated and unmyelinated nerve fibers of human diabetic peripheral nerves[104]. Ryle *et al* showed that peripheral nerve cytoskeletal proteins are vulnerable to AGE accumulation with increased duration of diabetes[105]. Excess AGE deposition in diabetic nerves and skin correlate with a reduction in myelinated fiber density and the onset of clinical manifestations of DPN[104,106]. Thus, enhanced AGEs play a role in the development of diabetic neuropathy.

Some biological effects of AGEs are modulated through the interaction with their cellular receptors (RAGEs), which are expressed in smooth muscle cells, macrophages, endothelial cells, astrocytes and microglia[107]. Dramatic increases in RAGE expression are found in peripheral epidermal axons, sural axons, SCs and DRG sensory neurons of diabetic mice along with progressive electrophysiological and structural abnormalities[108]. Interaction of AGE with RAGE increases oxidative stress and activates pro-inflammatory pathways through the transcription factor, NF-κB[100]. Vincent *et al* showed that activation of RAGE promoted neuronal injury via the formation of ROS by NAD(P)H oxidase in DRG sensory neurons[109]. Abolishing RAGE expression via genetic deletion attenuated the onset of DPN in diabetic RAGE knockout mice[108]. Consequently, these studies suggest that RAGE may be a potent therapeutic target for treating diabetic complications.

1.6 Oxidative Stress & Mitochondria Dysfunction.

Oxidative stress is a well-recognized mechanism in the pathogenesis of neurodegenerative diseases, and has been proposed as a central mechanism linking the aforementioned metabolic pathways with various biochemical abnormalities in diabetic neuropathy.

Reactive Oxygen Species

Although oxidative phosphorylation (OxPhos) is nearly always orchestrated with great rapidity and precision, reactive oxygen species (ROS) are occasionally generated as byproducts that readily react with a variety of cellular components[110]. The best known ROS is the superoxide radical ($O_2\cdot^-$). Approximately 4% of electrons that enter the mitochondria respiratory chain lead to the formation of $O_2\cdot^-$[111]. Superoxide can also act as a precursor for other reactive species[112]. The most potent oxygen species, hydroxyl radical is formed from $O_2\cdot^-$-driven Fenton reaction with hydrogen peroxide (H_2O_2) in the presence of transition metals (e.g., copper and iron; Eqns 1 & 2)[113]. Superoxide can also react directly with H_2O_2 (Eqn 3)[114].

$$O_2\cdot^- + Fe^{3+} \longrightarrow O_2 + Fe^{2+} \qquad (1)$$

$$H_2O_2 + Fe^{2+} \longrightarrow {}^{\cdot}OH + OH^- + Fe^{3+} \qquad (2)$$

$$O_2\cdot^- + H_2O_2 \longrightarrow O_2 + H_2O + {}^{\cdot}OH \qquad (3)$$

Oxidative free radicals are removed from the cell by antioxidants. The enzyme superoxide dismutase (SOD) is found in nearly all cells and is considered a first-line defense against ROS. SOD catalyzes the conversion of $O_2\cdot^-$ to H_2O_2. Nonetheless, the uncharged H_2O_2 is a powerful oxidizing agent too and is capable of diffusing rapidly across the mitochondrial membrane into the cytosol where it can potentially react to yield

other ROS[112]. H_2O_2 can be degraded to water and oxygen by enzymes such as catalase and glutathione peroxidase, which generates reduced glutathione (GSH).

Most free radicals are extremely short-lived, but they readily extract electrons from other molecules, converting them to free radicals and thereby initiating a chain reaction[115]. The random nature of free-radical attacks makes it difficult to characterize their reaction products, but all classes of biological molecules are susceptible to oxidative damage caused by ROS. ROS production can induce tissue damage through DNA and protein modifications and lead to endothelial injury and tissue hypoxia due to loss of vasodilation[110]. Because mitochondria are the major site of cellular oxidative metabolism, its lipids, DNA and proteins bear the brunt of ROS-related damage[116]. Many neurodegenerative diseases including Parkinson's, Alzheimer's and Huntington's diseases are associated with oxidative damage to mitochondria[117]. Such observations have led to the "free radical theory" of aging, which holds that reaction of free-radicals arising from oxidative metabolism are at least partially responsible for the aging process[93].

Mitochondrial Damage through Oxidative Stress

Although the contribution from individual sources may vary, mitochondrial oxidative phosphorylation (OxPhos) is the primary site of ROS production in most mammalian cells. As discussed above, all cells including neurons have the capacity to neutralize ROS under normal conditions via antioxidants. However, in diabetes, intracellular hyperglycemia increases mitochondrial activity leading to a surplus production of ROS. The buildup of ROS in neurons, coupled with the depletion of reducing equivalents as a result of activation of other metabolic and inflammatory pathways (Figure 1-2), eventually overwhelms the endogenous antioxidant reserves

leading to the damage of cellular proteins, DNA, membranes, organelles and neuronal function[116]. Given the typical distal-to-proximal progression of DPN, DRG sensory and motor neurons are especially vulnerable to damage because of their long – up to 1 meter in length – mitochondria-rich axon that directly accesses the nerve blood supply[118]. As a result, axonal mitochondria support a tremendous energy demand and become a primary source of ROS production [119]. Swollen mitochondria, disruption of internal cristae or, in some cases, shrinkage of organelles is observed in human diabetic nerve and skeletal muscle[120-122]. Similar structural abnormalities in mitochondria have been described in SCs of galactose-fed rats and in DRG neurons of long-term STZ-diabetic animals[123-124]. Ultrastructural analysis of the neuromuscular junction of short-term STZ-diabetic mice showed ballooning mitochondrial structure in nerve endings with altered cristae formation[125]. Collectively, these data suggest that an elevated rate of OxPhos increases oxidative stress and mitochondrial injury in DRG neurons and contributes to the pathogenesis of DPN.

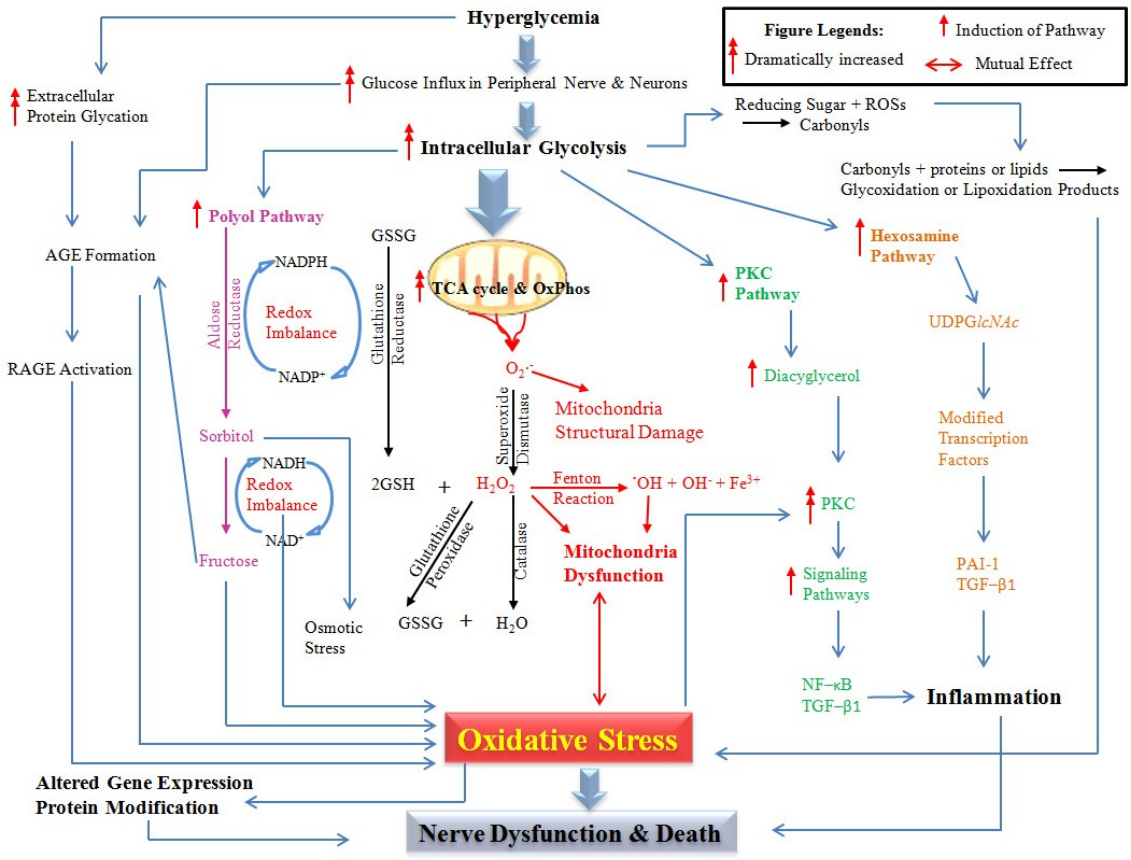

Figure 1-2 Schematic of hyperglycemic effects on biochemical pathways in DPN. A combination of hyperglycemic and oxidative stress activate the detrimental pathways such as AGE, polyol, hexosamine and PKC which lead to redox imbalance, gene expression disturbances, and further oxidative stress. These pathways also induce inflammation and neuronal dysfunction, contributing to axonal degeneration and impaired nerve re-innervation. Abbreviations: *NF- κB* nuclear factor kappa B, *PKC* protein kinase C, *AGE* advance glycation endproducts, *ROS* reactive oxygen species *GSH* glutathione, *GSSG* oxidized glutathione, *UDPGlcNAc* UDP-*N*-acetylglucosamine. (Modified from Figueroa-Romero *et al.* Rev Endocr Disord, 2008 9: 301-314)

Mitochondrial Dysfunction in Diabetic Neuropathy

There is mounting evidence indicating that hyperglycemia-induced mitochondria dysfunction caused by defects in energy metabolism and oxidative damage in peripheral neurons contributes to the pathogenesis of DPN. The modes of anatomical abnormalities and functional degeneration in DPN, however, have yet to be fully elucidated.

As the primary site of ROS formation, mitochondrial DNA (mtDNA), proteins and membrane are susceptible to oxidative modifications which ultimately compromise mitochondria function. Neuronal mtDNA is more prone to oxidative damage than that in glial cells[126]. Though little is known about the role of oxidative damage to mtDNA in DPN, analysis of patients with dominant optic atrophy, an axonopathy that shares pathological features with DPN, showed decreased neuronal mtDNA content[127]. Reduced antioxidants as a result of oxidative stress have been shown to destabilize mtDNA and prevent cAMP responsive element-binding protein (CREB)-mediated transcription in mitochondria[128]. As mtDNA encodes 13 essential protein subunits of the mitochondrial respiratory chain complexes, disruption of mtDNA will inevitably impair OxPhos activity, leading to energy failure. In fact, depolarization of mitochondrial membrane potential ($\Delta\Psi_m$) and depletion of high-energy phosphorylated intermediates have been reported in diabetic animals, supporting the view that ATP production by the mitochondria in diabetes is sub-optimal[129-132]. Several lines of evidence imply that the loss of $\Delta\Psi_m$ may be associated with mitochondria-mediated apoptosis in DPN. Studies in diabetic rats have demonstrated that elevated $\Delta\Psi_m$, along with decreased Bcl-2 levels and translocation of cytochrome *c*, increased apoptosis in both intact and acutely dissociated DRG neurons as early as 3 weeks after induction of diabetes[133]. Although few cell bodies

undergo apoptotic death, both *in vivo* and *in vitro* models of diabetes have shown caspase-mediated apoptosis along with ROS production and mitochondria dysfunction[73,130,134-135]. However, apoptotic death of neurons is not considered to substantially contribute to the pathogenesis of DPN.

Mitochondria have been reported to accumulate in demyelinated axonal segments and in regions of disrupted axo-glial junctions in pathologic states[118]. It is possible that prior to cellular apoptosis, hyperglycemia induces a local apoptotic program via damaged mitochondria at the axonal level. A shift in mitochondrial dynamics towards metabolic fission, yielding clumps of small, non-functional mitochondria may lead to the 'dying back' of axons with apoptotic feature[118]. This is evident by an increase in dynamin related protein 1 (Drp1), which initiates metabolic fission at times of stress, at mitochondria in models of diabetic neuropathy[136-138].

In summary, the injury cascade through oxidative stress and mitochondrial dysfunction outlined above suggest that DPN precipitates from an interaction and intersection of multiple pathways and mechanisms. Hence, potential therapeutic interventions may need to be directed at multiple pathogenic targets. Alternatively, we have proposed that the management of DPN may benefit from upregulating a broadly cytoprotective response in peripheral nerve. Induction of molecular chaperones promotes a pro-survival heat shock response that has been shown to be protective in neurodegenerative diseases and may also be applicable in the case of DPN.

1.7 Heat Shock Protein & Neurodegenerative Diseases

Accumulation of misfolded proteins concomitant with a decrease in proteasomal activity and altered functional capacity of molecular chaperones are considered a result of normal aging[139]. Nevertheless, many systemic and neurodegenerative diseases fall into a class of "protein-misfolding disorders", or "protein-conformational disorders"[140]. Post-mitotic cells such as neurons are particularly vulnerable to the detrimental effects of damaged proteins as they are less efficient in selectively degrading and replacing damaged proteins. This is evidenced by the accumulation of lipofusion inside the lysosomal compartment of post-mitotic cells which suggests an overload of normal chaperone capacity. Compromised lysosomal degradative capacity prevents efficient mitochondrial recycling, leading to irreversible functional decay and cell death[141]. Thus, promoting neuroprotection through induction of chaperone expression to help solubilize or clear protein aggregates become a rational therapeutic strategy. A detailed understanding of chaperone-mediated protection and its therapeutic potential against protein misfolding and aggregation are reviewed in this section.

Molecular Chaperones & Protein Folding

Of all the molecules found in living organisms, proteins are the most important biological workhorses that carry out vital functions in every cell. To accomplish their tasks, proteins must fold into a complex three-dimensional structure. Although the amino acid sequence of a protein may provide the blueprint that dictates proper folding, the crowded (300 mg/ml protein) intracellular milieu places constraints on such ordered protein folding, thereby promoting misfolding and aggregation[142]. To protect cells from the stress of misfolded proteins and guide proteins to their native states, molecular

chaperones are the first-line of supervision. Molecular chaperones selectively bind to nascent polypeptides and partially folded intermediates, prevent premature aggregation and misfolding of *de novo* protein and promote the refolding or targeted degradation of damaged proteins[140]. Molecular chaperones are an indispensable part of protein folding, targeting, transport, degradation and signal transduction[143].

In general, molecular chaperones are ubiquitous, highly conserved proteins, which function in a nucleotide-dependent manner, with an ATP-coupled conformational change to refold the substrate proteins[142]. While some chaperones are constitutively expressed, a subset of chaperones known as heat shock proteins (Hsps) are regulated by environmental and physiological stresses [144]. The Hsps are classified into six main families based on their molecular mass (in kDa): Hsp100, Hsp90, Hsp70, Hsp60, Hsp40 and small Hsps which weigh less than 40 kDa. While Hsps may be differentially expressed in tissues and subcellular compartments, Hsp90 has been shown to play an essential role in maintaining the functional stability and viability of cells under stress. Specifically, Hsp90 promotes protein disaggregation and degradation through regulation of the transcription factor, heat shock factor-1 (HSF-1).

In resting cells, Hsp90 binds to HSF-1 and maintains its inactive form in a monomeric state. During a protein damaging stress, heat shock or inhibition of Hsp90, HSF-1 is released from the cytoplasmic chaperone/HSF-1 complex[145]. The activation of HSF-1 proceeds through a multi-step pathway involving trimerization and phosphorylation, followed by its nuclear translocation. The HSF-1 trimer binds to heat shock elements present in the promoters of heat shock genes and initiates a heat shock response (HSR), manifested in part by the production of Hsp70, Hsp40 and other

chaperones[145-146]. Recent evidence implicates that pharmacological inhibition of Hsp90 modulates aberrant protein interactions through an HSF-1-dependent stress response[147]. Thus, regulating chaperone expression through Hsp90 inhibition has become a promising therapeutic target for protein conformational disorders.

Modulation of Hsp90 & Hsp70 in Neurodegenerative Disorders

In response to many metabolic disturbances and injuries, cells mount a stress response via the induction of a variety of chaperones, most notably Hsp70. Given that Hsp70 is usually not detectable under normal conditions in many cells, its induction suggests an upstream regulation by an Hsp90-mediated stress response. Induction of Hsp70 via pharmacological inhibition of Hsp90 is well-documented in models of stroke, neurodegenerative disease and diabetes and forms a powerful endogenous protective system[148-150]. Geldanamycin (GM), the first Hsp90 specific inhibitor, can decrease mis-folded proteins and protein aggregates in models of neurodegeneration and stroke, through an HSF-1-dependent stress response. Specifically, GM-mediated Hsp90 inhibition increased expression of Hsp70 and disaggregated mutant tau and improved binding of tau to microtubules in a cell model of Alzheimer's disease[151]. A more potent derivative of GM, 17-AAG, showed similar results where induction of Hsp70 correlated with degradation of mutant androgen receptor in polyglutamine diseases[152]. Besides GM's efficacy in neurodegeneration, induction of Hsp70 by GM also protects neural and cardiac cells against ischemic and toxic stress both *in vitro* and *in vivo*[153-154]. Additional studies, independent of Hsp90 inhibition, have confirmed the beneficial effects of Hsp70 induction in different models of nerve injury. Arimoclomol, a nontoxic Hsp60/Hsp70 co-inducer, has been shown to protect acute injury-induced and progressive motor-neuron

degeneration in mouse models of amyotrophic lateral sclerosis (ALS)[155]. Muchowski *et al* found that Hsp70 and its co-chaperone Hsp40 suppressed oligomerization of mutant huntingtin and attenuated the formation of detergent-insoluble amyloid-like fibrils in a cellular model of Huntington's disease[156]. These studies suggest that the primary protective mechanism of Hsp70 is related to its chaperone function by promoting disaggregation of proteins, but other mechanisms have also been proposed.

There might also be a relationship between protection by Hsp70 and oxidative injury. Work by Polla and co-workers showed that Hsp70 induction protects cells from H_2O_2-induced alteration of $\Delta\Psi_m$[157]. Similar observations were made in cultured glial cells where over-expression of Hsp70 increased glutathione levels and protected the cells from the H_2O_2, suggesting that Hsp70 might also protect antioxidant mechanisms[158]. Additionally, transgenic mice over-expressing Cu-Zn SOD (SOD1) showed prolonged expression of Hsp70 mRNA after focal and global ischemia in comparison to control[159-160]. Though the specific reason for this observation is unknown, altered oxidative stress with SOD1 over-expression may potentiate the expression of Hsp70.

Overall, these studies support the hypothesis that the stress response provides an organism with a cellular process for self-preservation. Hence, capitalizing on the natural cellular response to stress becomes an attractive therapeutic target for diseases that have multifactorial origins, such as DPN.

1.8 Dissertation Hypothesis

Despite the prevalence and severity of DPN, current therapeutic approaches focusing on "diabetic specific" targets/pathways have met with limited translational success as the disease progression differs among individuals and does not occur with biochemical uniformity. As reviewed above, the pathogenesis of DPN converges at mitochondrial dysfunction and oxidative stress-induced damage and resembles similar triggers seen in other neurodegenerative diseases. Although the etiology of DPN is not causally linked to the accrual of any one specific mis-folded or aggregated protein, hyperglycemia can trigger oxidative modification of amino acids and increase glycation and oxidative stress that can contribute to protein aggregation[161-162]. Thus, regulating chaperone expression in the context of DPN (Scheme 1-1) may mimic the broad cytoprotective effect seen in models of neurodegeneration. In fact, in its early phase of development, Arimoclomol (formerly known as BRX220), increased both insulin sensitivity and glutathione peroxidase activity, induced Hsp60 and Hsp70 and improved NCV, in diabetic animals[163-164]. Our lab has previously found that KU-32, a novobiocin-derived small molecule inhibitor of Hsp90, effectively reversed preexisting sensory and electrophysiologic deficits of DPN in diabetic mice[165]. Mechanistically, Hsp70 plays a central role in the neuroprotective efficacy of KU-32 as the drug was ineffective at reversing sensory deficits in diabetic Hsp70.1 and Hsp70.3 double knockout mice[165]. Evidence from these studies suggests that chaperone induction can promote a broad cytoprotective response that may be more efficacious against hyperglycemic insults than a highly selective single-target drug in DPN.

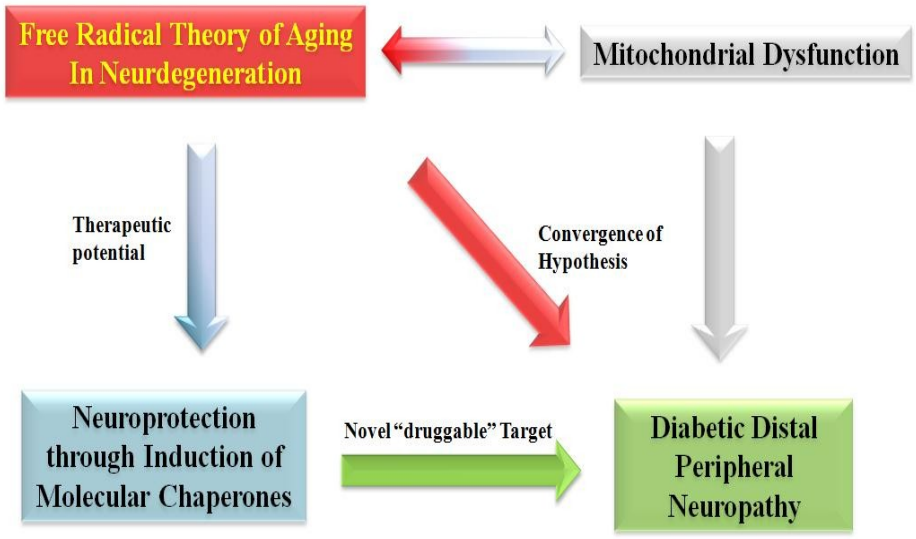

Scheme 1-1. Induction of molecular chaperones may be used as a novel drug target in DPN. Given that the free radical theory of aging converges with mechanisms contributing to the etiology of DPN, the neuroprotective effects of chaperone induction reported from neurodegenerative disease studies may also be applicable in the context of DPN. Moreover, the broad cytoprotective response from chaperone induction is indiscriminate against the biochemical inconsistency of disease progression in patients with DPN. Thus, pharmacological induction of molecular chaperones may be an attractive, novel, "druggable" target to treat DPN.

With the deleterious effect of hyperglycemia, this dissertation aimed at systematically characterizing and antagonizing the effect of hyperglycemia on mitochondrial function in the peripheral nervous system, namely DRG sensory neurons and SCs, by inducing chaperone expressions using KU-32. Specifically, this dissertation is divided into three areas of studies:

1. Using stable isotope labeling of cells in culture (SILAC) as an unbiased and systematic assessment to study the effect of hyperglycemia on the mitochondrial proteome in DRG neurons and SCs.
2. To antagonize hyperglycemic stress and promote neuroprotection in sensory neurons via pharmacological induction of chaperones using KU-32, a C-terminal Hsp90 inhibitor.
3. Enhance the neuroprotective properties of KU-32 by improving its interaction with the C-terminal Hsp90 binding site through structural modification.

In this dissertation, we have chosen SILAC as an unbiased, quantitative approach to systematically study the effect of hyperglycemia in neurons and glial cells on a molecular level. The rationale for choosing SILAC in this dissertation is reviewed below.

Stable Isotope Labeling Using Amino Acids in Cell Culture (SILAC) - An Unbiased, Quantitative Proteomic Approach

The most important and challenging technical task in proteomics is to accurately quantify the differences between two or more physiological states of a biological system. Many techniques in mass spectrometry involve creating a specific mass tag that can be recognized and quantified by the mass spectrometer. These mass tags or quantitative

features can be introduced into proteins or peptides metabolically, chemically, or by spiked synthetic peptide standards (Figure 1-3)[166]. In general, early introduction of quantitative features into the biological samples reduces the likelihood for quantification errors to occur. In contrast, label-free quantification approaches aim to compare the mass spectrometric intensity of the proteolytic peptides between two samples directly, but harbor a higher chance of quantification errors as no internal control is available.

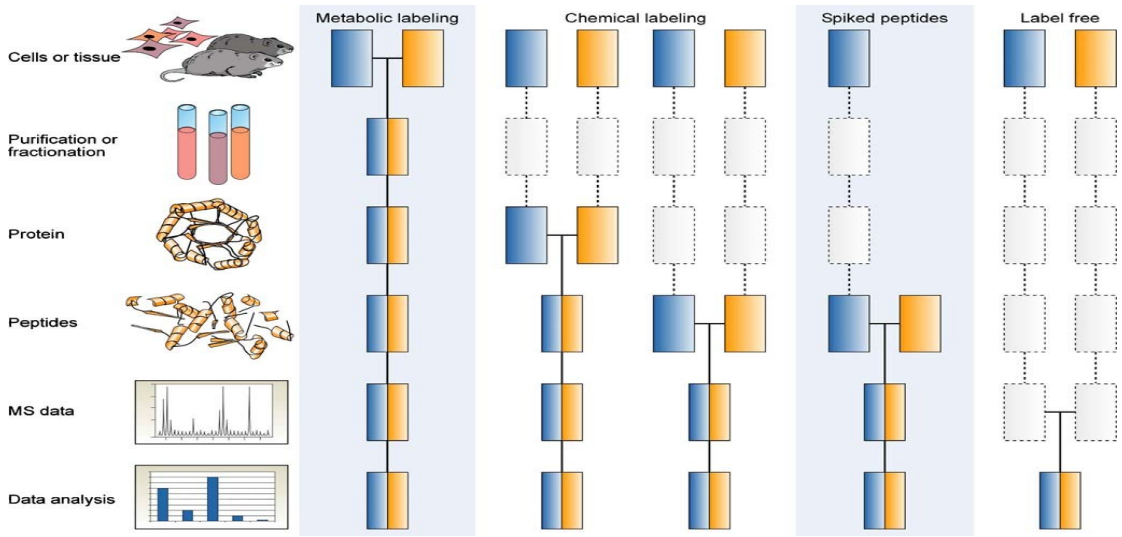

Figure 1-3. Common quantitative mass spectrometry workflows. Boxes in blue and yellow represent two experimental conditions. Horizontal lines indicate when samples are combined. Dashed lines indicate points at which experimental variation and thus quantification errors can occur. (Adapted from Bantscheff *et al.* Anal Bioanal Chem (2007) 389:1017–1031)

SILAC is a metabolic-based technique that has been used extensively to quantify relative protein changes in organellar proteomes. A specific essential amino acid in the media such as ^{12}C-Lys, is replaced by a non-radioactive, isotopically labeled form, $^{13}C_6$-Lys. Two distinct cell populations are supplied media containing the different isotopically labeled forms of lysine and the labels are metabolically incorporated into newly synthesized proteins during cell divisions. After the labeling period, one population of the cells serves as control while the other is subjected to treatment. After harvesting, protein populations from control and experimental samples are mixed directly in a 1:1 mass ratio, processed and analyzed by mass spectrometry. The molecular weight difference between the ^{12}C-Lys and $^{13}C_6$-Lys labeled proteins is 6 Da. The relative protein abundance in the mixture is then measured as the differential intensity between ^{12}C-Lys and $^{13}C_6$-Lys peptide fragments in the mass spectra. Generally, only incorporation of >95% is considered acceptable given that the labeled amino acid is the only available source for protein synthesis during incorporation. This level of incorporation can be achieved by doubling of cell population and calculated using $(1 - 0.5^n)$, where n denotes the number of population doublings[167]. As primary SCs readily undergo multiple population doublings before they begin to phenotypically change, we used SILAC to characterize the effect of hyperglycemia on the SC proteome and determine how changes in the proteome affected functional measures of oxidative stress and mitochondrial bioenergetics (Chapter 2). However, this "standard" SILAC method is not suitable for neurons.

Unlike dividing cells, neurons are post-mitotic cells and hence stable isotope incorporation can only be achieved by the rate of protein turnover[168]. We tracked the

levels of label incorporation in individual proteins in DRG neurons for up to 4 weeks (Figure 1-4). Despite the fact that the majority of proteins do indeed achieve significant levels of isotopic labeling, a subpopulation of the total quantified proteins was always partially labeled with less than 95% of incorporation. The partially labeled protein can contribute to the quantification inaccuracy and hence, this dissertation employed a variation of SILAC, pulsed SILAC (pSILAC) as an alternative approach to study changes in the sensory neuron proteome. Pulse-labeling with stable isotope has been used to measure protein turnover rates and can directly quantify the rate of protein translation on a proteome wide scale[169]. Thus, pSILAC was employed to study the effect of hyperglycemia and KU-32 on DRG sensory neurons and determine how these changes in protein expression affected functional measures of oxidative stress and mitochondrial bioenergetics (Chapter 3).

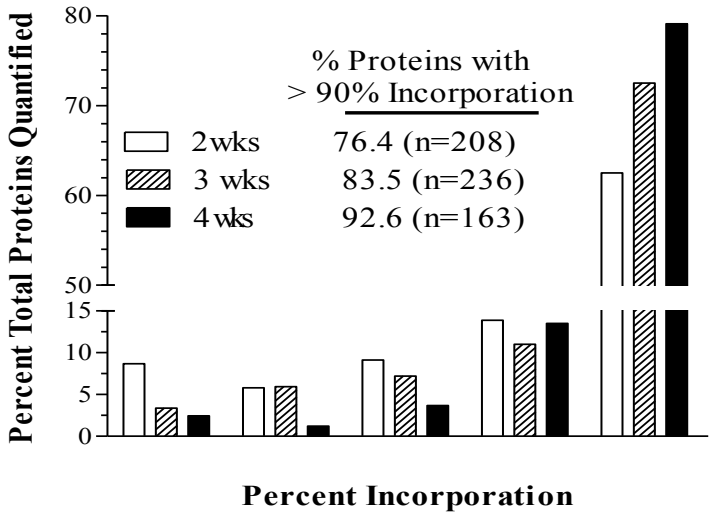

Figure 1-4. Isotopic enrichment increased with duration of incorporation but did not reach equilibrium labeling. The DRG neurons were maintained and labeled in SILAC media for up to 4weeks. Analysis of the proteome shows that only around 80% of the total protein quantified with 4 weeks of labeling has reached over 95% of SILAC incorporation.

References

1. Harris, M.I. Chapter 1 Summary Diabetes in America. *Diabetes in America, 2nd Edition* **110**, 1-15 (1995).
2. Zimmet, P., Alberti, K. & Shaw, J. Global and societal implications of the diabetes epidemic. *Nature* **414**, 782-787 (2001).
3. IDF. http://www.idf.org/diabetesatlas/5e/the-global-burden. (2011).
4. CDC. 2011 National Diabetes Fact Sheet. *Diabetes Public Health Resource* (2011).
5. NIDDK. http://diabetes.niddk.nih.gov/dm/pubs/diagnosis/index.aspx. (2012).
6. Authors, M. NIH publishes 2nd edition of "Diabetes in America". *Public Health Reports* **110**, 653-654 (1995).
7. WHO-IDF. Definition and diagnosis of diabetes mellitus and intermediate hyperglycemia. (2006).
8. Harris, M.I. Chapter 2 Classification, Diagnostic Criteria, and Screening for Diabetes. *Diabetes in America, 2nd Edition*, 15-36 (1995).
9. Knip, M.*, et al.* Environmental Triggers and Determinants of Type 1 Diabetes. *Diabetes* **54**, S125-S136 (2005).
10. Association, A.D. Diagnosis and Classification of Diabetes Mellitus. *Diabetes Care* **33**, S62-S69 (2010).
11. Unger, R.H. & Grundy, S. HYPERGLYCEMIA AS AN INDUCER AS WELL AS A CONSEQUENCE OF IMPAIRED ISLET CELL-FUNCTION AND INSULIN RESISTANCE - IMPLICATIONS FOR THE MANAGEMENT OF DIABETES. *Diabetologia* **28**, 119-121 (1985).
12. Poitout, V. & Robertson, R.P. Glucolipotoxicity: Fuel Excess and β-Cell Dysfunction. *Endocrine Reviews* **29**, 351-366 (2008).
13. Ben-Haroush, A., Yogev, Y. & Hod, M. Epidemiology of gestational diabetes mellitus and its association with Type 2 diabetes. *Diabetic Medicine* **21**, 103-113 (2004).
14. Committee, T.I.E. International Expert Committee Report on the Role of the A1C Assay in the Diagnosis of Diabetes. *Diabetes Care* **32**, 1327-1334 (2009).
15. Association, A.D. Economic Costs of Diabetes in the U.S. in 2007. *Diabetes Care* **31**, 596-615 (2008).
16. Palumbo, H.F.a.P.J. Chapter 13 Acute Metabolic Complications in Diabetes. *Diabetes in America, 2nd Edition*, 283-292 (1995).
17. Fowler, M.J. Microvascular and Macrovascular Complications of Diabetes. *Clinical Diabetes* **26**, 77-82 (2008).
18. DCCT. The Effect of Intensive Treatment of Diabetes on the Development and Progression of Long-Term Complications in Insulin-Dependent Diabetes Mellitus. *New England Journal of Medicine* **329**, 977-986 (1993).
19. UKPDS33. Intensive blood-glucose control with sulphonylureas or insulin compared with conventional treatment and risk of complications in patients with type 2 diabetes (UKPDS 33). *The Lancet* **352**, 837-853 (1998).
20. Beckman, J.A., Creager, M.A. & Libby, P. Diabetes and Atherosclerosis. *JAMA: The Journal of the American Medical Association* **287**, 2570-2581 (2002).
21. Boyle, P.J. Diabetes Mellitus and Macrovascular Disease: Mechanisms and Mediators. *The American Journal of Medicine* **120**, S12-S17 (2007).
22. Stratton, I.M.*, et al.* Association Of Glycaemia With Macrovascular And Microvascular Complications Of Type 2 Diabetes (UKPDS 35): Prospective Observational Study. *BMJ: British Medical Journal* **321**, 405-412 (2000).

23. Holman, R.R., Paul, S.K., Bethel, M.A., Matthews, D.R. & Neil, H.A.W. 10-Year Follow-up of Intensive Glucose Control in Type 2 Diabetes. *New England Journal of Medicine* **359**, 1577-1589 (2008).
24. Selvin, E.*, et al.* Meta-Analysis: Glycosylated Hemoglobin and Cardiovascular Disease in Diabetes Mellitus. *Annals of Internal Medicine* **141**, 421-W-481 (2004).
25. Cao, J.J., Hudson, M., Jankowski, M., Whitehouse, F. & Weaver, W.D. Relation of Chronic and Acute Glycemic Control on Mortality in Acute Myocardial Infarction With Diabetes Mellitus. *The American Journal of Cardiology* **96**, 183-186 (2005).
26. Watkins, P.J. Abc Of Diabetes: Retinopathy. *BMJ: British Medical Journal* **326**, 924-926 (2003).
27. Fong, D.S., Aiello, L.P., Ferris, F.L. & Klein, R. Diabetic Retinopathy. *Diabetes Care* **27**, 2540-2553 (2004).
28. Adler, A.I.*, et al.* Development and progression of nephropathy in type 2 diabetes: The United Kingdom Prospective Diabetes Study (UKPDS 64). *Kidney Int* **63**, 225-232 (2003).
29. Niskanen, L.K., Penttilã, I., Parviainen, M. & Uusitupa, M.I.J. Evolution, Risk Factors, and Prognostic Implications of Albuminuria in NIDDM. *Diabetes Care* **19**, 486-493 (1996).
30. Gross, J.L.*, et al.* Diabetic Nephropathy: Diagnosis, Prevention, and Treatment. *Diabetes Care* **28**, 164-176 (2005).
31. Eastman, R.C. Chapter 15 Neuropathy in Diabetes. *Diabetes in America, 2nd Edition*, 339-348 (1995).
32. Duby, J.J., Campbell, R.K., Setter, S.M., White, J.R. & Rasmussen, K.A. Diabetic neuropathy: An intensive review. *American Journal of Health-System Pharmacy* **61**, 160-173 (2004).
33. Boulton, A.J.M.*, et al.* Diabetic Neuropathies. *Diabetes Care* **28**, 956-962 (2005).
34. Vinik, A.I., Park, T.S., Stansberry, K.B. & Pittenger, G.L. Diabetic neuropathies. *Diabetologia* **43**, 957-973 (2000).
35. Dobretsov, M., Romanovsky, D. & Stimers, J.R. Early diabetic neuropathy: Triggers and mechanisms. *World Journal of Gastroenterology* **13**, 175-191 (2007).
36. Sugimoto, K., Murakawa, Y. & Sima, A.A.F. Diabetic neuropathy - a continuing enigma. *Diabetes-Metabolism Research and Reviews* **16**, 408-433 (2000).
37. Perkins, B.A., Greene, D.A. & Bril, V. Glycemic control is related to the morphological severity of diabetic sensorimotor polyneuropathy. *Diabetes Care* **24**, 748-752 (2001).
38. TOTH, C., BRUSSEE, V., CHENG, C. & ZOCHODNE, D.W. Diabetes Mellitus and the Sensory Neuron. *Journal of Neuropathology & Experimental Neurology* **63**, 561-573 (2004).
39. Kennedy, J.M. & Zochodne, D.W. Impaired peripheral nerve regeneration in diabetes mellitus. *Journal of the Peripheral Nervous System* **10**, 144-157 (2005).
40. Shun, C.T.*, et al.* Skin denervation in type 2 diabetes: correlations with diabetic duration and functional impairments. *Brain* **127**, 1593-1605 (2004).
41. Cameron, N.E., Eaton, S.E.M., Cotter, M.A. & Tesfaye, S. Vascular factors and metabolic interactions in the pathogenesis of diabetic neuropathy. *Diabetologia* **44**, 1973-1988 (2001).
42. Yagihashi, S., Kamijo, M., Ido, Y. & Mirrlees, D.J. EFFECTS OF LONG-TERM ALDOSE REDUCTASE INHIBITION ON DEVELOPMENT OF EXPERIMENTAL DIABETIC NEUROPATHY - ULTRASTRUCTURAL AND MORPHOMETRIC STUDIES OF SURAL NERVE IN STREPTOZOCIN-INDUCED DIABETIC RATS. *Diabetes* **39**, 690-696 (1990).

43. Mizisin, A.P., Calcutt, N.A., Tomlinson, D.R., Gallagher, A. & Fernyhough, P. Neurotrophin-3 reverses nerve conduction velocity deficits in streptozotocin-diabetic rats. *Journal of the Peripheral Nervous System* **4**, 211-221 (1999).
44. Zochodne, D.W. Neurotrophins and other growth factors in diabetic neuropathy. *Seminars in Neurology* **16**, 153-161 (1996).
45. Liuzzi, F.J., Bufton, S.M. & Vinik, A.I. Streptozotocin-induced diabetes mellitus causes changes in primary sensory neuronal cytoskeletal mRNA levels that mimic those caused by axotomy. *Experimental Neurology* **154**, 381-388 (1998).
46. Dyck, P.J. & Giannini, C. Pathologic alterations in the diabetic neuropathies of humans: A review. *Journal of Neuropathology and Experimental Neurology* **55**, 1181-1193 (1996).
47. Britland, S.T., Young, R.J., Sharma, A.K. & Clarke, B.F. ASSOCIATION OF PAINFUL AND PAINLESS DIABETIC POLYNEUROPATHY WITH DIFFERENT PATTERNS OF NERVE-FIBER DEGENERATION AND REGENERATION. *Diabetes* **39**, 898-908 (1990).
48. Mendell, J.R. & Sahenk, Z. Painful Sensory Neuropathy. *New England Journal of Medicine* **348**, 1243-1255 (2003).
49. Max, M.B.*, et al.* Effects of Desipramine, Amitriptyline, and Fluoxetine on Pain in Diabetic Neuropathy. *New England Journal of Medicine* **326**, 1250-1256 (1992).
50. Dyck, P.J.*, et al.* THE PREVALENCE BY STAGED SEVERITY OF VARIOUS TYPES OF DIABETIC NEUROPATHY, RETINOPATHY, AND NEPHROPATHY IN A POPULATION-BASED COHORT - THE ROCHESTER DIABETIC NEUROPATHY STUDY. *Neurology* **43**, 817-824 (1993).
51. Macleod, A.F.*, et al.* A MULTICENTER TRIAL OF THE ALDOSE-REDUCTASE INHIBITOR TOLRESTAT, IN PATIENTS WITH SYMPTOMATIC DIABETIC PERIPHERAL NEUROPATHY. *Diabetes & Metabolism* **18**, 14-20 (1992).
52. Didangelos, T.P., Karamitsos, D.T., Athyros, V.G. & Kourtoglou, G.I. Effect of aldose reductase inhibition on cardiovascular reflex tests in patients with definite diabetic autonomic neuropathy over a period of 2 years. *Journal of Diabetes and Its Complications* **12**, 201-207 (1998).
53. Greene, D.A., Arezzo, J.C., Brown, M.B. & Zenarestat Study, G. Effect of aldose reductase inhibition on nerve conduction and morphometry in diabetic neuropathy. *Neurology* **53**, 580-591 (1999).
54. Sima, A.A.F., Prashar, A., Zhang, W.X., Chakrabarti, S. & Greene, D.A. PREVENTIVE EFFECT OF LONG-TERM ALDOSE REDUCTASE INHIBITION (PONALRESTAT) ON NERVE-CONDUCTION AND SURAL NERVE STRUCTURE IN THE SPONTANEOUSLY DIABETIC BIO-BREEDING RAT. *Journal of Clinical Investigation* **85**, 1410-1420 (1990).
55. Kihara, M.*, et al.* AMINOGUANIDINE EFFECTS ON NERVE BLOOD-FLOW, VASCULAR-PERMEABILITY, ELECTROPHYSIOLOGY, AND OXYGEN FREE-RADICALS. *Proceedings of the National Academy of Sciences of the United States of America* **88**, 6107-6111 (1991).
56. Yagihashi, S., Kamijo, M., Baba, M., Yagihashi, N. & Nagai, K. EFFECT OF AMINOGUANIDINE ON FUNCTIONAL AND STRUCTURAL ABNORMALITIES IN PERIPHERAL-NERVE OF STZ-INDUCED DIABETIC RATS. *Diabetes* **41**, 47-52 (1992).
57. Cameron, N.E., Cotter, M.A., Dines, K. & Love, A. EFFECTS OF AMINOGUANIDINE ON PERIPHERAL-NERVE FUNCTION AND POLYOL PATHWAY METABOLITES IN STREPTOZOTOCIN-DIABETIC RATS. *Diabetologia* **35**, 946-950 (1992).

58. Goova, M.T., *et al.* Blockade of Receptor for Advanced Glycation End-Products Restores Effective Wound Healing in Diabetic Mice. *The American Journal of Pathology* **159**, 513-525 (2001).
59. Park, L., *et al.* Suppression of accelerated diabetic atherosclerosis by the soluble receptor for advanced glycation endproducts. *Nat Med* **4**, 1025-1031 (1998).
60. Jamal, G.A. & Carmichael, H. THE EFFECT OF GAMMA-LINOLENIC ACID ON HUMAN DIABETIC PERIPHERAL NEUROPATHY - A DOUBLE-BLIND PLACEBO-CONTROLLED TRIAL. *Diabetic Medicine* **7**, 319-323 (1990).
61. Wolever, T.M.S. Comments on "Treatment of diabetic neuropathy with γ-linolenic acid" by The γ-Linolenic Multicenter Trial Group. *Diabetes Care* **16**, 1309 (1993).
62. Nagamatsu, M., *et al.* LIPOIC ACID IMPROVES NERVE BLOOD-FLOW, REDUCES OXIDATIVE STRESS, AND IMPROVES DISTAL NERVE-CONDUCTION IN EXPERIMENTAL DIABETIC NEUROPATHY. *Diabetes Care* **18**, 1160-1167 (1995).
63. Haugaard, N. & Haugaard, E.S. STIMULATION OF GLUCOSE UTILIZATION BY THIOCTIC ACID IN RAT DIAPHRAGM INCUBATED IN-VITRO. *Biochimica Et Biophysica Acta* **222**, 583-& (1970).
64. Jacob, S., *et al.* The antioxidant alpha-lipoic acid enhances insulin-stimulated glucose metabolism in insulin-resistant rat skeletal muscle. *Diabetes* **45**, 1024-1029 (1996).
65. Ziegler, D. & Gries, F.A. alpha-lipoic acid in the treatment of diabetic peripheral and cardiac autonomic neuropathy. *Diabetes* **46**, S62-S66 (1997).
66. Ziegler, D., *et al.* Effects of treatment with the antioxidant alpha-lipoic acid on cardiac autonomic neuropathy in NIDDM patients - A 4-month randomized controlled multicenter trial (DEKAN study). *Diabetes Care* **20**, 369-373 (1997).
67. Ziegler, D., *et al.* Treatment of symptomatic diabetic polyneuropathy with the antioxidant alpha-lipoic acid - A 7-month multicenter randomized controlled trial (ALADIN III Study). *Diabetes Care* **22**, 1296-1301 (1999).
68. Reljanovic, M., *et al.* Treatment of diabetic polyneuropathy with the antioxidant thioctic acid (alpha-lipoic acid): A two year multicenter randomized double-blind placebo-controlled trial (ALADIN II). *Free Radical Research* **31**, 171-179 (1999).
69. Apfel, S.C. & Kessler, J.A. NEUROTROPHIC FACTORS IN THE THERAPY OF PERIPHERAL NEUROPATHY. *Baillieres Clinical Neurology* **4**, 593-606 (1995).
70. Apfel, S.C., *et al.* Recombinant human nerve growth factor in the treatment of diabetic polyneuropathy. *Neurology* **51**, 695-702 (1998).
71. Dyck, P.J., *et al.* Intradermal recombinant human nerve growth factor induces pressure allodynia and lowered heat-pain threshold in humans. *Neurology* **48**, 501-505 (1997).
72. Sima, A.A.F. PERIPHERAL NEUROPATHY IN THE SPONTANEOUSLY DIABETIC BB-WISTAR-RAT - AN ULTRASTRUCTURAL-STUDY. *Acta Neuropathologica* **51**, 223-227 (1980).
73. Russell, J.W., Sullivan, K.A., Windebank, A.J., Herrmann, D.N. & Feldman, E.L. Neurons undergo apoptosis in animal and cell culture models of diabetes. *Neurobiology of Disease* **6**, 347-363 (1999).
74. Magnani, P., *et al.* Regulation of glucose transport in cultured Schwann cells. *Journal of the Peripheral Nervous System* **3**, 28-36 (1998).
75. Patel, N.J., Llewelyn, J.G., Wright, D.W. & Thomas, P.K. Glucose and leucine uptake by rat dorsal root ganglia is not insulin sensitive. *Journal of the Neurological Sciences* **121**, 159-162 (1994).
76. Muona, P., Sollberg, S., Peltonen, J. & Uitto, J. GLUCOSE TRANSPORTERS OF RAT PERIPHERAL-NERVE - DIFFERENTIAL EXPRESSION OF GLUT1 GENE BY SCHWANN-CELLS AND PERINEURIAL CELLS INVIVO AND INVITRO. *Diabetes* **41**, 1587-1596 (1992).

77. Tomlinson, D.R. & Gardiner, N.J. Glucose neurotoxicity. *Nature Reviews Neuroscience* **9**, 36-45 (2008).
78. Bell, G.I.*, et al.* MOLECULAR-BIOLOGY OF MAMMALIAN GLUCOSE TRANSPORTERS. *Diabetes Care* **13**, 198-208 (1990).
79. Magnani, P.*, et al.* Glucose transporters in rat peripheral nerve: Paranodal expression of GLUT1 and GLUT3. *Metabolism-Clinical and Experimental* **45**, 1466-1473 (1996).
80. Eckersley, L. Role of the Schwann cell in diabetic neuropathy. *Neurobiology of Diabetic Neuropathy* **50**, 293-321 (2002).
81. Greene, D.A. & Winegrad, A.I. EFFECTS OF ACUTE EXPERIMENTAL DIABETES ON COMPOSITE ENERGY-METABOLISM IN PERIPHERAL-NERVE AXONS AND SCHWANN-CELLS. *Diabetes* **30**, 967-974 (1981).
82. Obrosova, I.G.*, et al.* Role of poly(ADP-Ribose) polymerase activation in diabetic neuropathy. *Diabetes* **53**, 711-720 (2004).
83. Vincent, A.M., Brownlee, M. & Russell, J.W. Oxidative stress and programmed cell death in diabetic neuropathy. in *Increasing Healthy Life Span: Conventional Measures and Slowing the Innate Aging Process*, Vol. 959 (ed. Harman, D.) 368-383 (2002).
84. Song, Z.T.*, et al.* Transgenic mice overexpressing aldose reductase in Schwann cells show more severe nerve conduction velocity deficit and oxidative stress under hyperglycemic stress. *Molecular and Cellular Neuroscience* **23**, 638-647 (2003).
85. Anand, P. Neurotrophins and Peripheral Neuropathy. *Philosophical Transactions: Biological Sciences* **351**, 449-454 (1996).
86. Russell, J. & Feldman, E.L. Insulin-like growth factor-I protects sensory neurons from glucotoxicity. *Annals of Neurology* **40**, M81-M81 (1996).
87. Ohi, T.*, et al.* Therapeutic effects of aldose reductase inhibitor on experimental diabetic neuropathy through synthesis/secretion of nerve growth factor. *Experimental Neurology* **151**, 215-220 (1998).
88. Eckersley, L., Ansselin, A.D. & Tomlinson, D.R. Effects of experimental diabetes on axonal and Schwann cell changes in sciatic nerve isografts. *Molecular Brain Research* **92**, 128-137 (2001).
89. Edwards, J.L., Vincent, A.M., Cheng, H.T. & Feldman, E.L. Diabetic neuropathy: Mechanisms to management. *Pharmacology & Therapeutics* **120**, 1-34 (2008).
90. Yabe-Nishimura, C. Aldose reductase in glucose toxicity: A potential target for the prevention of diabetic complications. *Pharmacological Reviews* **50**, 21-33 (1998).
91. Stewart, M.A., Sherman, W.R. & Anthony, S. FREE SUGARS IN ALLOXAN DIABETIC RAT NERVE. *Biochemical and Biophysical Research Communications* **22**, 488-& (1966).
92. Bagnasco, S., Balaban, R., Fales, H.M., Yang, Y.M. & Burg, M. PREDOMINANT OSMOTICALLY ACTIVE ORGANIC SOLUTES IN RAT AND RABBIT RENAL MEDULLAS. *Journal of Biological Chemistry* **261**, 5872-5877 (1986).
93. Figueroa-Romero, C., Sadidi, M. & Feldman, E.L. Mechanisms of disease: The oxidative stress theory of diabetic neuropathy. *Reviews in Endocrine & Metabolic Disorders* **9**, 301-314 (2008).
94. Obrosova, I.G., Fathallah, L. & Stevens, M.J. Taurine counteracts oxidative stress and nerve growth factor deficit in early experimental diabetic neuropathy. *Experimental Neurology* **172**, 211-219 (2001).
95. Kashiwagi, A.*, et al.* ABNORMAL GLUTATHIONE METABOLISM AND INCREASED CYTOTOXICITY CAUSED BY H2O2 IN HUMAN UMBILICAL VEIN ENDOTHELIAL-CELLS CULTURED IN HIGH GLUCOSE MEDIUM. *Diabetologia* **37**, 264-269 (1994).
96. Cameron, N., Cotter, M., Dines, K. & Maxfield, E. Pharmacological manipulation of vascular endothelium function in non-diabetic and streptozotocin-diabetic rats: effects on

nerve conduction, hypoxic resistance and endoneurial capillarization. *Diabetologia* **36**, 516-522 (1993).
97. Stevens, M.J., *et al.* THE LINKED ROLES OF NITRIC-OXIDE, ALDOSE REDUCTASE AND, (NA+,K+)-ATPASE IN THE SLOWING OF NERVE-CONDUCTION IN THE STREPTOZOTOCIN-DIABETIC RAT. *Journal of Clinical Investigation* **94**, 853-859 (1994).
98. Ludvigson, M.A. & Sorenson, R.L. IMMUNOHISTOCHEMICAL LOCALIZATION OF ALDOSE REDUCTASE .1. ENZYME-PURIFICATION AND ANTIBODY PREPARATION - LOCALIZATION IN PERIPHERAL-NERVE, ARTERY, AND TESTIS. *Diabetes* **29**, 438-449 (1980).
99. Ahmed, N. Advanced glycation endproducts - role in pathology of diabetic complications. *Diabetes Research and Clinical Practice* **67**, 3-21 (2005).
100. Huijberts, M.S.P., Schaper, N.C. & Schalkwijk, C.G. Advanced glycation end products and diabetic foot disease. *Diabetes/Metabolism Research and Reviews* **24**, S19-S24 (2008).
101. Singh, R., Barden, A., Mori, T. & Beilin, L. Advanced glycation end-products: a review. *Diabetologia* **44**, 129-146 (2001).
102. Karachalias, N., Babaei-Jadidi, R., Ahmed, N. & Thornalley, P.J. Accumulation of fructosyl-lysine and advanced glycation end products in the kidney, retina and peripheral nerve of streptozotocin-induced diabetic rats. *Biochemical Society Transactions* **31**, 1423-1425 (2003).
103. Schalkwijk, C.G., Stehouwer, C.D.A. & van Hinsbergh, V.W.M. Fructose-mediated non-enzymatic glycation: sweet coupling or bad modification. *Diabetes-Metabolism Research and Reviews* **20**, 369-382 (2004).
104. Sugimoto, K., Nishizawa, Y., Horiuchi, S. & Yagihashi, S. Localization in human diabetic peripheral nerve of N epsilon-carboxymethyllysine-protein adducts, an advanced glycation endproduct. *Diabetologia* **40**, 1380-1387 (1997).
105. Ryle, C., Leow, C.K. & Donaghy, M. Nonenzymatic glycation of peripheral and central nervous system proteins in experimental diabetes mellitus. *Muscle & Nerve* **20**, 577-584 (1997).
106. Meerwaldt, R., *et al.* Increased accumulation of skin advanced glycation end-products precedes and correlates with clinical manifestation of diabetic neuropathy. *Diabetologia* **48**, 1637-1644 (2005).
107. Thornalley, P.J. Cell activation by glycated proteins. AGE receptors, receptor recognition factors and functional classification of AGEs. *Cellular and Molecular Biology* **44**, 1013-1023 (1998).
108. Toth, C., *et al.* Receptor for advanced glycation end products (RAGEs) and experimental diabetic neuropathy. *Diabetes* **57**, 1002-1017 (2008).
109. Vincent, A.M., *et al.* Receptor for advanced glycation end products activation injures primary sensory neurons via oxidative stress. *Endocrinology* **148**, 548-558 (2007).
110. Vincent, A.M., Russell, J.W., Low, P. & Feldman, E.L. Oxidative Stress in the Pathogenesis of Diabetic Neuropathy. *Endocrine Reviews* **25**, 612-628 (2004).
111. Fridovich, I. Superoxide Radical and Superoxide Dismutases. *Annual Review of Biochemistry* **64**, 97-112 (1995).
112. Zhang, D.X. & Gutterman, D.D. Mitochondrial reactive oxygen species-mediated signaling in endothelial cells. *American Journal of Physiology - Heart and Circulatory Physiology* **292**, H2023-H2031 (2007).
113. Radi, R., Beckman, J.S., Bush, K.M. & Freeman, B.A. Peroxynitrite oxidation of sulfhydryls. The cytotoxic potential of superoxide and nitric oxide. *Journal of Biological Chemistry* **266**, 4244-4250 (1991).

114. Evans, J.L., Goldfine, I.D., Maddux, B.A. & Grodsky, G.M. Oxidative Stress and Stress-Activated Signaling Pathways: A Unifying Hypothesis of Type 2 Diabetes. *Endocrine Reviews* **23**, 599-622 (2002).
115. Valko, M.*, et al.* Free radicals and antioxidants in normal physiological functions and human disease. *International Journal of Biochemistry & Cell Biology* **39**, 44-84 (2007).
116. Leinninger, G.M., Edwards, J.L., Lipshaw, M.J. & Feldman, E.L. Mechanisms of disease: mitochondria as new therapeutic targets in diabetic neuropathy. *Nature Clinical Practice Neurology* **2**, 620-628 (2006).
117. Wallace, D.C. A mitochondrial paradigm of metabolic and degenerative diseases, aging, and cancer: A dawn for evolutionary medicine. in *Annual Review of Genetics*, Vol. 39 359-407 (2005).
118. Baloh, R.H. Mitochondrial dynamics and peripheral neuropathy. *Neuroscientist* **14**, 12-18 (2008).
119. Pieczenik, S.R. & Neustadt, J. Mitochondrial dysfunction and molecular pathways of disease. *Experimental and Molecular Pathology* **83**, 84-92 (2007).
120. Kelley, D.E., He, J., Menshikova, E.V. & Ritov, V.B. Dysfunction of Mitochondria in Human Skeletal Muscle in Type 2 Diabetes. *Diabetes* **51**, 2944-2950 (2002).
121. Schroer, J.A., Plurad, S.B. & Schmidt, R.E. FINE-STRUCTURE OF PRESYNAPTIC AXONAL TERMINALS IN SYMPATHETIC AUTONOMIC GANGLIA OF AGING AND DIABETIC HUMAN-SUBJECTS. *Synapse* **12**, 1-13 (1992).
122. Tay, S.S.W. & Wong, W.C. SHORT-TERM AND LONG-TERM EFFECTS OF STREPTOZOTOCIN-INDUCED DIABETES ON THE DORSAL MOTOR NUCLEUS OF THE VAGUS NERVE IN THE RAT. *Acta Anatomica* **150**, 274-281 (1994).
123. Kalichman, M.W., Powell, H.C. & Mizisin, A.P. Reactive, degenerative, and proliferative Schwann cell responses in experimental galactose and human diabetic neuropathy. *Acta Neuropathologica* **95**, 47-56 (1998).
124. Sasaki, H., Schmelzer, J.D., Zollman, P.J. & Low, P.A. Neuropathology and blood flow of nerve, spinal roots and dorsal root ganglia in longstanding diabetic rats. *Acta Neuropathologica* **93**, 118-128 (1997).
125. Fahim, M.A., Hasan, M.Y. & Alshuaib, W.B. Early morphological remodeling of neuromuscular junction in a murine model of diabetes. *Journal of Applied Physiology* **89**, 2235-2240 (2000).
126. Harrison, J.F.*, et al.* Oxidative stress-induced apoptosis in neurons correlates with mitochondrial DNA base excision repair pathway imbalance. *Nucleic Acids Research* **33**, 4660-4671.
127. Kim, J.Y.*, et al.* Mitochondrial DNA content is decreased in autosomal dominant optic atrophy. *Neurology* **64**, 966-972 (2005).
128. Ryu, H., Lee, J., Impey, S., Ratan, R.R. & Ferrante, R.J. Antioxidants modulate mitochondrial PKA and increase CREB binding to D-loop DNA of the mitochondrial genome in neurons. *Proceedings of the National Academy of Sciences of the United States of America* **102**, 13915-13920 (2005).
129. Huang, T.J.*, et al.* Insulin prevents depolarization of the mitochondrial inner membrane in sensory neurons of type 1 diabetic rats in the presence of sustained hyperglycemia. *Diabetes* **52**, 2129-2136 (2003).
130. Russell, J.W.*, et al.* High glucose-induced oxidative stress and mitochondrial dysfunction in neurons. *Faseb Journal* **16**, 1738-1748 (2002).
131. Obrosova, I.G.*, et al.* Evaluation of alpha 1-adrenoceptor antagonist on diabetes-induced changes in peripheral nerve function, metabolism, and antioxidative defense. *Faseb Journal* **14**, 1548-1558 (2000).

132. Stevens, M.J., Obrosova, I., Cao, X., Van Huysen, C. & Greene, D.A. Effects of DL-alpha-lipoic acid on peripheral nerve conduction, blood flow, energy metabolism, and oxidative stress in experimental diabetic neuropathy. *Diabetes* **49**, 1006-1015 (2000).
133. Srinivasan, S., Stevens, M. & Wiley, J.W. Diabetic peripheral neuropathy - Evidence for apoptosis and associated mitochondrial dysfunction. *Diabetes* **49**, 1932-1938 (2000).
134. Vincent, A.M., McLean, L.L., Backus, C. & Feldman, E.L. Short-term hyperglycemia produces oxidative damage and apoptosis in neurons. *The FASEB Journal* (2005).
135. Schmeichel, A.M., Schmelzer, J.D. & Low, P.A. Oxidative Injury and Apoptosis of Dorsal Root Ganglion Neurons in Chronic Experimental Diabetic Neuropathy. *Diabetes* **52**, 165-171 (2003).
136. Yu, T., Robotham, J.L. & Yoon, Y. Increased production of reactive oxygen species in hyperglycemic conditions requires dynamic change of mitochondrial morphology. *Proceedings of the National Academy of Sciences of the United States of America* **103**, 2653-2658 (2006).
137. Leinninger, G.M.*, et al.* Mitochondria in DRG neurons undergo hyperglycemic mediated injury through Bim, Bax and the fission protein Drp1. *Neurobiology of Disease* **23**, 11-22 (2006).
138. Arnoult, D.*, et al.* Bax/Bak-Dependent Release of DDP/TIMM8a Promotes Drp1-Mediated Mitochondrial Fission and Mitoptosis during Programmed Cell Death. *Current Biology* **15**, 2112-2118 (2005).
139. Söti, C. & Csermely, P. Chaperones and aging: role in neurodegeneration and in other civilizational diseases. *Neurochemistry International* **41**, 383-389 (2002).
140. Muchowski, P.J. & Wacker, J.L. Modulation of neurodegeneration by molecular chaperones. *Nat Rev Neurosci* **6**, 11-22 (2005).
141. Rodgers, K.J., Ford, J.L. & Brunk, U.T. Heat shock proteins: keys to healthy ageing? *Redox Report* **14**, 147-153 (2009).
142. Boshoff, A.*, et al.* Molecular chaperones in biology, medicine and protein biotechnology. *South African Journal of Science* **100**, 665-677 (2004).
143. Voisine, C., Pedersen, J.S. & Morimoto, R.I. Chaperone networks: Tipping the balance in protein folding diseases. *Neurobiology of Disease* **40**, 12-20 (2010).
144. Lindquist, S. The Heat-Shock Response. *Annual Review of Biochemistry* **55**, 1151-1191 (1986).
145. Zou, J., Guo, Y., Guettouche, T., Smith, D.F. & Voellmy, R. Repression of Heat Shock Transcription Factor HSF1 Activation by HSP90 (HSP90 Complex) that Forms a Stress-Sensitive Complex with HSF1. *Cell* **94**, 471-480 (1998).
146. Vigh, L.*, et al.* Bimoclomol: A nontoxic, hydroxylamine derivative with stress protein-inducing activity and cytoprotective effects. *Nat Med* **3**, 1150-1154 (1997).
147. Luo, W.J., Sun, W.L., Taldone, T., Rodina, A. & Chiosis, G. Heat shock protein 90 in neurodegenerative diseases. *Molecular Neurodegeneration* **5**(2010).
148. Vass, K., Welch, W.J. & Nowak, T.S. LOCALIZATION OF 70-KDA STRESS PROTEIN INDUCTION IN GERBIL BRAIN AFTER ISCHEMIA. *Acta Neuropathologica* **77**, 128-135 (1988).
149. Nowak, T.S. LOCALIZATION OF 70-KDA STRESS PROTEIN MESSENGER-RNA INDUCTION IN GERBIL BRAIN AFTER ISCHEMIA. *Journal of Cerebral Blood Flow and Metabolism* **11**, 432-439 (1991).
150. Armstrong, J.N., Plumier, J.C.L., Robertson, H.A. & Currie, R.W. The inducible 70,000 molecular weight heat shock protein is expressed in the degenerating dentate hilus and piriform cortex after systemic administration of kainic acid in the rat. *Neuroscience* **74**, 685-693 (1996).

151. Dou, F., *et al.* Chaperones Increase Association of tau Protein with Microtubules. *Proceedings of the National Academy of Sciences of the United States of America* **100**, 721-726 (2003).
152. Waza, M., *et al.* 17-AAG, an Hsp90 inhibitor, ameliorates polyglutamine-mediated motor neuron degeneration. *Nat Med* **11**, 1088-1095 (2005).
153. Conde, A.G., Lan, S.S., Dillmann, W.H. & Mestril, R. Induction of heat shock proteins by tyrosine kinase inhibitors in rat cardiomyocytes and myogenic cells confers protection against simulated ischemia. *Journal of Molecular and Cellular Cardiology* **29**, 1927-1938 (1997).
154. Lu, A., Ran, R., Parmentier-Batteur, S., Nee, A. & Sharp, F.R. Geldanamycin induces heat shock proteins in brain and protects against focal cerebral ischemia. *Journal of Neurochemistry* **81**, 355-364 (2002).
155. Kieran, D., *et al.* Treatment with arimoclomol, a coinducer of heat shock proteins, delays disease progression in ALS mice. *Nat Med* **10**, 402-405 (2004).
156. Muchowski, P.J., *et al.* Hsp70 and Hsp40 chaperones can inhibit self-assembly of polyglutamine proteins into amyloid-like fibrils. *Proceedings of the National Academy of Sciences* **97**, 7841-7846 (2000).
157. Polla, B.S., *et al.* Mitochondria are selective targets for the protective effects of heat shock against oxidative injury. *Proceedings of the National Academy of Sciences of the United States of America* **93**, 6458-6463 (1996).
158. Xu, L.J. & Giffard, R.G. HSP70 protects murine astrocytes from glucose deprivation injury. *Neuroscience Letters* **224**, 9-12 (1997).
159. Kamii, H., *et al.* PROLONGED EXPRESSION OF HSP70 MESSENGER-RNA FOLLOWING TRANSIENT FOCAL CEREBRAL-ISCHEMIA IN TRANSGENIC MICE OVEREXPRESSING CUZN-SUPEROXIDE DISMUTASE. *Journal of Cerebral Blood Flow and Metabolism* **14**, 478-486 (1994).
160. Kondo, T., *et al.* Expression of hsp70 mRNA is induced in the brain of transgenic mice overexpressing human CuZn-superoxide dismutase following transient global cerebral ischemia. *Brain Research* **737**, 321-326 (1996).
161. Wells-Knecht, K.J., Zyzak, D.V., Litchfield, J.E., Thorpe, S.R. & Baynes, J.W. Identification of Glyoxal and Arabinose as Intermediates in the Autoxidative Modification of Proteins by Glucose. *Biochemistry* **34**, 3702-3709 (1995).
162. Kaneto, H., *et al.* Reducing sugars trigger oxidative modification and apoptosis in pancreatic beta-cells by provoking oxidative stress through the glycation reaction. *Biochem. J.* **320**, 855-863 (1996).
163. KÜRthy, M., *et al.* Effect of BRX-220 against Peripheral Neuropathy and Insulin Resistance in Diabetic Rat Models. *Annals of the New York Academy of Sciences* **967**, 482-489 (2002).
164. Rakonczay Jr, Z., *et al.* Nontoxic heat shock protein coinducer BRX-220 protects against acute pancreatitis in rats. *Free Radical Biology and Medicine* **32**, 1283-1292 (2002).
165. Urban, M.J., *et al.* Inhibiting heat-shock protein 90 reverses sensory hypoalgesia in diabetic mice. *Asn Neuro* **2**(2010).
166. Bantscheff, M., Schirle, M., Sweetman, G., Rick, J. & Kuster, B. Quantitative mass spectrometry in proteomics: a critical review. *Analytical and Bioanalytical Chemistry* **389**, 1017-1031 (2007).
167. Yu, C., Alterman, M. & Dobrowsky, R.T. Ceramide displaces cholesterol from lipid rafts and decreases the association of the cholesterol binding protein caveolin-1. *Journal of Lipid Research* **46**, 1678-1691 (2005).
168. Spellman, D.S., Deinhardt, K., Darie, C.C., Chao, M.V. & Neubert, T.A. Stable Isotopic Labeling by Amino Acids in Cultured Primary Neurons. *Molecular & Cellular Proteomics* **7**, 1067-1076 (2008).

169. Schwanhäusser, B., Gossen, M., Dittmar, G. & Selbach, M. Global analysis of cellular protein translation by pulsed SILAC. *PROTEOMICS* **9**, 205-209 (2009).

Chapter 2: Hyperglycemia Alters the Schwann Cell Mitochondrial Proteome and Decreases Coupled Respiration in the Absence of Superoxide Production

(Zhang, L., Yu, C., Vasquez, F.E., Galeva, N., Onyango, I., Swerdlow, R.H., Dobrowsky, R.T. (2010) Hyperglycemia Alters the Schwann Cell Mitochondrial Proteome and Decreases Coupled Respiration in the Absence of Superoxide Production. *J. Proteome Res.* **9**, 458-471.)

Abstract

Hyperglycemia-induced mitochondrial dysfunction contributes to sensory neuron pathology in diabetic neuropathy. Although Schwann cells (SCs) also undergo substantial degeneration in diabetic neuropathy, the effect of hyperglycemia on the SC mitochondrial proteome and mitochondrial function has not been examined. Stable isotope labeling with amino acids in cell culture (SILAC) was used to quantify the temporal effect of hyperglycemia on the mitochondrial proteome of primary SCs isolated from neonatal rats. Of 317 mitochondrial proteins identified, about 78% were quantified and detected at multiple time points. Pathway analysis indicated that proteins associated with mitochondrial dysfunction, oxidative phosphorylation, the TCA cycle, and detoxification were significantly increased in expression and over-represented. Assessing mitochondrial respiration in intact SCs indicated that hyperglycemia increased the overall rate of oxygen consumption but decreased the efficiency of coupled respiration. Although a glucose-dependent increase in superoxide production occurs in embryonic sensory neurons, hyperglycemia did not induce a substantial change in superoxide levels in SCs. This correlated with a 1.9-fold increase in Mn superoxide dismutase expression,

which was confirmed by immunoblot and enzymatic activity assays. These data support that hyperglycemia alters mitochondrial respiration and can cause remodeling of the SC mitochondrial proteome independent of significant contributions from glucose-induced superoxide production.

2.1 Introduction

A severe and prevalent complication of diabetes is the development of diabetic peripheral neuropathy (DPN)[1]. Hyperglycemia and poor control of blood glucose are precipitating events that initiate a series of complex and inter-related metabolic and vascular insults that underlie the etiology of diabetic neuropathy. Two pathogenetic components that contribute to DPN are enhanced oxidative stress and mitochondrial dysfunction in both sensory neurons and Schwann cells (SCs)[2-3]. Using cultured endothelial cells, Brownlee and colleagues were the first to suggest that increased mitochondrial superoxide production may be a unifying biochemical lesion that promotes hyperglycemia-induced increases in polyol synthesis, protein kinase C activity, protein modification by *N*-acetyl glucosamine, and formation of advanced glycation end products in endothelial cells[4-5]. Consistent with this hypothesis, pharmacological interventions that decrease superoxide production and protein nitration in peripheral nerve improve morphological and physiological indices of nerve damage that contribute to diabetic neuropathy[6-9].

Although hyperglycemia can increase oxidative stress in mitochondria[10], it is unclear whether glucose-induced superoxide production may contribute to changes in mitochondrial protein expression and function. SCs undergo substantial degeneration in DPN, but the broad effect of hyperglycemia on the SC mitochondrial proteome has not been examined. To this end, we used stable isotope labeling of cells in culture (SILAC) to establish an unbiased and temporally dynamic assessment of the effect of hyperglycemia on the SC mitochondrial proteome. SILAC has been used extensively for quantifying changes in organellar proteomes[11] and requires at least two distinct

populations of SCs that are differentially labeled with, for example, ^{12}C-Lys or $^{13}C_6$-Lys. After 5-6 population doublings, the SCs readily incorporate the $^{13}C_6$-Lys into their proteome such that at least 95% incorporation is obtained within 10 days[12]. After the labeling period, one population of the cells serves as a control and the other is subjected to hyperglycemic stress for various periods of time. Cell lysates are then prepared, mixed together in a 1:1 mass ratio and specific subproteomes are enriched prior to analysis[13].

In the present study, SCs subjected to hyperglycemic stress for 2, 6, or 16 days exhibited an overall increase in the expression of numerous mitochondrial proteins associated with a broad range of biochemical functions. Although hyperglycemia increased the expression of protein components of the respiratory chain, this correlated with a decreased mitochondrial efficiency toward ATP generation. Concurrent measures of the rate of extracellular acidification indicated a shift toward glycolysis. Unexpectedly, we found that hyperglycemia did not significantly increase superoxide production either acutely (<6 h) or under conditions of more prolonged hyperglycemia (6 days) using two fluorometric dyes. The lack of glucose-induced superoxide generation may arise in part from an increase in mitochondrial Mn-SOD. These data suggest that neonatal rat SCs are rather insensitive to glucose-induced superoxide generation in the mitochondria and that hyperglycemia affects the mitochondrial proteome independent of this marker of oxidative stress.

2.2 Experimental Section

Schwann Cell Isolation & Metabolic Labeling.

Schwann cells (SCs) were isolated as described and were cultured in low glucose (5.5 mM) DMEM that was custom prepared and conformed to Gibco DMEM (#12320), with the exception that L-arginine and L-lysine were omitted[12]. Complete medium contained the specified isotopic forms of Lys or Arg, 100 U/mL penicillin, 100 µg/mL streptomycin, 10% dialyzed FCS (dFCS, Atlas Biologicals, Fort Collins, CO), and 2 µM forskolin. In experiments not requiring stable isotopes, the medium was supplemented with 84 mg/L ^{12}C-Arg and 125 mg/L ^{12}C-Lys (K0). For SILAC analysis, the cells were incubated in medium supplemented with ^{12}C-Arg and U-[$^{13}C_6$]-L-Lys ($^{13}C_6$-Lys, K6). Primary SCs were used for 5 passages and were maintained in the labeling medium for at least 10 days prior to mass spectrometric analysis since this is the minimal labeling period necessary to obtain about 95% isotopic enrichment of the proteome[12]. All the amino acids were prepared as 100× stock solutions in serum-free Arg/Lys deficient DMEM, sterile filtered and added to working volumes of medium. Unlabeled amino acids were obtained from Sigma Chemicals (St. Louis, MO) and >98% isotopically enriched amino acids were a product of Cambridge Isotopes (Andover, MA); no correction for isotopic purity was made in the quantitative measures.

Cell Fractionation for SILAC Analysis

For proteomic analysis, 10 × 15 cm plates of SCs were expanded in K0 or K6 complete medium yielding about 4 × 10^7 cells per treatment. Since it was necessary to passage the primary SCs twice to obtain a sufficient cell number to seed into the 10

plates, they have already been labeled to metabolic equilibrium. At this point, the Lys concentration was also decreased to 62.5 mg/L in both the K0 and K6 cultures to conserve the metabolic label and forskolin was not added to the medium to avoid possible confounding effects due to the growth promoting activity of the drug. After the cells became established, hyperglycemia was induced by adjusting the glucose concentration to 30 mM in the K6 or cultures (K0 in the reverse labeling experiment) and both sets of cells were incubated for 2, 6, or 16 days with a medium change every third day. The cells were trypsinized, washed twice with ice-cold phosphate-buffered saline (PBS), and resuspended in 10 mL of mitochondrial isolation buffer (MIBA) containing 10 mM Tris-HCl, pH 7.4, 1 mM EDTA, 0.2 M D-mannitol, 0.05 M sucrose, 0.5 mM sodium orthovanadate, 1 mM sodium fluoride, and 1× Complete Protease Inhibitors (Roche Diagnostics)[14]. The cells were homogenized with the aid of a Teflon pestle and lysis was confirmed microscopically. The protein concentration of each lysate was measured in quadruplicate using the Bradford assay and bovine serum albumin as the standard. The coefficient of variation was determined for each set of quadruplicate measures and if the variability exceeded 5%, the protein assay was repeated for that set of samples. The samples were then mixed together in a 1:1 mass ratio yielding 24–30mg of protein.

Nuclei were isolated from the pooled lysates by centrifugation at 500× *g* at 4°C for 5 min. The crude nuclei were washed with PBS and further purified as described below. The remaining S1 supernatant was centrifuged at 8,000 × g for 10 min at 4°C, yielding the S2 supernatant and the heavy mitochondrial (HM) fraction. The HM fraction was washed twice with MIBA and resuspended in 3 mL of 25% Nycodenz prepared in 10 mM Tris-HCl, pH 7.4,1 mM EDTA, and 0.25 M sucrose. Mitochondria were purified by

centrifugation at 50 000× *g* for 90 min at 4°C in a SW41 rotor over a discontinuous gradient of 40, 34, 30, 25 (HM), 23, and 20% Nycodenz as described[14]. The mitochondria that sedimented at the 25-30% interface were recovered, the fraction was diluted with MIBA and the mitochondria pelleted by centrifugation at 10 000× *g* for 10 min at 4 °C. The final mitochondrial pellet was resuspended in 0.1-0.15 mL MIBA.

A cytosolic fraction was obtained from the S2 supernatant by centrifugation at 100 000× *g* for 60 min at 4°C. The resulting cytosol was concentrated at 4°C to less than 0.5 mL using an Amicon Ultra filter device with a 10 000 nominal molecular weight limit. Nuclei were purified following the procedure of Hwang et al[15]. Briefly, the crude nuclei were resuspended in 20 mM HEPES-KOH, pH 7.5, 10 mM KCl, 1 mM EDTA, 1 mM DTT, 0.25 M sucrose and mixed with an equal volume of 20 mM HEPES-KOH, pH 7.5, 10 mM KCl, 1 mM EDTA, 1 mM DTT, 2.3 M sucrose (both buffers contained the Complete protease inhibitor cocktail). The nuclei sample was then layered directly over the 2.3 M sucrose buffer and centrifuged at 60 000× *g* for 90 min at 4°C in a SW41 rotor. The nuclear pellet was washed with MIBA and resuspended in 0.1-0.15 mL of this buffer.

To assess organelle enrichment, 3 µg of protein was fractionated by SDS-PAGE. After transfer to nitrocellulose, immunoblot analysis was performed using the following antibodies against marker proteins for mitochondria, MnSOD (Upstate Biotechnology, Lake Placid, NY) and prohibitin-1 (Neomarkers, Freemeont, CA); nuclei, p62 nucleoporin (BD Transduction Laboratories, Lexington, KY); endoplasmic reticulum, GRP 78 (Santa Cruz Biotechnology, Santa Cruz, CA); and cytosol, lactate dehydrogenase (Sigma-Aldrich, St. Louis, MO).

Mass Spectrometry & Protein Identification

Proteins were identified following one-dimensional SDS-PAGE coupled to RP-HPLC linear quadrupole ion trap Fourier transform ion cyclotron resonance tandem mass spectrometry (GeLC-LTQ-FT MS/MS)[16]. About 75-100 µg of protein was fractionated by SDS-PAGE, the proteins were visualized by staining the gel and the lane was cut into 12-15 sections for in-gel tryptic digestion.

The gel pieces were placed in silanized microfuge tubes and destained with 100 mM ammonium bicarbonate in 50% acetonitrile[17]. Following reduction (10 mM dithiothreitol at 55 °C for 1 h) and alkylation (55 mM iodoacetamide for 30 min in the dark at room temperature), the gel pieces were washed with 100 mM ammonium bicarbonate in 50% acetonitrile, dehydrated with 100% acetonitrile and dried. The gel pieces were rehydrated on ice in a minimal volume of 25 mM ammonium bicarbonate, pH 7.5 containing 12.5 ng/µL Trypsin Gold (Promega Corp., Madison, WI), covered with a sufficient volume of 25 mM ammonium bicarbonate, pH 7.5 and the proteins were digested overnight at 37 °C. The peptides were extracted from the gel particles with 5% formic acid in 100 mM ammonium bicarbonate and 5% formate in 100% acetonitrile. The combined supernatants were concentrated to ~25 µL in a Speed-Vac prior to analysis.

Peptides were separated on a microcapillary reverse-phase column (either 0.30 × 150 mm, Pepmap C18, or 0.32 × 50 mm, MicroTech Scientific) at a flow rate of 5 -10 µL/min with a linear gradient from 5 to 65% acetonitrile in 0.06% aqueous formic acid (v/v) over 55 min and the eluate was introduced into the LTQ-FT tandem mass spectrometer (ThermoFinnigan, Waltham, MA). All experiments were performed in

data-dependent mode using dynamic exclusion with survey MS spectra (*m*/*z* 300-2000) acquired in the FT-ICR cell with resolution R = 25 000 at *m*/*z* 400 and accumulation to a target value of 5×10^5 charges or a maximum ion accumulation time of 2000 ms. The three most intense ions were isolated and fragmented with a target value of 2×10^3 accumulated ions and an ion selection threshold of 3000 counts. Dynamic exclusion duration was typically 200 s with early expiration if ion intensity fell below a S/N threshold of 2. The ESI source was operated with a spray voltage of 2.8 kV, a tube lens offset of 170 V and a capillary temperature of 200 °C. All other source parameters were optimized for maximum sensitivity of a synthetic YGGFL peptide ion at *m*/*z* 556.27.

The MS/MS peak list was generated from the Xcalibur raw files using DTA Supercharge (v 1.17) (http://msquant. sourceforge.net). The individual text files were linked to their corresponding LTQ-FT raw file and concatenated with the aid of an in-house modified Perl script (MultiRawPrepare) originally obtained from the MSQUANT web address. The concatenated file was submitted to Mascot (v. 2.1, Matrix Science, London, United Kingdom) and proteins were identified by searching a combined IPI mouse/rat (v3.26) database concatenated with their reverse sequences (188 450 total sequences). Search parameters specified a maximum mass deviation of 10 ppm, a fragment tolerance of 0.5 Da, up to 1 missed cleavage, and carboxyamidomethylated cysteine as a fixed modification. Variable modifications were set to consider protein N-terminal acetylation, N-terminal pyro-glutamine, methionine oxidation, and the presence of $^{13}C_6$-Lys. The Mascot search results were imported into Scaffold Protein Identification software (v 2.0, Proteome Software, Portland, OR) and reanalyzed using the X! Tandem search algorithm to enhance and further validate peptide and protein

identification. The peptide filter was set to a 95% confidence level and proteins validated by Scaffold at this confidence level or greater were considered identified without further verification. Manual verification of other proteins, especially those identified by a single peptide, followed an acceptance criteria which required a fully tryptic peptide that was at least 7 amino acids in length, had a detected series of at least 4 consecutive y-ions or b-ions, and a had Mascot ion score of 25 or greater at a mass deviation of $\leq$ 6 ppm (3 times the dispersion of the mass deviations). Using these criteria for peptide identification, the overall false positive rate was estimated[18] as <0.5% between the various time points used in the proteomic analyses.

To assess the statistical mass accuracy between the experiments, the distribution of calibrated mass errors for all peptides initially identified in the search was obtained from MSQUANT and the errors were binned by 2 ppm intervals[19]. The errors between the mitochondrial analyses followed a normal distribution and the average calibrated absolute mass deviation was 2.63 ± 0.21 ppm and the average dispersion was 1.97 ± 0.19 ppm (Figure 2-1).

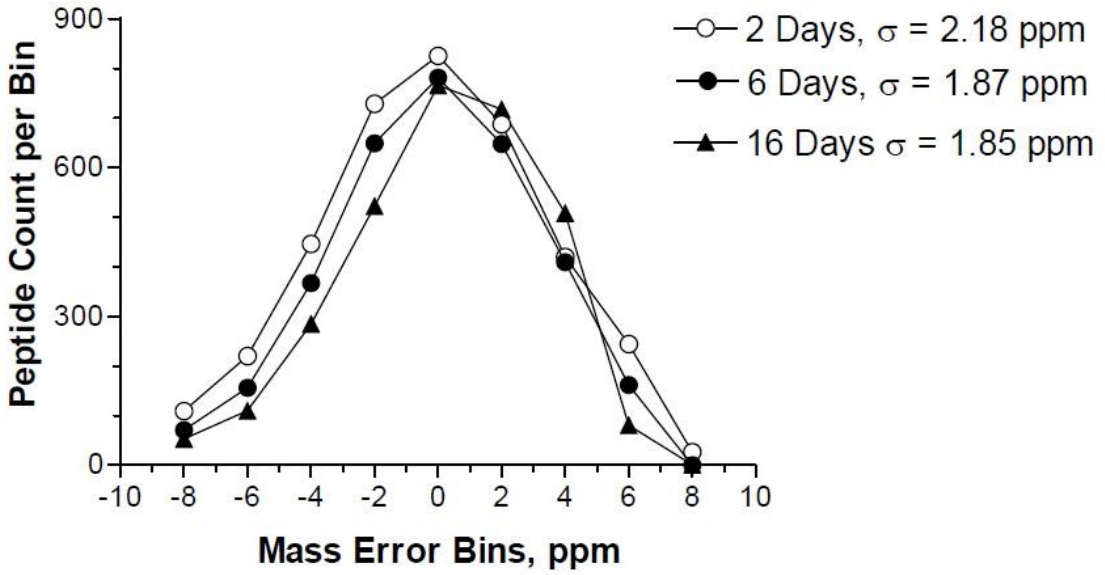

Figure 2-1. Distribution of Mass Errors and Estimation of Statistical MassAccuracy. At each time point, the calibrated mass errors (ppm) for all the peptides identified from the mitochondrial fractions by Mascot were obtained from the MSQUANT peptide report. Mass errors were binned to a width of 2 ppm and the number of peptides per bin counted. Data shows the Gaussian nature of the distribution of mass deviations and the average dispersion was 1.97$\pm$ 0.19 ppm.

Protein Quantification, Statistical & Bioinformatic Analyses

The expression ratio of individual peptide pairs was obtained using MSQUANT[20]. However, it was also necessary to manually quantify peptide pairs and verify a subset of the MSQUANT results using peak intensities from Xcalibur software (v2.0 SR1). If similar peptides of different charge states were detected, only the peptide with the highest ion score was counted toward identification and quantified. Similarly, redundant peptides containing a modification were only counted toward identification and quantified if an unmodified peptide was not detected. If multiple peptide pairs were quantified for the same protein, an overall protein expression ratio was taken as the average of these measures and the standard deviation was determined. The protein lists from MSQUANT were imported into Protein Center (Proxeon Bioinformatics, Odense, Denmark) and redundant mouse-rat orthologs and database entries were removed after clustering at 60% homology. The anchor protein used for clustering a given group of proteins is indicated in Supplementary Tables 1-3 (Appendix).

As previously reported, 3 times the average standard deviation of all the expression ratios at a given time point was assigned as the threshold for indicating a significant change[21]. For example, of 1251 proteins identified at all times points in the mitochondrial fractions, 991 (79%) were quantified and 556 were quantified by ≥2 unique peptides. The average standard deviation obtained in these three separate experiments was 0.111 ± 0.02, indicating that the analytic variability was tightly clustered at about 11%. Using the above criterion, proteins whose expression ratios were <0.67 or >1.33 were defined as showing a significant change.

Proteins were automatically annotated with respect to cell localization using Protein Center and via manual annotation from the SwissProt database. Bioinformatic analyses were performed using Ingenuity Pathway Analysis (v 7.0, Ingenuity Systems, Redwood CA) and BinGO[22]. After setting a bidirectional 1.3 fold change as the threshold, the program identified statistically over or under represented molecular networks. Pathways with $p < 0.001$ using the HyperGeometric test after correcting for multiple term testing by the Benjamini and Hochberg False Discovery Rate (B-H FDR) were deemed enriched.

Mitochondrial Respiration & Extracellular Acidification Measures

The rates of O_2 consumption (OCR) and extracellular acidification (ECAR) were assessed on intact SCs using an Extracellular Flux Analyzer (Seahorse Biosciences, North Billerica, MA). Extracellular flux analysis is a non-invasive assay which uses two calibrated optical sensors which directly measure OCR and ECAR in cells that remain attached to the culture plate. This technique avoids variability associated with trypsinization and mechanical stirring of the cells to determine OCR. Primary SCs were treated with 5.5 mM or 30 mM glucose for 3 days and baseline respiration was determined. Respiratory chain inhibitors were sequentially injected into the wells and ATP-coupled oxygen consumption was calculated as the oxygen consumption rate sensitive to 1 µM oligomycin, an ATP synthase inhibitor, after correcting for non-mitochondrial respiration. Proton leak was calculated as the mitochondrial rate insensitive to oligomycin, after correcting for non-mitochondrial respiration. The maximal uncoupled respiration rate was determined by depolarizing the mitochondrial membrane potential with 1 µM FCCP (carbonylcyanide-4-(trifluoromethoxy)-

phenylhydrazone) and non-mitochondrial respiration was determined as the activity remaining after inhibition of complexes 1 and 3 with 1 μM rotenone and 1 μM myxothiazol, respectively. Changes in ECAR are an indirect assessment of glycolytic activity due to lactic acid production and proton extrusion and were measured concurrent with oxygen consumption[23]. After the measures, the cells were harvested, protein concentration of each well was determined and experimental rate values were normalized to protein content.

Superoxide Assessment & Mn-SOD Activity Assay

Superoxide levels were measured by following the oxidation of dihydroethidine (Invitrogen-Molecular Probes, Carlsbad, CA) to ethidium[24]. SCs were seeded at 1×10^4 cells per well in 96-well plates and were treated with 5.5 mM or 30 mM glucose for the indicated times once reaching about 90% confluency. At the end of the incubation, the cells were incubated with 15 μM dihydroethidine for 15 min at 37 °C. The cells were washed with PBS and the ratio of ethidium (excitation 530 nm, emission 590 nm) to dihydroethidine (excitation 485 nm, emission 530 nm) was determined with the cells attached to the plate using a fluorescence spectrometer.

For assessing superoxide production using MitoSOX Red[25], SCs were grown in low glucose DMEM in six well plates until confluent. Cells were incubated in medium containing 5.5 mM or 30 mM glucose for 6 days and the cells were washed once with OPTI-MEM medium. MitoTracker Green (80 nM) was added to each well and after 10 min, 2.25 μM MitoSOX Red was added into the wells and the cells incubated for an additional 10 min. The cells were washed twice with fresh OPTI-MEM medium prior to imaging on an Olympus 3I Spinning Disk confocal microscope using excitation/ emission wavelengths of 575/624 nm (MitoSox Red) and 494/531 nm (MitoTracker Green). As a positive control, some cells were treated with 1.8 μg/mL Antimycin A in OPTI-MEM medium with 1% BSA for 25 min. Fluorescence intensity of the red and green signals of at least 200 cells per treatment was obtained using CellProfiler and CellProfiler Analyst image analysis software.

To assess manganese superoxide dismutase (Mn-SOD) activity, SCs were seeded into 10 cm plates and treated with 5.5 mM or 30 mM glucose for the indicated times after

reaching about 90% confluency. The cells were trypsinized and three plates per treatment were combined to isolate a heavy mitochondrial fraction as described above. Mn-SOD activity was determined as described by the manufacturer (Dojindo Molecular Technologies, Gaithersburg, MD) using 0.5-3µg of the heavy mitochondrial fraction. To inhibit Cu/Zn SOD, the protein was pre-incubated with 2 mM KCN for 30 min at 4 °C prior to assaying for MnSOD activity[14].

2.3 Results

Analysis of the SC Organellar Fractions

Although the primary focus of the study was on assessing the effect of hyperglycemia on altering the mitochondrial proteome, nuclei and cytosolic fractions were also isolated as described in the Experimental Methods (Figure 2-2A). Organelle purity was assessed following SDS-PAGE and immunoblot analysis for the presence of established protein markers of nuclei, mitochondria, endoplasmic reticulum and cytosol (Figure 2-2B). As expected, the mitochondrial fraction was enriched in the inner mitochondrial membrane and matrix proteins, prohibitin 1 and MnSOD. Neither marker protein for cytosol (lactate dehydrogenase) or nuclei (p62 nucleoporin) was detected in the purified mitochondrial fraction but it did remain contaminated with endoplasmic reticulum. Indeed, we repeatedly found GRP78 in most fractions and it proved difficult to remove from the mitochondrial fraction by using either Nycodenz or Percoll discontinuous gradients. Although GRP78 is a resident protein of the endoplasmic reticulum, it is also secreted from the organelle which may contribute to its cytosolic localization.

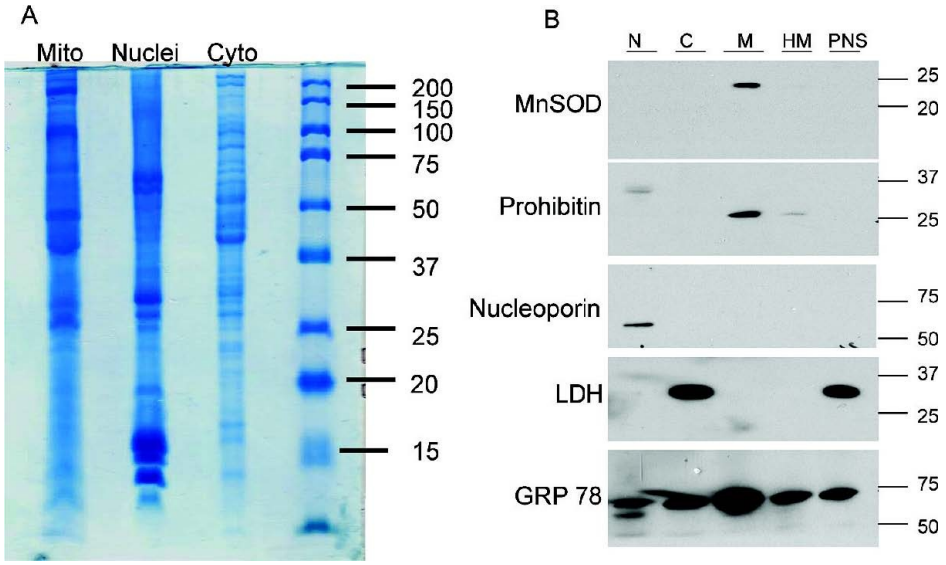

Figure 2-2. Assessment of organelle purity. K0 and K6 primary SCs were cultured for 16 days in 30 mM glucose, lysates were prepared and mixed together in a 1:1 mass ratio. Nuclear, mitochondrial and cytosolic fractions were isolated and (A) 75 µg of protein was separated by SDS-PAGE for proteomic analysis or (B) 3 µg was subjected to immunoblot analysis for the indicated organelle marker.

Hyperglycemia Has Temporally Distinct Effects on Nuclear & Mitochondrial Protein Expression

To perform a temporal analysis of the effect of hyperglycemia on the SC proteome, metabolically labeled cells (K6) were treated with 30 mM glucose for 2, 6, or 16 days while unlabeled control cells (K0) were maintained in 5.5 mM glucose at each time point. This time course was chosen to model the effect of acute and more chronic hyperglycemia on the primary SCs. Although triple labeling can be performed for temporal analyses by SILAC[26], we only used $^{13}C_6$-Lys as a single metabolic label and performed three separate experiments to cover the time course. Mitochondrial, nuclear and cytosolic proteins were separated by SDS-PAGE, in-gel digested with trypsin and the peptides were analyzed by GeLC-LTQ-FT MS/MS. The acquired mass spectra were searched against a combined mouse-rat IPI database and we identified 1673 proteins from the various cell fractions at all time points and 1198 (71.6%) of these proteins were unique.

Analysis of the nuclear fraction identified 332 total proteins, of which, 64% were detected at 2 or more time points (Figure 2-3A). Among the total proteins identified in this fraction, resident nuclear proteins were identified by their gene ontology (GO) annotation and 213 nuclear proteins were quantified using 1145 peptides (Supplementary Table 1-1, Appendix). In order to broadly compare the temporal effect of hyperglycemia on the nuclear proteome, the quantified proteins were ranked by their expression ratio and plotted versus protein number (Figure 2-3B) or the expression ratios were binned and the percent of proteins per bin was determined (Figure 2-3C). Increases in nuclear protein expression were rather similar between 2 and 16 days of hyperglycemia with 40% and

51% of the quantified proteins showing a statistically relevant increase, respectively. In contrast, 6 days of hyperglycemia led to 35% of the nuclear proteins showing a decreased expression. On the other hand, hyperglycemia had little effect on proteins identified in the cytoplasmic fraction (Supplementary Table 1-2, Appendix). Although the majority of cytoplasmic proteins showed no significant change after 2 (91.7%) or 6 (84.0%) days of hyperglycemia, about 34% of the quantified proteins showed an increased expression after 16 days (Figure 2-3D & E).

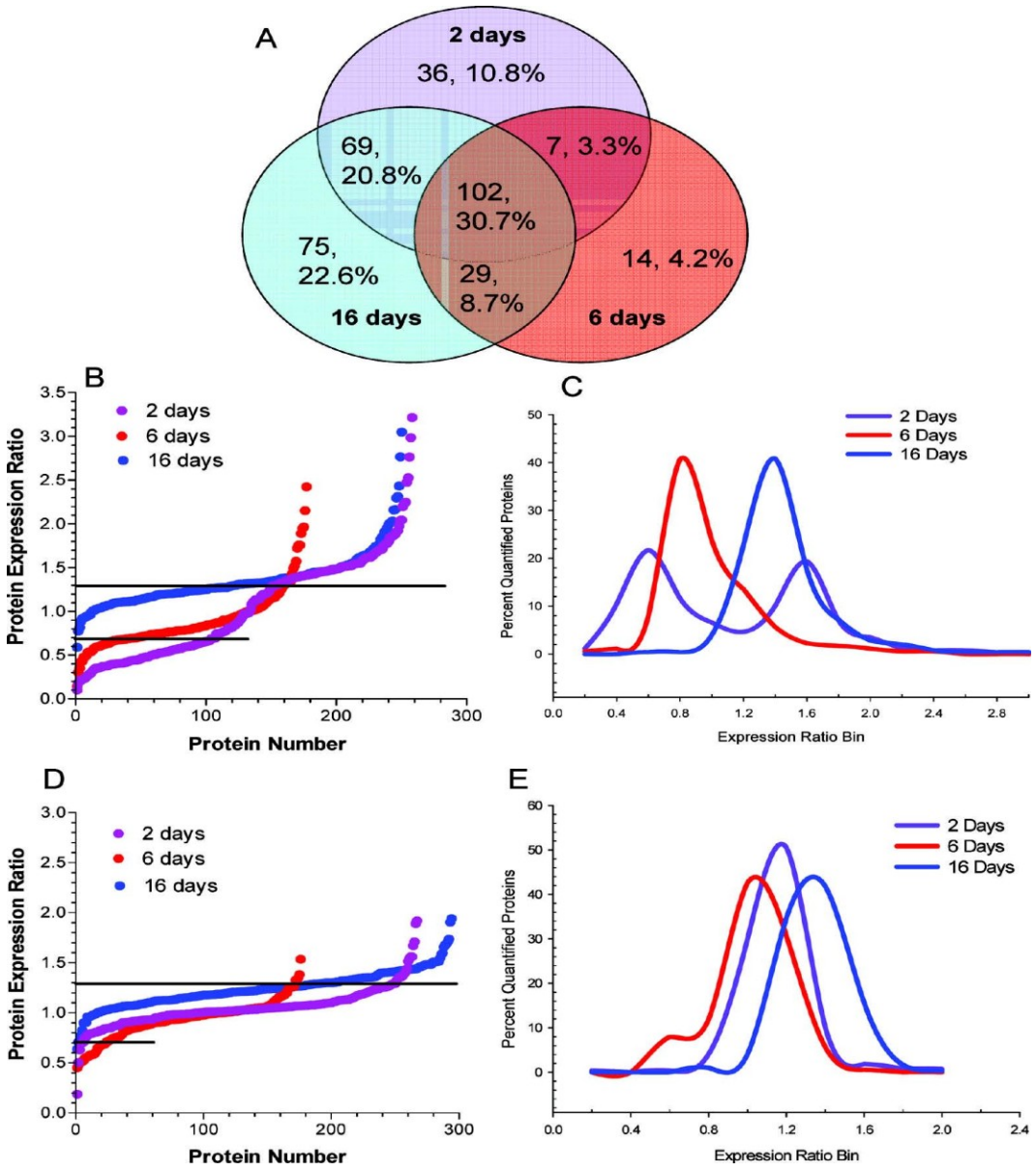

Figure 2-3. Hyperglycemia has differential effects on the nuclear and cytoplasmic proteomes. SCs were incubated in medium containing 5.5 mM (K0) or 30 mM (K6) medium for 2, 6, or 16 days and nuclear and cytoplasmic fractions were analyzed by GeLC-LTQ-FT MS/MS. (A) Venn diagram of number and percent of annotated nuclear proteins identified at each time point. To compare the effect of 2, 6, or 16 days hyperglycemia on the (B, C) nuclear or (D, E) cytoplasmic proteomes, the expression ratios were (B, D) plotted versus protein number or (C, E) binned by 0.2 units and expressed as a percent of the total quantified proteins. Line indicates

three times the standard deviation of the analytic variability and proteins between the lines did not show a significant change.

BinGO was used to determine if any biological processes were over-represented among the nuclear proteins that showed a significant change in their expression ratio after hyperglycemic stress[22]. Proteins affecting chromatin regulation, DNA remodeling and transcription were over-represented after 2 days of hyperglycemia (Figure 2-4A). This result was consistent with the pathway analysis which found that the top two molecular networks affected by hyperglycemia were associated with increases in mRNA processing, splicing and modification and DNA repair (Figure 2-4B). Conversely, proteins associated with protein transport, biosynthesis and metabolism were either marginally decreased or unchanged, especially since the majority of these proteins are cytoplasmic.

Mitochondrial proteins were identified by their GO annotation in Protein Center and by filtering against a reference set of 1,022 mouse mitochondrial proteins downloaded from the MitoP2 project (http://141.39.186.157:8080/mitop2/, last updated Nov. 2008). Using this approach, we identified 317 unique proteins that either reside or are associated with mitochondria and detected 242 proteins (76.3%) at two or more time points (Figure 2-5A). Using 1,599 peptides, 248 proteins were quantified but the detection of only Arg-containing tryptic peptides negated quantification of the remaining 69 proteins. Only 16 (5.0%) non-quantifiable mitochondrial proteins were identified by a single peptide at a single time point and the ion scores and MS^2 spectra for these peptides are shown in Supplementary Table 1-3 (Appendix).

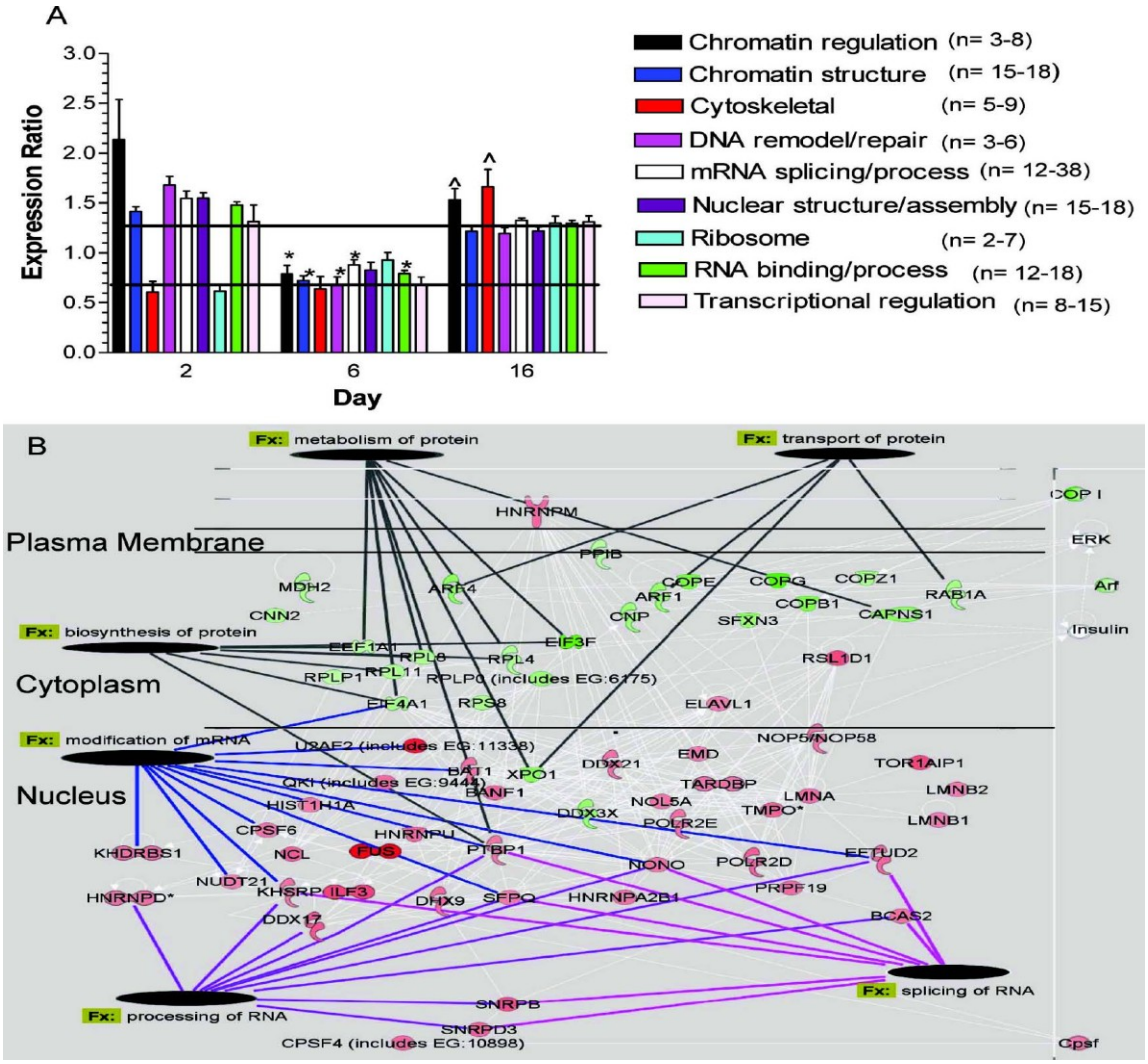

Figure 2-4. Identification of functional classes of nuclear proteins affected by hyperglycemia. (A) Quantified proteins were grouped based upon their annotated function. The expression ratios of all proteins associated with a function were averaged and the line indicates three times the standard deviation of the analytic variability associated with the quantitation. Categories above or below these limits define a significant change in expression. The number of quantified proteins per category is indicated in the legend. Significant differences between time points were determined using a one-way ANOVA and Tukey's post hoc test. *, $p < 0.05$ compared to 2 days, ^, $p < 0.05$ compared to 6 days. (B) Top two molecular networks affected after 2 days of hyperglycemia were identified using Ingenuity Pathway Analysis, merged and graphically presented to highlight the increase in proteins regulating mRNA processing and the

decrease in proteins regulating protein synthesis, metabolism and transport. Gene names are identified in Supplementary Table 1-4 (Appendix).

After 2 or 6 days of hyperglycemia, approximately 90% of all mitochondrial proteins showed a statistically relevant increase (Figure 2-5B). However, about 21% of the proteins increased expression ≥1.9-fold after 6 days of hyperglycemia compared to only 7.0% and 1.1% after 2 or 16 days of glycemic stress (Figure 2-5C). Indeed, after 16 days of hyperglycemia, only 56% of the mitochondrial proteins increased above 1.3 fold.

The analytic and biologic confidence of these changes is strengthened by the observation that when the SILAC experiment was reversed (K6 cells as control and K0 subjected to 6 days of hyperglycemia), the overall effect on the mitochondrial proteome was similar (Figure 2-5B). Second, immunoblot analysis for prohibitin 1 showed a similar increase in expression after 6 days of hyperglycemia as was determined by the SILAC analysis (Figure 2-6). Additionally, proteins known to exist in a 1:1 subunit stoichiometry showed similar changes at each time point[27]. For example, after 2 days of hyperglycemia, quantitation of 6-10 peptides identifying the α and β subunits of ATP synthase indicated an increase of 1.66 ± 0.11 and 1.49 ± 0.11, respectively. Agreement between changes in ATP synthase subunit levels was also preserved after 6 (1.50 ± 0.09 and 1.59 ± 0.11) or 16 days (1.30 ± 0.12 and 1.369 ± 0.11) of hyperglycemia. Similarly, the relative change in the α and β subunits of the E1 component of the pyruvate dehydrogenase were tightly correlated (Supplementary Table 1-3, Appendix). Lastly, the average expression ratio of all contaminating non-mitochondrial proteins did not show a statistically relevant change after 6 (176 proteins) or 16 (228 proteins) days of hyperglycemia although a 1.42 fold increase was noted after 2 days of hyperglycemia (145 proteins).

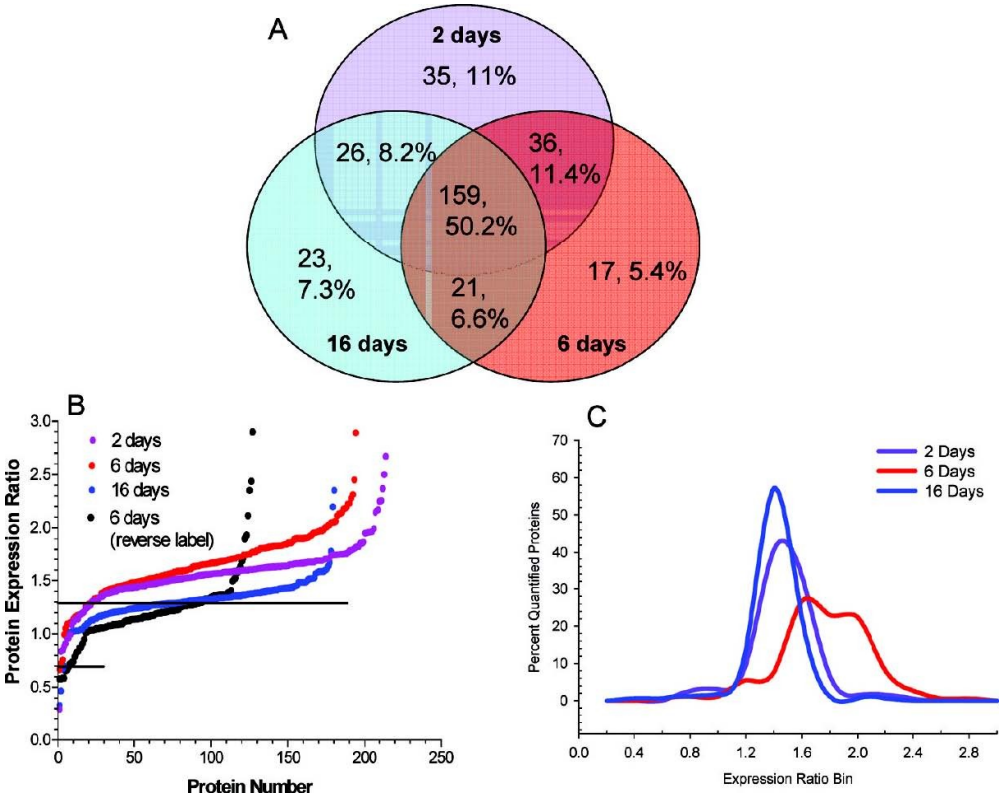

Figure 2-5. Temporal Profile of the Effect of Hyperglycemia on the Mitochondrial Proteome. SCs were incubated in medium containing 5.5 mM (K0) or 30 mM (K6) medium for 2, 6, or 16 days and mitochondrial fractions were analyzed by GeLC-LTQ-FT MS/MS. (A) Venn diagram of number and percent of annotated mitochondrial proteins identified at each time point. To compare the effect of 2, 6, or 16 days hyperglycemia on the mitochondrial proteome, the expression ratios were (B) plotted versus protein number or (C) binned by 0.2 units and expressed as a percent of the total quantified proteins. Reverse label indicates results from an experiment where control cells were labeled in K6 medium. Line indicates three times the standard deviation of the analytic variability and proteins between the lines did not show a significant change.

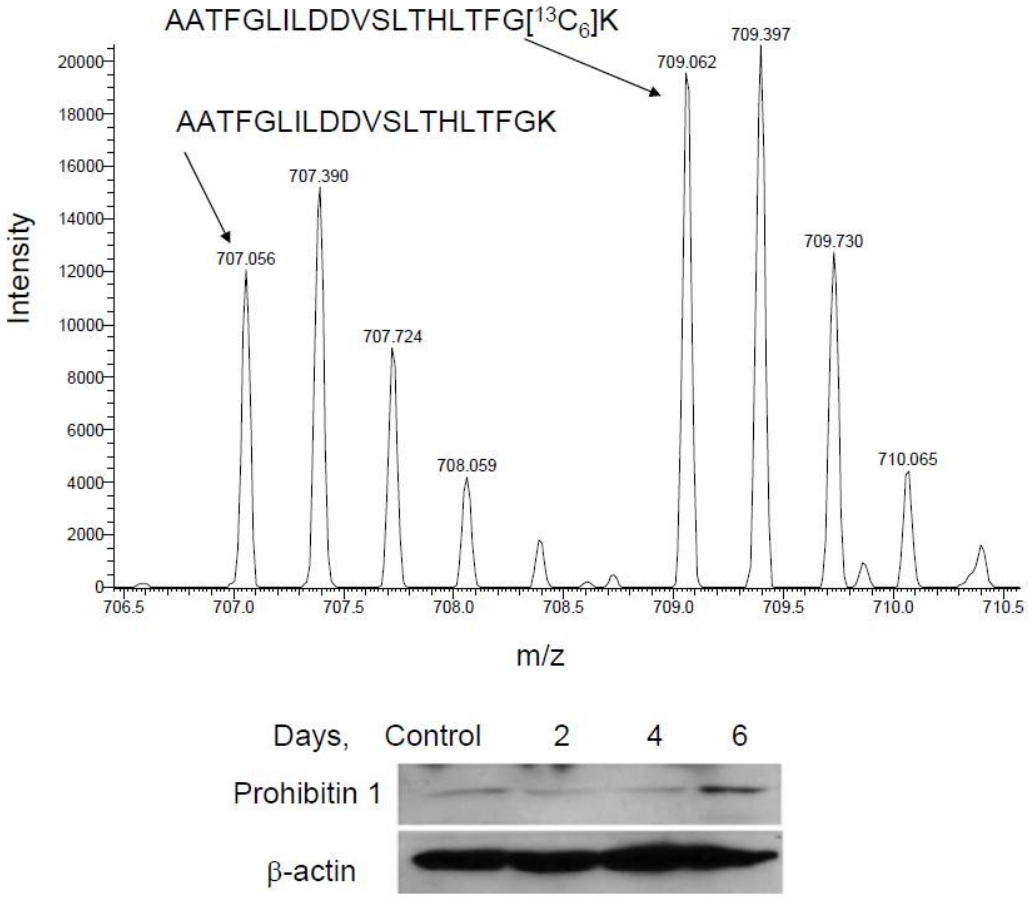

Figure.2-6 Hyperglycemia Increased Prohibitin 1. SCs were incubated with 5.5 mM (K0) or 30 mM (K6) glucose for 6 days. **(A)** Spectra show MS1 scan indicating a 1.6 fold increase for the prohibitin peptide AATFGLILDDVSLTHLTFGK. **(B)** The expression of prohibitin 1 from a heavy mitochondrial fraction obtained from SCs subjected to hyperglycemia for the indicated time. β-Actin was used as a loading control.

Hyperglycemia Increased the Expression of Proteins Contributing to Mitochondrial Dysfunction & Decreases the Efficiency of Oxidative Phosphorylation.

The above analysis strongly suggests that the mitochondrial proteome undergoes a marked increase in protein expression during hyperglycemic stress. This response would suggest that proteins involved in coordinated metabolic functions such as glucose metabolism, oxidative phosphorylation, lipid metabolism, stress response mediators and gene expression may respond in a concerted manner. Clustering the mitochondrial proteins by functional class showed that the quantified components of the mitochondrial respiratory chain exhibited a significant increase in expression after 2 and 6 days of hyperglycemia (Figure 2-7A). This corresponded with a 1.6-to 1.8-fold increase in components of the TCA cycle which provides the reducing equivalents utilized by the respiratory chain. However, after 16 days, there was a significant decline in expression of proteins associated with the TCA cycle as well as with complexes I and V.

To identify the top metabolic processes affected by hyperglycemia over time, the data sets were subjected to pathway analysis. Mitochondrial dysfunction, oxidative phosphorylation and the TCA cycle were among the top over-represented canonical pathways after 2 or 6 days of hyperglycemia (Figure 2-7B). These data are consistent with previous work which demonstrated that hyperglycemia increased the transcript levels for components of oxidative phosphorylation[28]. Proteins annotated to mitochondrial dysfunction were linked primarily to the regulation of respiration and detoxification of reactive oxygen species.

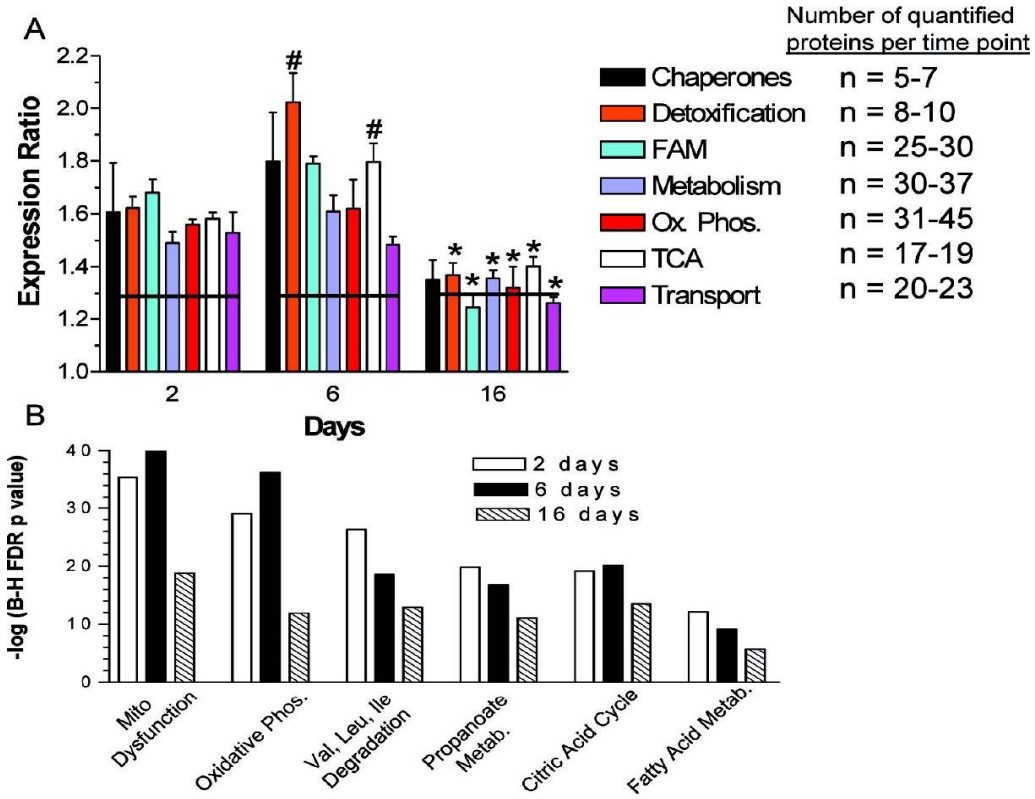

Figure 2-7. Temporal effect of hyperglycemia on functional classes of mitochondrial proteins. (A) Quantified proteins were grouped based upon their annotated function. The expression ratios of all proteins associated with a function were averaged and the line indicates three times the standard deviation of the analytic variability associated with the quantitation. Categories above or below these limits define a significant change in expression. The number of quantified proteins per category is indicated in the legend. Significant differences between time points were determined using a one-way ANOVA and Tukey's post hoc test. #, $p < 0.05$ compared to 2 days, *, $p < 0.05$ compared to 2 and 6 days. FAM, fatty acid metabolism; Ox Phos, oxidative phosphorylation. (B) Top over-represented toxicologic functions were identified using Ingenuity Pathway Analysis. Ordinate values are -log of the Benjamini-Hochberg False Discovery Rate *p*-value.

Since proteins associated with the TCA cycle and oxidative phosphorylation were increased, this suggested that hyperglycemia was affecting mitochondrial activity. SCs were subjected to hyperglycemic stress for three days and the rate of oxygen consumption was measured over 2 h using intact SCs. Since the oxygen consumption rates (OCR) and extracellular acidification rates (ECAR) are affected by metabolic activity and the number of cells[23], both indices were normalized to total protein. Hyperglycemia increased the overall rate of oxygen consumption and part of this effect was related to a 1.5 fold increase in non-mitochondrial oxygen consumption by hyperglycemia: basal OCR minus rotenone + myxothiazol insensitive OCR (Figure 2-8A). Coupled respiration and proton leak were determined using the ATP synthase inhibitor, oligomycin. In the presence of 5.5 mM glucose, SCs devoted 88.2 ± 16.6% of their mitochondrial respiration for ATP production and 11.8% to proton leak. Under hyperglycemic conditions, ATP coupled respiration decreased to 64.5 ± 12.2% and proton leak increased to 35.4%. Thus, hyperglycemia decreased mitochondrial efficiency by uncoupling oxygen consumption from ATP production. Consistent with a decrease in the efficiency of oxidative phosphorylation, hyperglycemia increased extracellular acidification by 2.1 ± 0.4 fold, suggesting an increase in the rate of glycolysis (Figure 2-8B)[29].

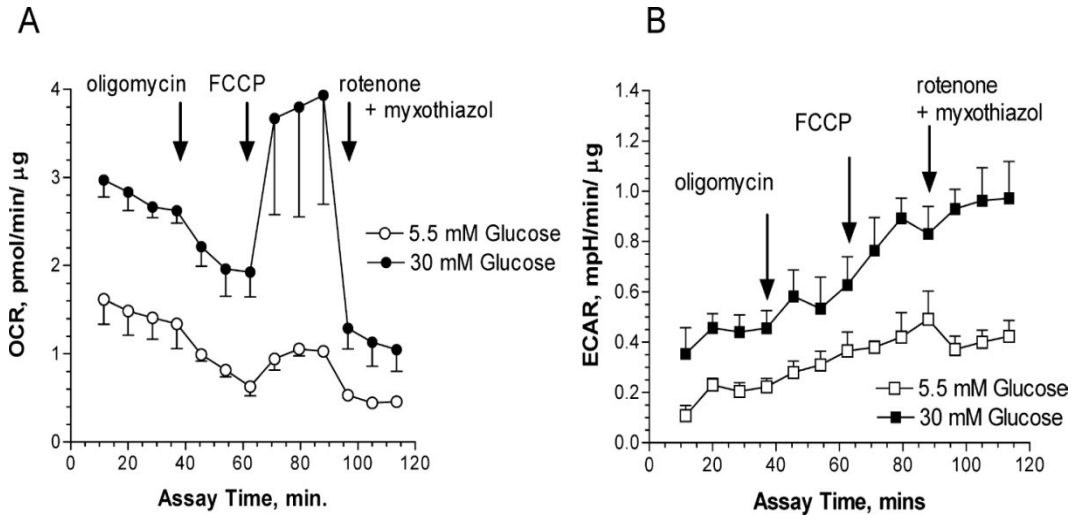

Figure 2-8. Hyperglycemia increased the oxygen consumption rate and extracellular acidification. SCs were subjected to hyperglycemic stress for 3 days and (A) the oxygen consumption rate (OCR) and (B) extracellular acidification rate (ECAR) were measured in intact cells using an Extracellular Flux Analyzer. Oligomycin, FCCP and rotenone/myxothiazole were added at the indicated times to determine the rate of proton leak and O2 coupled ATP production. Respiration experiments were repeated three times and the results presented are four replicate measures per time point from one representative experiment.

Hyperglycemia Increased the Expression of MnSOD but Not the Production of Superoxide Anion

Proteins annotated as mediating mitochondrial detoxification responses showed the largest increase as a class after 6 days of hyperglycemia. Among this group, SILAC analysis indicated that MnSOD (Figure 2-9A) expression increased about 2.0 fold after 6 days of hyperglycemia. The increase in Mn-SOD was specific since a similar change was not observed in the cytosolic Cu/Zn SOD (Figure 2-9B). These differences were confirmed in separate experiments by immunoblot analysis as well. SCs were treated with 5.5 mM or 30 mM glucose for 2-6 days, and heavy mitochondrial and cytosolic fractions were obtained. Curiously, the magnitude of the increase in MnSOD in the heavy mitochondrial fraction seemed slightly greater by immunoblot analysis but was nonetheless consistent with that observed in the purified mitochondria (Figure 2-9C & E). Confirming the mass spectrometric analysis, hyperglycemia did not increase cytosolic levels of CuZn SOD (Figure 2-9D). Consistent with our proteomic data, MnSOD activity also increased by 2-2.5 fold after 4-6 days of hyperglycemia (Figure 2-10A). Lastly, to rule out that the observed changes were the result of osmotic stress, SCs were incubated with 30 mM L-glucose or mannitol for 6 days and a heavy mitochondrial fraction was isolated. No change was observed in the expression of Mn-SOD and prohibitin 1 (data not shown). Since L-glucose is not metabolized, these data suggest that osmotic stress was not sufficient to alter mitochondrial protein expression.

Glucose-induced production of superoxide within mitochondria has been suggested to be a key biochemical feature of glucotoxicity[9,30]. Surprisingly, no significant change in total cellular superoxide levels was observed in the SCs even after

prolonged hyperglycemia (Figure 2-10B). On the other hand, previous studies in embryonic sensory neurons cultured for several days in vitro have suggested that glucose-induced superoxide generation may occur shortly after exposure to high glucose[24]. However, even after 4-6 h of hyperglycemia, we observed no significant increase in superoxide generation (data not shown). Since the above study monitored the cellular conversion of hyroethidine to ethidium, we next used the mitochondrially targeted derivative of hydroethidine, MitoSox Red along with co-staining for mitochondria using MitoTracker Green to more directly visualize if hyperglycemia increased superoxide in the mitochondria. Similar to the above results, six days of hyperglycemia did not significantly enhance mitochondrial superoxide production (Figure 2-10 C & D). However, the mitochondria were actively capable of producing this molecule since a brief incubation with antimycin A clearly increased mitochondrial superoxide generation as shown by the increase intensity of the yellow fluorescence.

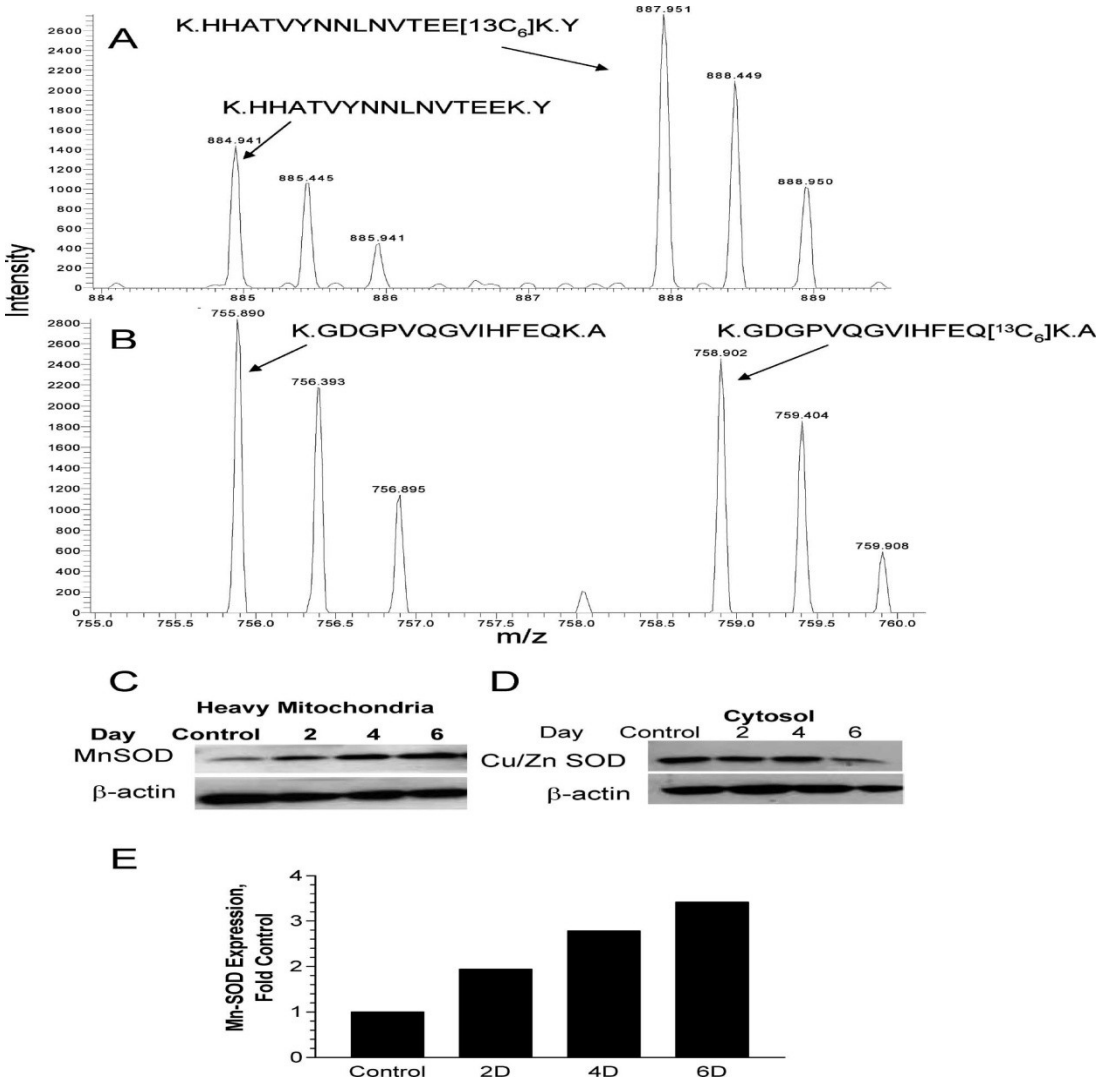

Figure 2-9. MnSOD but not Cu/Zn SOD Increased with Hyperglycemic Stress. SCs were incubated with 5.5 mM (K0) or 30 mM (K6) glucose for 6 days and mitochondrial and cytosolic fractions were isolated. Spectra show MS1 scans indicating (A) an increase in intensity of a representative labeled peptide from mitochondrial MnSOD but (B) no change in intensity of a labeled peptide for cytosolic Cu/Zn SOD. The expression of (C) MnSOD or (D) CuZn SOD was determined by immunoblot analysis using a heavy mitochondrial fraction and cytosolic fraction prepared from SCs were treated for the indicated days with 30 mM glucose. (E) MnSOD expression was normalized to β-actin levels and the average of two separate experiments is expressed as a fold control.

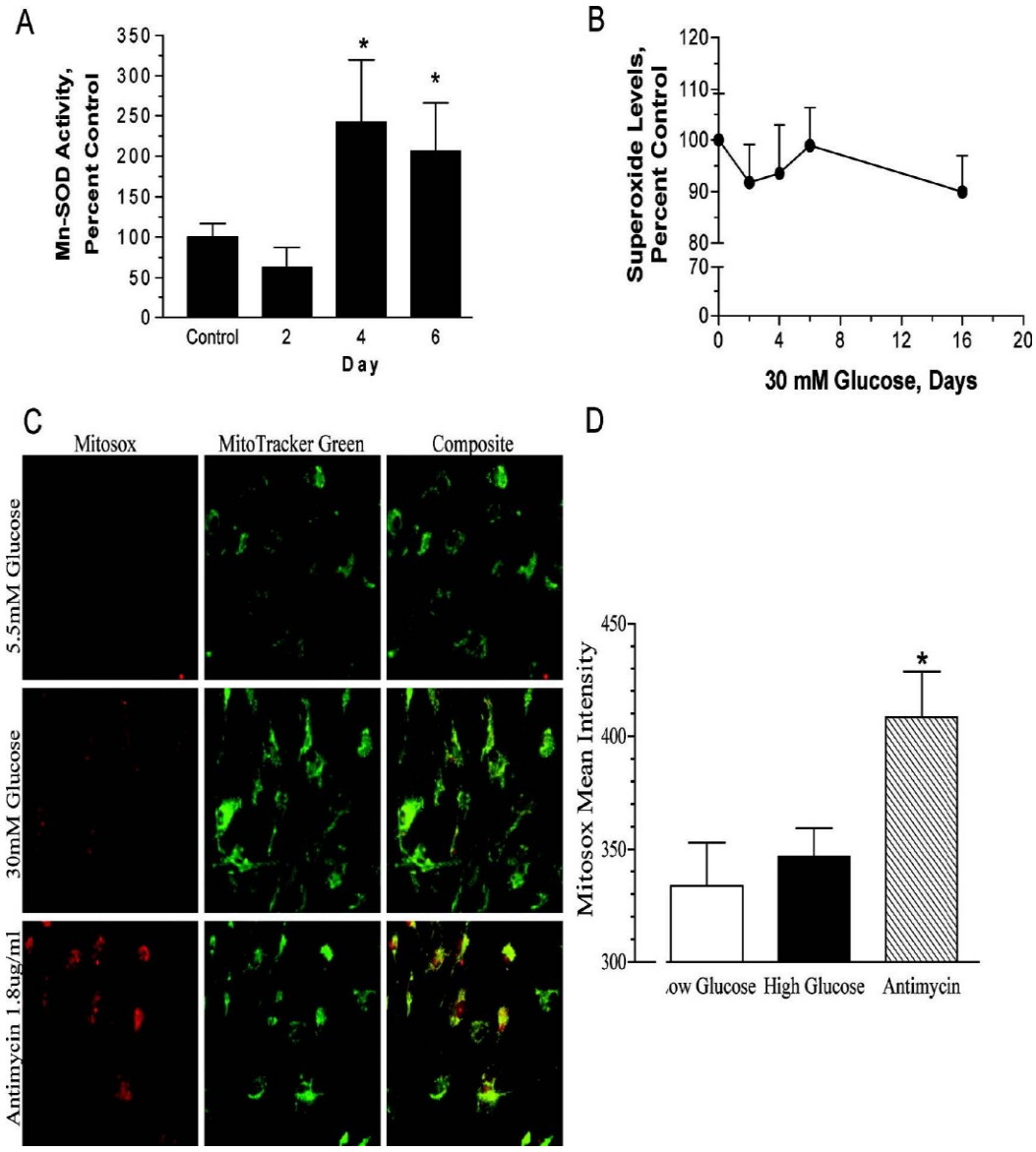

Figure 2-10. Acute hyperglycemia increased MnSOD activity but not superoxide production. (A) SCs were incubated with 5.5 mM or 30 mM glucose for the indicated time and a heavy mitochondrial fraction was isolated. MnSOD activity was determined after a 30 min preincubation with 2 mM NaCN to inhibit residual Cu/Zn SOD activity and results are the mean ± SEM from three separate experiments. *, $p < 0.05$ compared to control. (B) SCs were incubated with 5.5 mM or 30 mM glucose for the indicated time and cellular superoxide levels were determined after the addition of 3 μM dihydroethidine. Results are the mean of four experiments perform with 8 replicates each and are expressed as a percent of control. (C) SCs

were incubated with 5.5 mM or 30 mM glucose for 6 days, treated with MitoSox Red and MitoTracker Green and mitochondrial levels of superoxide were visualized by confocal microscopy. Incubation with Antimycin A served as a positive control for mitochondrial superoxide generation. (D) Quantitative image analysis of superoxide levels. Results are from a representative experiment performed twice and are the mean ± SEM from at least 200 cells per treatment. *, $p < 0.05$ versus low and high glucose treatments.

2.4 Discussion

To date, few studies have used SILAC as an approach to examine the effect of hyperglycemic stress on primary cells that regulate glucose uptake or contribute to diabetic complications. However, the utility of SILAC in identifying novel proteins that may contribute to diabetes is highlighted by a recent report showing that cultured myotubes from extremely obese women secreted almost 3 times more myostatin than myotubes obtained from lean or moderately obese patients[31]. Additionally, SILAC has been used to characterize the phosphoproteome of the insulin signaling pathway[21,32-33]. In the present study, we provide the first quantitative characterization of the temporal effect of hyperglycemia on the proteome of cultured primary SCs using SILAC.

One benefit of the SILAC approach is that the isotopically enriched amino acid is not preferentially incorporated into a given sub-proteome if a sufficient labeling period is performed. Therefore, we characterized the broad effect of hyperglycemia on the SC proteome by isolating cytoplasmic, nuclear and mitochondrial subcellular fractions. After 2 days of hyperglycemia, nuclear proteins affecting chromatin regulation, DNA remodeling and transcription increased but the mean expression ratio was 1.03 for all the proteins identified in the nuclear fraction, suggesting a limited global effect. Similarly, hyperglycemia had little effect on altering cytoplasmic proteins at all time points, but one cytoplasmic enzyme worth noting is aldose reductase. It is well recognized that an increase in aldose reductase activity contributes to the pathophysiology of diabetic neuropathy[34-35]. Although we did not assess aldose reductase activity in the present study, the unbiased identification of aldose reductase indicated that its expression was unaffected by hyperglycemic stress in the cultured SCs. This lack of change in aldose

reductase expression is consistent with previous reports that its mRNA level is not induced in hyperglycemic rat SCs[36] and that aldose reductase immunoreactivity does not increase in SCs of diabetic rat sciatic nerve[37].

In large part, hyperglycemia had the greatest effect on the SC mitochondrial proteome since the average expression ratio was 1.51 for all proteins identified in the mitochondrial fraction. This result is consistent with previous reports that numerous mitochondrial proteins were increased in hearts obtained from OVE26 mice that were diabetic for 18 weeks[38] and in cardiomyocytes from acutely hyperglycemic rats[39]. For example, aconitase, ATP synthase , prohibitin, ATP synthase D chain, and GTP specific succinyl CoA synthetase increased to a similar level in both the hyperglycemically stressed SCs and in diabetic rat heart mitochondria[38]. Interestingly, we also observed an increase in up-regulated during skeletal muscle growth protein 5, a poorly characterized mitochondrial protein which associates with ATP synthase[40]. This protein is also known as diabetes-associated protein in insulin sensitive tissues (DAPIT) since its mRNA decreased in muscle but not brain of diabetic rats[41]. Thus, DAPIT may be a novel glucose-responsive protein that affects mitochondrial function in diabetic tissues. Although we did not explore the mechanism by which high glucose caused such a broad increase in mitochondrial proteins, evidence exists for an increase in mitochondrial biogenesis in diabetic heart[38]. Consistent with the possibility of an acute increase in mitochondrial biogenesis, mitochondrial transcription factor A is critical for the replication of mitochondrial DNA,[42] and it was increased approximately 1.7 fold after 2 or 6 days of hyperglycemia.

A recent report has demonstrated that diabetes induced a tissue-specific remodeling of the mitochondrial proteome in organs derived from 6-week old diabetic Akita mice that did not necessarily correlate with changes in mitochondrial function[43]. For example, despite a diabetes-induced increase in proteins involved in oxidative phosphorylation and the TCA cycle, no changes were observed in mitochondrial respiration in organelles obtained from liver, brain or kidney[43]. However, in heart mitochondria, diabetes decreased the expression of proteins involved in oxidative phosphorylation and the TCA cycle and this correlated with a decrease in mitochondrial respiration. These data highlight the issue that hyperglycemic stress can differentially affect the mitochondrial proteome and respiratory activity. Since it is difficult to model chronic diabetes in a cell culture model, the overall increase in the SC mitochondrial proteome in our acute cell culture model may more reflect early protective responses to hyperglycemic rather than chronic damage. Proteomic analysis of mitochondria isolated from dorsal root ganglia and sciatic nerve of animals rendered diabetic for various durations will provide further insight into the utility of the primary cell models to address more mechanistic issues contributing to changes in the proteome associated with protective versus degenerative responses.

Despite the increase in mitochondrial respiratory proteins in heart mitochondria from diabetic mice, the respiratory control ratio was actually lower but the coupling of ATP production and oxygen consumption (P/O ratio) was not affected[38]. Although mitochondrial respiration is often measured using purified mitochondria, the use of the XF24 Extra-cellular Flux Analyzer allowed us to use intact SCs to assess both mitochondrial and non-mitochondrial effects of glucose on oxygen consumption and

medium acidification. In 5.5 mM glucose, ~88% of the mitochondrial oxygen consumption was coupled to ATP production in intact SCs. In contrast, hyperglycemia decreased the amount of ATP-coupled oxygen consumption by 27% and increased the extent of proton leak 3-fold. The decreased efficiency and increased proton leak suggests that hyperglycemia is lowering the P/O ratio, but we did not directly assess this parameter. Although our data does reflect the physiological response of the intact SCs to high glucose, it is difficult to directly compare these data with the lack of a change in the P/O ratio observed in mitochondria from diabetic heart[38] due to the different experimental conditions. Lastly, although glycolytic proteins did not increase in expression after 2-6 days of hyperglycemia, 3 days of hyperglycemia increased ECAR, which is an indirect measure of glycolytic activity (lactic acid production) and non-glycolytic acidification from CO_2 production[23]. These data suggest that the cultured SCs are highly glycolytic even in the absence of protein upregulation.

The putative physiological role of proton leak is to contribute to the uncoupling of electron transport from ATP synthesis (heat generation) and decrease oxidative stress by reactive oxygen species[44]. Although increases in the mitochondrial membrane surface area and phospholipid composition can affect the basal leak rate, changes in the expression of the adenine nucleotide transporter 1 protein (ANT1) can also contribute to mild uncoupling[44]. Previous data has shown that a 1.7 fold increase in ANT1 can increase proton leak by about 1.5 fold in isolated mitochondria[45]. We found that hyperglycemia induced a 1.5 fold increase in ANT1 expression after 2-6 days (Supplementary Table 1-3, Appendix) and this correlated with an increased proton leak from a basal level of 12% in 5.5 mM glucose to about 35%. Although uncoupling

proteins may also contribute to enhanced proton leak, a genomic study of mouse peripheral nerve from embryonic day 17 through adulthood found that transcripts for the uncoupling proteins (UCP1-3) were not expressed[46]. Thus, it is unlikely that hyperglycemia also increases UCPs, but additional studies are needed to determine if ANT1 directly contributes to the increased proton leak.

Previous reports have proposed that mitochondrial superoxide production may be a unifying biochemical lesion that contributes to increases in polyol synthesis and other molecular pathologies of hyperglycemia[4-5]. However, we were not able to detect a significant increase in superoxide production in SC following up to 6 days of hyperglycemia and this correlated with an increase in mitochondrial Mn-SOD expression and activity. Vincent and colleagues recently reported a similar resistance of SCs to glucose-dependent oxidative stress that correlated with a rapid increase in nuclear levels of Nrf2, a critical transcription factor which regulates the expression of antioxidant genes such as superoxide dismutase, catalase, and heme oxygenase 1[47]. Indeed, the basal activity of catalase in SCs was about 4-fold greater than the corresponding activity in sensory neurons[47]. It is also interesting to note that increased proton leak can also protect against mitochondrial damage induced by reactive oxygen species, such as superoxide[48-49]. Together, these results suggest that in neonatal SCs, mitochondria may possess multiple pathways to help minimize short-term glucose-induced oxidative stress and that hyperglycemia can alter the SC mitochondrial proteome independent of superoxide generation. On the other hand, 24 h of hyperglycemic stress increased superoxide levels and overall protein nitration in commercially supplied, cultured adult human SCs[6,50]. Unfortunately, the reason for the discrepant results between primary neonatal rat and the

adult human SCs is unclear. One possibility may reside in the maturity or natural history of the adult human SCs. Precedence exists that developmental maturity can affect the response of cells to hyperglycemia since 24 h of hyperglycemia induces death of rat embryonic sensory neurons after 3 days in culture[24,51]. However, adult rat sensory neurons and embryonic sensory neurons that have been permitted to mature and differentiate in culture for 3 weeks are both resistant to glucose-induced apoptosis[52-53]. Importantly, it is unlikely that the neonatal cells have lost the SC phenotype and/or the ability to respond to hyperglycemic stress since they are competent to myelinate[53], a hallmark of SC function. Whether the adult human SCs are myelination competent is unclear. Additionally, the myelinated neonatal SCs can respond to hyperglycemic stress since the extent of neuregulin-induced demyelination was increased by high glucose concentrations[53]. Thus, primary neonatal and adult SCs may serve as complementary models to examine the effect of glucose on the mitochondrial proteome and function in the absence or presence of substantial superoxide production, respectively.

It is important to note that SCs undergo degeneration in diabetic neuropathy[54] and that increased superoxide production, protein nitration, and mitochondrial dysfunction contributes to DPN[55]. At first blush, these results would appear contradictory with our findings. However, it is not surprising that the *in vivo* increase in superoxide and nitrotyrosine levels in SCs after 4 or more weeks of diabetes does not mimic what we observed in the primary SC cultures. Although there are numerous possibilities for this difference, one explanation consistent with a recent report is that protective antioxidant responses may be overwhelmed with increasing duration of diabetes. For example, diabetic adult sensory neurons mount a transient antioxidant response in response to *ex*

vivo hyperglycemia that is characterized by a brief upregulation of Mn-SOD after one day of hyperglycemia followed by a subsequent decline[52]. Additional studies are needed to determine if adult SCs mount a transient antioxidant response during the early onset of diabetes that may be eventually overwhelmed with disease duration.

In conclusion, we have used quantitative proteomics to assess the effect of hyperglycemia on the SC proteome. Hyperglycemia increased the expression of numerous mitochondrial proteins but whether this effect is due to an increase in overall mitochondrial mass, as previously reported in diabetic heart, remains to be determined. Glucose did not increase superoxide production in SCs and this correlated with an increase in MnSOD and the extent of proton leak, which may function in reducing oxidative stress. Consistent with a recent report[47], our data support that primary, neonatal rat SCs are rather insensitive to glucose-induced oxidative stress and that the mitochondrial proteome can undergo dynamic remodeling in response to hyperglycemia.

References

1. Said, G. Diabetic neuropathy[mdash]a review. *Nat Clin Pract Neuro* **3**, 331-340 (2007).
2. Fernyhough, P., Huang, T.-J. & Verkhratsky, A. Mechanism of mitochondrial dysfunction in diabetic sensory neuropathy. *Journal of the Peripheral Nervous System* **8**, 227-235 (2003).
3. Huang, T.-J.*, et al.* Insulin Prevents Depolarization of the Mitochondrial Inner Membrane in Sensory Neurons of Type 1 Diabetic Rats in the Presence of Sustained Hyperglycemia. *Diabetes* **52**, 2129-2136 (2003).
4. Du, X.-L.*, et al.* Hyperglycemia-induced mitochondrial superoxide overproduction activates the hexosamine pathway and induces plasminogen activator inhibitor-1 expression by increasing Sp1 glycosylation. *Proceedings of the National Academy of Sciences* **97**, 12222-12226 (2000).
5. Nishikawa, T.*, et al.* Normalizing mitochondrial superoxide production blocks three pathways of hyperglycaemic damage. *Nature* **404**, 787-790 (2000).
6. Obrosova, I.G.*, et al.* Oxidative-Nitrosative Stress and Poly(ADP-Ribose) Polymerase (PARP) Activation in Experimental Diabetic Neuropathy. *Diabetes* **54**, 3435-3441 (2005).
7. Drel, V.R., Pacher, P., Stevens, M.J. & Obrosova, I.G. Aldose reductase inhibition counteracts nitrosative stress and poly(ADP-ribose) polymerase activation in diabetic rat kidney and high-glucose-exposed human mesangial cells. *Free Radical Biology and Medicine* **40**, 1454-1465 (2006).
8. Obrosova, I.G.*, et al.* Role of nitrosative stress in early neuropathy and vascular dysfunction in streptozotocin-diabetic rats. *American Journal of Physiology - Endocrinology And Metabolism* **293**, E1645-E1655 (2007).
9. Pop-Busui, R., Sima, A. & Stevens, M. Diabetic neuropathy and oxidative stress. *Diabetes/Metabolism Research and Reviews* **22**, 257-273 (2006).
10. Vincent, A.M., Russell, J.W., Low, P. & Feldman, E.L. Oxidative Stress in the Pathogenesis of Diabetic Neuropathy. *Endocrine Reviews* **25**, 612-628 (2004).
11. Andersen, J.S. & Mann, M. Organellar proteomics: turning inventories into insights. *EMBO Rep* **7**, 874-879 (2006).
12. Yu, C., Alterman, M. & Dobrowsky, R.T. Ceramide displaces cholesterol from lipid rafts and decreases the association of the cholesterol binding protein caveolin-1. *Journal of Lipid Research* **46**, 1678-1691 (2005).
13. Zhang, G., Spellman, D.S., Skolnik, E.Y. & Neubert, T.A. Quantitative Phosphotyrosine Proteomics of EphB2 Signaling by Stable Isotope Labeling with Amino Acids in Cell Culture (SILAC). *Journal of Proteome Research* **5**, 581-588 (2006).
14. Okado-Matsumoto, A. & Fridovich, I. Subcellular Distribution of Superoxide Dismutases (SOD) in Rat Liver. *Journal of Biological Chemistry* **276**, 38388-38393 (2001).
15. Hwang, S.-I.*, et al.* Systematic Characterization of Nuclear Proteome during Apoptosis. *Molecular & Cellular Proteomics* **5**, 1131-1145 (2006).
16. Steen, H. & Mann, M. The abc's (and xyz's) of peptide sequencing. *Nat Rev Mol Cell Biol* **5**, 699-711 (2004).
17. Shevchenko, A., Tomas, H., Havlis, J., Olsen, J.V. & Mann, M. In-gel digestion for mass spectrometric characterization of proteins and proteomes. *Nat. Protocols* **1**, 2856-2860 (2007).
18. Peng, J.M., Elias, J.E., Thoreen, C.C., Licklider, L.J. & Gygi, S.P. Evaluation of multidimensional chromatography coupled with tandem mass spectrometry (LC/LC-MS/MS) for large-scale protein analysis: The yeast proteome. *Journal of Proteome Research* **2**, 43-50 (2003).

19. Zubarev, R. & Mann, M. On the Proper Use of Mass Accuracy in Proteomics. *Molecular & Cellular Proteomics* **6**, 377-381 (2007).
20. Schulze, W.X. & Mann, M. A Novel Proteomic Screen for Peptide-Protein Interactions. *Journal of Biological Chemistry* **279**, 10756-10764 (2004).
21. Foster, L.J.*, et al.* Insulin-dependent Interactions of Proteins with GLUT4 Revealed through Stable Isotope Labeling by Amino Acids in Cell Culture (SILAC)*. *Journal of Proteome Research* **5**, 64-75 (2005).
22. Maere, S., Heymans, K. & Kuiper, M. BiNGO: a Cytoscape plugin to assess overrepresentation of Gene Ontology categories in Biological Networks. *Bioinformatics* **21**, 3448-3449.
23. Wu, M.*, et al.* Multiparameter metabolic analysis reveals a close link between attenuated mitochondrial bioenergetic function and enhanced glycolysis dependency in human tumor cells. *American Journal of Physiology - Cell Physiology* **292**, C125-C136 (2007).
24. Vincent, A.M., McLean, L.L., Backus, C. & Feldman, E.L. Short-term hyperglycemia produces oxidative damage and apoptosis in neurons. *The FASEB Journal* (2005).
25. Robinson, K.M., Janes, M.S. & Beckman, J.S. The selective detection of mitochondrial superoxide by live cell imaging. *Nat. Protocols* **3**, 941-947 (2008).
26. Blagoev, B., Ong, S.-E., Kratchmarova, I. & Mann, M. Temporal analysis of phosphotyrosine-dependent signaling networks by quantitative proteomics. *Nat Biotech* **22**, 1139-1145 (2004).
27. Johnson, D.T.*, et al.* Tissue heterogeneity of the mammalian mitochondrial proteome. *American Journal of Physiology - Cell Physiology* **292**, C689-C697 (2007).
28. Price, S.A., Zeef, L.A.H., Wardleworth, L., Hayes, A. & Tomlinson, D.R. Identification of Changes in Gene Expression in Dorsal Root Ganglia in Diabetic Neuropathy: Correlation With Functional Deficits. *Journal of Neuropathology & Experimental Neurology* **65**, 722-732 710.1097/1001.jnen.0000228199.0000289420.0000228190 (2006).
29. Choi, S.W., Gerencser, A.A. & Nicholls, D.G. Bioenergetic analysis of isolated cerebrocortical nerve terminals on a microgram scale: spare respiratory capacity and stochastic mitochondrial failure. *Journal of Neurochemistry* **109**, 1179-1191 (2009).
30. Tomlinson, D.R. & Gardiner, N.J. Glucose neurotoxicity. *Nat Rev Neurosci* **9**, 36-45 (2008).
31. Hittel, D.S., Berggren, J.R., Shearer, J., Boyle, K. & Houmard, J.A. Increased Secretion and Expression of Myostatin in Skeletal Muscle From Extremely Obese Women. *Diabetes* **58**, 30-38 (2009).
32. Krüger, M.*, et al.* Dissection of the insulin signaling pathway via quantitative phosphoproteomics. *Proceedings of the National Academy of Sciences* **105**, 2451-2456 (2008).
33. Hanke, S. & Mann, M. The Phosphotyrosine Interactome of the Insulin Receptor Family and Its Substrates IRS-1 and IRS-2. *Molecular & Cellular Proteomics* **8**, 519-534 (2009).
34. Obrosova, I.G.*, et al.* Aldose Reductase Inhibition Counteracts Oxidative-Nitrosative Stress and Poly(ADP-Ribose) Polymerase Activation in Tissue Sites for Diabetes Complications. *Diabetes* **54**, 234-242 (2005).
35. Ho, E.C.M.*, et al.* Aldose Reductase–Deficient Mice Are Protected From Delayed Motor Nerve Conduction Velocity, Increased c-Jun NH2-Terminal Kinase Activation, Depletion of Reduced Glutathione, Increased Superoxide Accumulation, and DNA Damage. *Diabetes* **55**, 1946-1953 (2006).
36. Maekawa, K.*, et al.* Expression of aldose reductase and sorbitol dehydrogenase genes in Schwann cells isolated from rat: effects of high glucose and osmotic stress. *Molecular Brain Research* **87**, 251-256 (2001).

37. Jiang, Y., Calcutt, N.A., Rames, K.M. & Mizisin, A.P. Novel sites of aldose reductase immunolocalization in normal and streptozotocin-diabetic rats. *Journal of the Peripheral Nervous System* **11**, 274-285 (2006).
38. Shen, X.*, et al.* Cardiac mitochondrial damage and biogenesis in a chronic model of type 1 diabetes. *American Journal of Physiology - Endocrinology And Metabolism* **287**, E896-E905 (2004).
39. Warda, M.*, et al.* Simulated hyperglycemia in rat cardiomyocytes: A proteomics approach for improved analysis of cellular alterations. *PROTEOMICS* **7**, 2570-2590 (2007).
40. Meyer, B., Wittig, I., Trifilieff, E., Karas, M. & Schägger, H. Identification of Two Proteins Associated with Mammalian ATP Synthase. *Molecular & Cellular Proteomics* **6**, 1690-1699 (2007).
41. Paivarinne, H. & Kainulainen, H. DAPIT, a novel protein down-regulated in insulin-sensitive tissues in streptozotocin-induced diabetes. *Acta Diabetologica* **38**, 83-86 (2001).
42. Tsutsui, H., Kinugawa, S. & Matsushima, S. Mitochondrial oxidative stress and dysfunction in myocardial remodelling. *Cardiovascular Research* **81**, 449-456 (2009).
43. Bugger, H.*, et al.* Tissue-Specific Remodeling of the Mitochondrial Proteome in Type 1 Diabetic Akita Mice. *Diabetes* **58**, 1986-1997 (2009).
44. Brand, M.D. The efficiency and plasticity of mitochondrial energy transduction. *Biochemical Society Transactions* **33**, 897-904 (2005).
45. Brand, M.D.*, et al.* The basal proton conductance of mitochondria depends on adenine nucleotide translocase content. *Biochemical Journal* **392**, 353-362 (2005).
46. Verheijen, M.H.G., Chrast, R., Burrola, P. & Lemke, G. Local regulation of fat metabolism in peripheral nerves. *Genes & Development* **17**, 2450-2464 (2003).
47. Vincent, A.M., Kato, K., McLean, L.L., Soules, M.E. & Feldman, E.L. Sensory Neurons and Schwann Cells Respond to Oxidative Stress by Increasing Antioxidant Defense Mechanisms. *Antioxidants & Redox Signaling* **11**, 425-438 (2009).
48. Brand, M.D.*, et al.* Mitochondrial superoxide: production, biological effects, and activation of uncoupling proteins. *Free Radical Biology and Medicine* **37**, 755-767 (2004).
49. Echtay, K.S., Pakay, J.L., Esteves, T.C. & Brand, M.D. Hydroxynonenal and uncoupling proteins: A model for protection against oxidative damage. *Biofactors* **24**, 119-130 (2005).
50. Askwith, T., Zeng, W., Eggo, M.C. & Stevens, M.J. Oxidative stress and dysregulation of the taurine transporter in high-glucose-exposed human Schwann cells: implications for pathogenesis of diabetic neuropathy. *American Journal of Physiology - Endocrinology And Metabolism* **297**, E620-E628 (2009).
51. Russell, J.W., Sullivan, K.A., Windebank, A.J., Herrmann, D.N. & Feldman, E.L. Neurons Undergo Apoptosis in Animal and Cell Culture Models of Diabetes. *Neurobiology of Disease* **6**, 347-363 (1999).
52. Zherebitskaya, E., Akude, E., Smith, D.R. & Fernyhough, P. Development of Selective Axonopathy in Adult Sensory Neurons Isolated From Diabetic Rats. *Diabetes* **58**, 1356-1364 (2009).
53. Yu, C., Rouen, S. & Dobrowsky, R.T. Hyperglycemia and downregulation of caveolin-1 enhance neuregulin-induced demyelination. *Glia* **56**, 877-887 (2008).
54. Eckersley, L. Role of the Schwann cell in diabetic neuropathy. *Neurobiology of Diabetic Neuropathy* **50**, 293-321 (2002).
55. Vareniuk, I., Pavlov, I. & Obrosova, I. Inducible nitric oxide synthase gene deficiency counteracts multiple manifestations of peripheral neuropathy in a streptozotocin-induced mouse model of diabetes. *Diabetologia* **51**, 2126-2133 (2008).

Chapter 3: C-Terminal Heat Shock Protein 90 Inhibitor Decreases Hyperglycemia-induced Oxidative Stress and Improves Mitochondrial Bioenergetics in Sensory Neurons

Zhang, L., Zhao, H., Blagg, B.S.J. and Dobrowsky, R.T. (2012) A C-Terminal Heat Shock Protein 90 Inhibitor Decreases Hyperglycemia-induced Oxidative Stress and Improves Mitochondrial Bioenergetics in Sensory Neurons. J. Proteome Res. ***11***, 2581-2593.*)*

Abstract

Diabetic peripheral neuropathy (DPN) is a common complication of diabetes in which hyperglycemia-induced mitochondrial dysfunction and enhanced oxidative stress contribute to sensory neuron pathology. KU-32 is a novobiocin-based, C-terminal inhibitor of the molecular chaperone, heat shock protein 90 (Hsp90). KU-32 ameliorates multiple sensory deficits associated with the progression of DPN and protects unmyelinated sensory neurons from glucose-induced toxicity. Mechanistically, KU-32 increased the expression of Hsp70, and this protein was critical for drug efficacy in reversing DPN. However, it remained unclear if KU-32 had a broader effect on chaperone induction and if its efficacy was linked to improving mitochondrial dysfunction. Using cultures of hyperglycemically stressed primary sensory neurons, the present study investigated whether KU-32 had an effect on the translational induction of other chaperones and improved mitochondrial oxidative stress and bioenergetics. A variation of stable isotope labeling with amino acids in cell culture called pulse SILAC (pSILAC) was used to unbiasedly assess changes in protein translation. Hyperglycemia decreased the translation of numerous mitochondrial proteins that affect superoxide levels

and respiratory activity. Importantly, this correlated with a decrease in mitochondrial oxygen consumption and an increase in superoxide levels. KU-32 increased the translation of Mn superoxide dismutase and several cytosolic and mitochondrial chaperones. Consistent with these changes, KU-32 decreased mitochondrial superoxide levels and significantly enhanced respiratory activity. These data indicate that efficacy of modulating molecular chaperones in DPN may be due in part to improved neuronal mitochondrial bioenergetics and decreased oxidative stress.

3.1 Introduction

Diabetic peripheral neuropathy (DPN) is a neurodegenerative complication of diabetes that develops in 50−60% of diabetic patients[1]. DPN has proven difficult to manage pharmacologically since it does not result from a single biochemical etiology that is manifested uniformly for the disease's duration (10−30 yrs). Molecular targets that are relatively "diabetes specific" (polyol and hexosamine pathways, advanced glycation end products) or which are altered in numerous disease states (PKC activation, altered neurotrophic support, enhanced oxidative stress) contribute to the progressive degeneration of small and large sensory fibers in DPN[2]. However, current small molecule inhibitors of the above pathways/products have yielded few therapeutic agents. Clearly, the rational identification of new molecular paradigms that ameliorate DPN and offer "druggable" targets affords translational potential for improving the medical management of DPN.

Many neurodegenerative diseases fall into a class of protein-conformational disorders since their etiology is linked to the accumulation of specific mis-folded or aggregated proteins (for example, β-amyloid and tau in Alzheimer's disease)[3]. Though the etiology of DPN is not causally linked to the accrual of any one specific mis-folded or aggregated protein, hyperglycemia can increase oxidative stress[4]. The oxidative modification of amino acids[5-6] can impair protein folding[3], decrease mitochondrial function and protein import[2,5,7] and increase interaction with molecular chaperones[8].

Molecular chaperones such as heat shock proteins 90 and 70 (Hsp90, Hsp70) are critical for folding nascent proteins. However, both of these chaperones are components of the cellular heat shock response (HSR). Numerous conditions that promote cell stress

lead to the Hsp90-dependent induction of the HSR which, in part, promotes the transient up-regulation of Hsp70 to aid the refolding or clearance of aggregated and damaged proteins[8]. Hsp70 upregulation can also prevent neuronal apoptosis[9] and decrease oxidative stress in neurodegenerative disorders[10]. Importantly, the HSR can be pharmacologically activated by inhibiting Hsp90 and we have developed and validated KU-32 as a novel, novobiocin-based, C-terminal Hsp90 inhibitor[11-12] that protects against in vitro neuronal cell death[13-14]. KU-32 also effectively reversed preexisting psychosensory and electrophysiologic deficits of DPN in mice and its efficacy required Hsp70 since the drug was ineffective at reversing DPN modeled in Hsp70.1 and Hsp70.3 double knockout mice[15]. While these data clearly support that modulating molecular chaperones offers a potentially novel approach toward treating sensory neuron dysfunction in DPN, additional insight into the mechanism by which KU-32 may improve the function of glycemically stressed neurons is needed.

Increased oxidative stress and mitochondrial dysfunction are strongly implicated in the pathogenesis of DPN[5,16]. Using variations of stable isotope labeling of amino acids in culture (SILAC), we have recently shown that numerous mitochondrial proteins are downregulated in response to hyperglycemia in cultured primary Schwann cells and dorsal root ganglia obtained from diabetic rats[17-18]. Importantly, decreases in the mitochondrial proteome correlated with a decrease in mitochondrial respiratory capacity[18]. However, as the level of all proteins is affected by the balance between their rates of synthesis versus degradation, these studies provided no insight into possible effects of hyperglycemia on the rate of protein translation. Indeed, little is known regarding the effect of hyperglycemia on rates of protein translation in sensory neurons.

In the present study, we took an unbiased approach to address the effect of hyperglycemia on protein translation using pulse SILAC (pSILAC)[19]. Moreover, since the mechanism of KU-32 invokes an increase in chaperone translation, we assessed the effect of hyperglycemia and KU-32 treatment on translation of mitochondrial proteins in sensory neurons. We identify that hyperglycemia decreases the translation of numerous mitochondrial proteins and this correlates with an increase in mitochondrial superoxide levels and a decrease in mitochondrial respiratory function. KU-32 increased the overall rate of protein translation in glycemically stressed neurons, including several cytosolic and mitochondrial chaperones, components of the mitochondrial respiratory chain and Mn superoxide dismutase (MnSOD). Importantly, these changes correlated with a decrease in mitochondrial superoxide levels and increased mitochondrial respiratory capacity. Collectively, these data suggest that KU-32 may improve the sensory deficits associated with DPN by enhancing chaperone levels and improving mitochondrial function.

3.2 Experimental Procedure

Preparation of Embryonic Dorsal Root Ganglion Sensory Neurons

Dorsal root ganglion (DRG) neurons were dissected from embryonic day 15−18 rat pups and the ganglia were collected into L15 medium[20]. The tissue was dissociated with 0.25% trypsin at 37 °C for 30 min, the cells resuspended in DMEM containing 25 mM glucose, 10% fetal calf serum (FCS, Atlas Biologicals, Fort Collins, CO) and triturated with a fire-polished glass pipette. The cells were counted and plated in the center of collagen coated (0.1 mg/mL collagen followed by overnight air drying in a laminar flow hood) 35 mm dishes at a density of (2−3) × 10^5 cells per dish. The cells were cultured in maintenance medium composed of DMEM (4.5 mg/mL glucose, 25 mM) containing 10% dialyzed FCS, 1× penicillin/streptomycin, 1× gentamicin and 50 ng/mL NGF (Harlan Biosciences, Indianapolis, IN). To remove proliferating cells, the neurons were treated with 40 μM of fluorodeoxyuridine and 10 μM cytosine β-D-arabinoside for two days and the drugs withdrawn for 2 days; this cycle was repeated two more times. As the basal glucose concentration in the culture medium was 25 mM, hyperglycemia was induced by the addition of 20 mM excess glucose as we and others have described previously[15,21-22]. All animal procedures were performed in accordance with protocols approved by the Institutional Animal Care and Use Committee and in compliance with standards and regulations for care and use of laboratory rodents set by the National Institutes of Health.

[^{3}H]Leucine Pulse

To assess the global effect of hyperglycemia and KU-32 on protein translation,

neurons were seeded in 12 well plates at 1×10^5 cells per well and treated for 5 days in the absence or presence of 45 mM glucose. During the final 24 h of the incubation, the cells were treated with DMSO or 1 μM KU-32 and pulsed with 1 μCi/ml L-[2,3,4,5-^{3}H]Leucine (American Radiolabeled Chemicals, St. Louis, MO). The cells were washed with ice-cold phosphate-buffered saline (PBS), scraped into 50 mM Tris-HCl, pH 7.4, 150 mM NaCl, 1 mM EDTA, 1% NP40, 1x Complete protease inhibitors (Roche Diagnostics, Indianapolis, IN) and an aliquot removed for protein determination. Equal amounts of total protein were precipitated by the addition of ice cold trichloroacetic acid to a final concentration of 25% and the precipitate was pelleted by centrifugation. The pellet was washed twice with −20 °C acetone, air-dried and radioactivity quantified by scintillation spectrometry.

pSILAC Labeling

Lysine (Lys)/Arginine (Arg) deficient DMEM and isotopically enriched (>98%) [$^2H_4$] L-Lys; [$^{13}C_6$] L-Arg; [$^{13}C_6$, $^{15}N_2$] L-Lys and [$^{13}C_6$, $^{15}N_4$] L-Arg were purchased from Sigma-Isotec (St. Louis, MO). For each neuron preparation, we performed three different sets of experiments to analyze the effect of hyperglycemia and KU-32 on protein translation. The isotopic mixtures and treatments used in the pSILAC[19] experiments are summarized in Table 1. To assess the effect of hyperglycemia on translation, the neurons were cultured in maintenance medium containing 125 mg/L ^{12}C-Lys and 84 mg/L ^{12}C-Arg (K0R0) in the absence or presence of 45 mM glucose for 5 days. For the final 48 h of the incubation, control cultures were isotopically pulsed in DMEM supplemented with [$^2H_4$] Lys and [$^{13}C_6$] Arg (K4R6) while cells subjected to hyperglycemia were pulsed in

culture medium containing [$^{13}C_6$, $^{15}N_2$] Lys and [$^{13}C_6$, $^{15}N_4$] Arg (K8R10). To assess the effect of KU-32 on translation under normoglycemic conditions, the drug was added for the final 24 h to neurons pulsed with K8R10; cells pulsed with K4R6 received DMSO. When assessing the effect of KU-32 on translation under hyperglycemic conditions, neurons were maintained in medium containing 45 mM glucose for 5 days and 1 μM KU-32 was added for the final 24 h to neurons pulsed with K4R6; DMSO was added to the cultures pulsed with K8R10. KU-32 [N-(7-((2R,3R,4S,5R)-3,4-dihydroxy-5-methoxy-6,6-dimethyl-tetrahydro-2H–pyran-2-yloxy)-8-methyl-2-oxo-2H-chromen-3-yl) acetamide] was synthesized and structural purity (>95%) verified as previously described[23].

At the end of the incubations, the cells were washed with ice-cold PBS and resuspended in 0.5 mL of mitochondrial isolation buffer (MIBA) containing 10 mM Tris-HCl, pH 7.4, 1 mM EDTA, 0.2 M D-mannitol, 0.05 M sucrose, 0.5 mM sodium orthovanadate, 1 mM sodium fluoride and 1× Complete protease inhibitors[24]. The cells were homogenized and the protein concentration of each lysate was measured in quadruplicate using the Bradford assay and bovine serum albumin as the standard. The samples were then mixed together in a 1:1 mass ratio and the combined lysate was centrifuged at 800× g for 10 min at 4 °C. The supernatant was recovered, a heavy mitochondrial fraction isolated by centrifugation at 8000× g for 5 min at 4 °C and the pellet washed twice with ice-cold MIBA buffer. Three biological replicates were performed for the MS analysis using neurons obtained from separate litters of embryonic rat pups. Three additional biologic replicates using neurons obtained from separate litters were performed to validate some of the MS data using immunoblot analysis: monoclonal

antibodies included Hsp70, mitochondrial Hsp70 and Hsc70 (Stressgen/Enzo Life Sciences, Farmingdale, NY); MnSOD (Upstate Biotechnology/Millipore, Billerica, MA) and β-actin (MP Biomedicals, Solon, OH). Hsp60 and Hsp70 protein 12A polyclonal and secondary antibodies were from Santa Cruz Biotechnology (Santa Cruz, CA).

Mass Spectrometry and Protein Identification

Proteins were identified following one-dimensional SDS-PAGE coupled to RP-HPLC linear quadrupole ion trap Fourier transform ion cyclotron resonance tandem mass spectrometry (GeLC-LTQ-FT MS/MS)[25]. About 50 μg of protein was fractionated by SDS-PAGE, the proteins were visualized by staining the gel and the lanes were cut into 10−12 × 0.5 cm sections for in-gel tryptic digestion.

Tryptic digestion of the proteins was performed as described previously[17-18]. The peptides were separated on a 0.30 × 150 mm, Pepmap C_{18} microcapillary reverse-phase column at a flow rate of 5−10 μL/min with a linear gradient from 5 to 65% acetonitrile in 0.06% aqueous formic acid (v/v) over 65 min. The eluate was introduced into the LTQ-FT tandem mass spectrometer (ThermoFinnigan, Waltham, MA) and mass spectra were acquired in the positive ion mode. All experiments were performed in data-dependent mode using dynamic exclusion with survey MS spectra (m/z 300−2000) acquired in the FT-ICR cell with resolution R = 50000 at m/z 400 and accumulation to a target value of 5×10^5 charges, or a maximum ion accumulation time of 2000 ms. The five most intense ions were isolated and fragmented with a target value of 2×10^3 accumulated ions and an ion selection threshold of 3000 counts. Dynamic exclusion duration was typically 180 s with early expiration if ion intensity fell below a S/N threshold of 2. The ESI source was

operated with a spray voltage of 2.8 kV, a tube lens offset of 130 V and a capillary temperature of 200 °C. All other source parameters were optimized for maximum sensitivity of a synthetic YGGFL peptide ion at m/z 556.27.

Protein Identification and Quantification

Peak lists were acquired from the Xcalibur .raw files using MaxQuant v1.1.1.36[26]. Protein identification utilized the integrated Andromeda search engine[27] queried against the rat IPI database (v3.80, 39,473 entries) that was concatenated with forward plus reverse sequences and supplemented with common contaminants. Search parameters specified a MS tolerance of 20 ppm, a fragment tolerance of 0.5 Da, up to 2 missed cleavages, 3 labeled amino acids per peptide and carboxyamidomethylated cysteine as a fixed modification. Variable modifications were set to consider methionine oxidation and protein N-terminal acetylation. It is not necessary to specify the isotopic labels as variable modifications when using the MaxQuant software[28] but the multiplicity was set to three to consider the K4R6 and K8R10 isotope combinations.

The experimental design template of MaxQuant was constructed such that the Xcalibur .raw MS files were grouped together for the three biological replicates (including any technical duplicates) for each treatment group shown in Table 1. For identification, peptides were required to be at least 6 amino acids in length and protein identification required at least one razor plus unique peptide. A protein was only included in the final analysis if it was identified by at least one peptide in two treatment groups. The false discovery rates were set to 1% at the peptide and protein levels. Posterior error probabilities (PEP, false hit probability given the peptide score and length)[26] ranged from 0 to 0.54 (95% of proteins had a PEP < 0.05), and after mass

recalibration, the average absolute mass deviation was 1.62 ppm. Annotated MS/MS spectra were derived from the .raw files using the Viewer feature of MaxQuant.

For protein quantitation, we activated the requant feature and specified a single ratio count of unmodified and variably modified peptides for quantitation. For all the quantified peptides of a given protein, MaxQuant reports the median of these expression ratios and the non-normalized ratios are reported in Supplemental Table 2-1 (Appendix). Gene ontology (GO) annotations were obtained using the Uniprot identifier and the Perseus component of the MaxQuant software suite. Enrichment analyses were performed using the Database for Visualization and Integrated Discovery (DAVID)[29] and the Biological Networks Gene Ontology (BinGO)[30] plug-in of Cytoscape[31].

Superoxide Assessment

Superoxide levels were measured by following the oxidation of dihydroethidine (Invitrogen-Molecular Probes, Carlsbad, CA) to ethidium[32]. Neurons were seeded at 1×10^4 cells per well in black 96-well plates, treated overnight with 1 μM KU-32 then for 6h with 25 mM or 45 mM glucose. After 6h, the cells were subsequently treated with 15 μM dihydroethidine for 15 min at 37 °C. After washing with PBS, the ratio of ethidium (excitation 530 nm, emission 590 nm) to dihydroethidine (excitation 485 nm, emission 530 nm) was determined using a fluorescence spectrometer.

To directly assess mitochondrial superoxide production, the cells were treated as above and washed twice with phenol free Neurobasal medium. MitoTracker Green (80 nM) and 0.4 μM MitoSOX Red were added to each well and incubated for 15 min[33]. The cells were washed twice with fresh Neurobasal medium prior to imaging on an Olympus

3I Spinning Disk confocal microscope using excitation/emission wavelengths of 575/624 nm (MitoSox Red) and 494/531 nm (MitoTracker Green)[34]. As a positive control, some cells were treated with 1.8 μg/mL antimycin A for 25 min. Fluorescence intensity of the red and green signals of at least 200 cells per treatment was obtained using CellProfiler and CellProfiler Analyst image analysis software.

Mitochondrial Respiration

O2 consumption rate (OCR) was assessed using intact DRG sensory neurons and a XF96 Extracellular Flux Analyzer (Seahorse Biosciences, North Billerica, MA). Extracellular flux analysis is a noninvasive assay which uses two calibrated optical sensors to directly measure OCR in real-time in neurons that remain attached to the culture plate[35]. Primary embryonic sensory neurons were seeded in the 96 well plates at 1.5×10^4 cells per well and treated for 5 days in 25 or 45 mM glucose. Cells were treated with 1 μM KU-32 or DMSO for the final 24 h of the incubation and the cells were placed in fresh bicarbonate-free DMEM containing 5 mM glucose and 1 mM pyruvate. Baseline OCR was assessed in the XF96 analyzer using 4 measurement loops consisting of a 2 min mix cycle and a 5 min measurement cycle. Respiratory chain inhibitors were then sequentially injected into the wells and ATP-coupled oxygen consumption was calculated as the fraction of the basal OCR sensitive to 1 μg/mL oligomycin, an ATP synthase inhibitor. The maximal uncoupled respiration rate was determined by depolarizing the mitochondrial membrane potential with 1 μM FCCP (carbonylcyanide-4-(trifluorome-thoxy)-phenylhydrazone). The cell seeding density and inhibitor concentrations were optimized in preliminary experiments. After the respiratory measures, the cells were harvested and experimental rate values were normalized to protein content of each well.

Maximal respiratory capacity, spare respiratory capacity and respiratory state apparent ($State_{app}$) were determined from the rate data as described[36-37].

Statistical Analyses

All statistical differences between treatments were determined using ProStat (v4.83). Data were analyzed using either a one-way ANOVA and Tukey's post hoc test or a Kruskal−Wallis test and Dunn's posthoc analysis.

3.3 Results

We have shown previously that 2−3 week old cultures of embryonic sensory neurons can serve as a cell model to examine mechanisms of hyperglycemic stress. After two weeks in culture, embryonic sensory neurons were subjected to five days of hyperglycemia and the global effect on protein translation was measured by pulsing the cells with [^{3}H] Leu for the final 24 h. Hyperglycemically stressed neurons showed a 22% decrease in [^{3}H]Leu incorporation and treating the cells with 1 μM KU-32 for 24 h prior to the Leu pulse significantly increased overall translation (Figure 3-1). These results suggest that modulating chaperones may broadly increase protein translation.

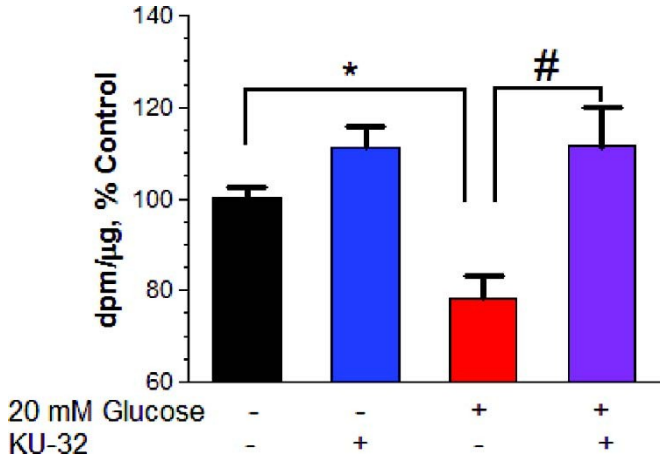

Figure 3-1. Hyperglycemia decreases the incorporation of [3H]Leucine into protein. Primary sensory neurons were cultured for 5 days in medium with 25 mM or 45 mM glucose and treated with DMSO or 1 µM KU-32 for the final 24 h. Coincident with the addition of KU-32, the cells were pulsed with 1 µCi/ml [^{3}H]Leu and the incorporation of of [^{3}H]Leu into total protein was determined as described in Experimental Procedures. The total dpm/µg protein was determined and the results are expressed as the percent of control. The data are the mean ± SEM from three experiments. *, $p < 0.05$ compared to control; #, $p < 0.05$ compared to glucose minus KU-32.

To identify specific proteins whose translation was differentially effected by hyperglycemia and KU-32, we utilized the pSILAC strategy that has been previously described[19] and is outlined in Figure 3-2. To assess the effect of KU-32 on protein translation in hyperglycemically stressed sensory neurons, the cells were incubated in K0R0 culture medium containing 45 mM glucose. After 3 days, the K0R0 cultures were divided such that one set of cells was placed in hyperglycemic culture medium containing medium-heavy forms of Lys and Arg (K4R6). The cells were pulsed with K4R6 for 48 h and treated with 1 μM KU-32 for the final 24 h of the incubation. The remaining K0R0 cells were placed in hyperglycemic culture medium containing heavy isotope forms of Lys and Arg (K8R10) and treated with DMSO for the final 24 h of the incubation. During the isotopic pulse, all newly synthesized proteins can only incorporate the K4R6 or K8R10 forms of Lys and Arg. Total cell lysates were prepared from the two treatment groups and mixed in a 1:1 mass ratio prior to isolation of subcellular fractions. Following mass spectrometric analysis, the abundance ratio of a K4/K8 or R6/R10 peptide reflects the difference in translation of the associated protein due to KU-32 treatment under hyperglycemic conditions (Table 3-1). Since all the K0R0 peptides associated with a given protein are present prior to the pulse, they can be ignored as they do not represent newly translated protein[19].

Label Combination	Treatment	Ratio Analyzed	Interpretation
K4R6 (M) : K8R10 (H)	25 mM glucose : 45 mM glucose	H/M	Effect of 5 day hyperglycemia on translation
K4R6 (M) : K8R10 (H)	25 mM glucose : 25 mM glucose + KU-32	H/M	Effect of 24 h KU-32 treatment on translation in basal glucose
K4R6 (M) : K8R10 (H)	45 mM glucose + KU-32 : 45 mM glucose	M/H	Effect of 24 h KU-32 treatment on translation under hyperglycemic conditions

Table 3-1. Isotopic Combinations for pSILAC Experiments

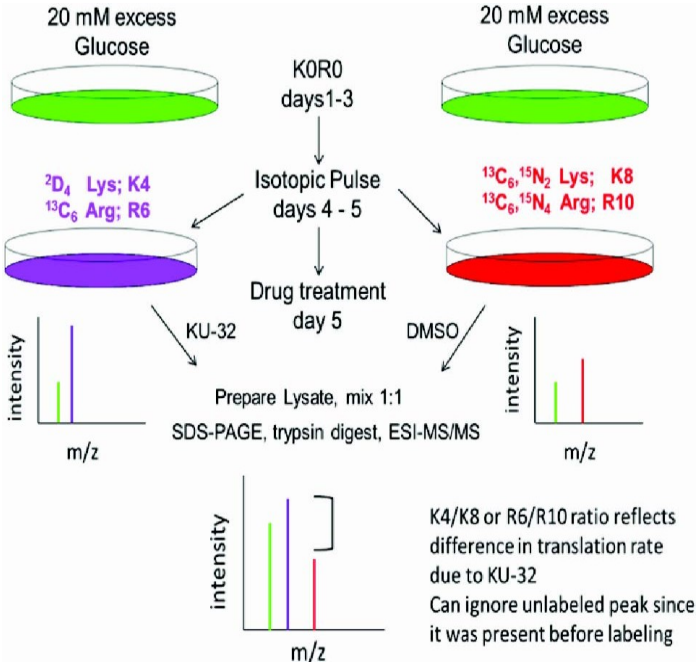

Figure 3-2. Experimental strategy for pSILAC analyses. Primary neurons were cultured in medium containing 45 mM glucose and light forms of Lys and Arg (K0R0) for 3 days. The K0R0 cultures were divided in half and one set of cells was placed in hyperglycemic culture solution containing medium-heavy forms of Lys and Arg (K4R6). The cells were pulsed with

K4R6 for 48 h and treated with 1 μM KU-32 for the final 24 h. The remaining K0R0 cells were placed in hyperglycemic culture medium containing heavy isotope forms of Lys and Arg (K8R10) and treated with DMSO for the final 24 h of the incubation. Total cell lysates were prepared and mixed in a 1:1 mass ratio, a heavy mitochondrial fraction was isolated, and the proteins were separated by SDS-PAGE prior to tryptic digestion and MS/MS analysis.

MaxQuant identified 743 proteins, of which 577 were identified by at least 2 peptides and 280 were quantified (Supplementary Table 2-2, Appendix). Approximately one-third of the 280 quantified proteins were present in all of the treatments (Figure 3-3A) and of the 156 proteins annotated as mitochondrial, 79 were quantified. Though the log 2 distributions of the protein expression ratios for each treatment were relatively unimodal, they were asymmetric and consistent with hyperglycemia decreasing protein translation and KU-32 treatment of hyperglycemically stressed cells increasing translation (Figure 3-3B). To determine what biological processes may be over-represented following KU-32 treatment, proteins showing at least a 1.5 fold increase were submitted to enrichment analysis using DAVID and the BinGO plug-in of Cytoscape. Both analyses supported that protein folding and response to reactive oxygen species were among the enriched biological processes identified (both ~11-fold enrichment).

KU-32 Effects Expression of Multiple Molecular Chaperones

The effect of hyperglycemia in absence and presence of KU-32 treatment on the expression of chaperones (green) and proteins with a mitochondrial annotation (red) is shown in Figure 3-3C. We have shown previously that KU-32 induces cytosolic Hsp70[13] and rather unexpectedly, we did not detect this Hsp70 paralog in any treatment group. This may be due to its relatively low abundance in the neurons compared to the constitutive form of Hsp70 (Hsc70), which is highly abundant and has a similar molecular weight (Figure 3-3D). Although an enriched mitochondrial preparation was used in the analysis, cytosolic Hsc70 was among the top ten identifications based on total number of peptides identified, but was not significantly modified in any treatment. However, immunoblot analysis of whole cell lysates revealed that KU-32 significantly

increased Hsp70 expression in hyperglycemically stressed neurons (Figure 3-3D).

A surprising finding of the pSILAC analysis was that KU-32 also increased mitochondrial chaperones under hyperglycemic conditions. Hsp60 is necessary to ensure the proper folding of proteins imported into the mitochondrial matrix[38] and compared to hyperglycemia alone, KU-32 promoted a median increase in translation of 3.7-fold (Figure 3-3C). An example of a pSILAC isotopic triplet of mtHsp60 is shown in Figure 3-4A. As expected, the unlabeled AAVEEGIVIGGGCAII(R0) peptide is of substantially greater intensity than the newly translated labeled peptides (note 5× scale amplification for the K4R6 and K8R10 peaks) since it existed prior to the pulse, and its intensity has additive contributions from sample mixing. When comparing the R6 and R10 forms of the peptide as indicative of newly translated protein, KU-32 treatment (R6 peptide at m/z 845.97) clearly enhanced the translation of Hsp60 relative to hyperglycemia alone (note that the mass differences between the peaks are one-half the expected amu shift since the peptides are doubly charged). In contrast, Hsp10 is a mitochondrial chaperone that was identified but not quantified in any treatment, suggesting that it had a lower rate of translation.

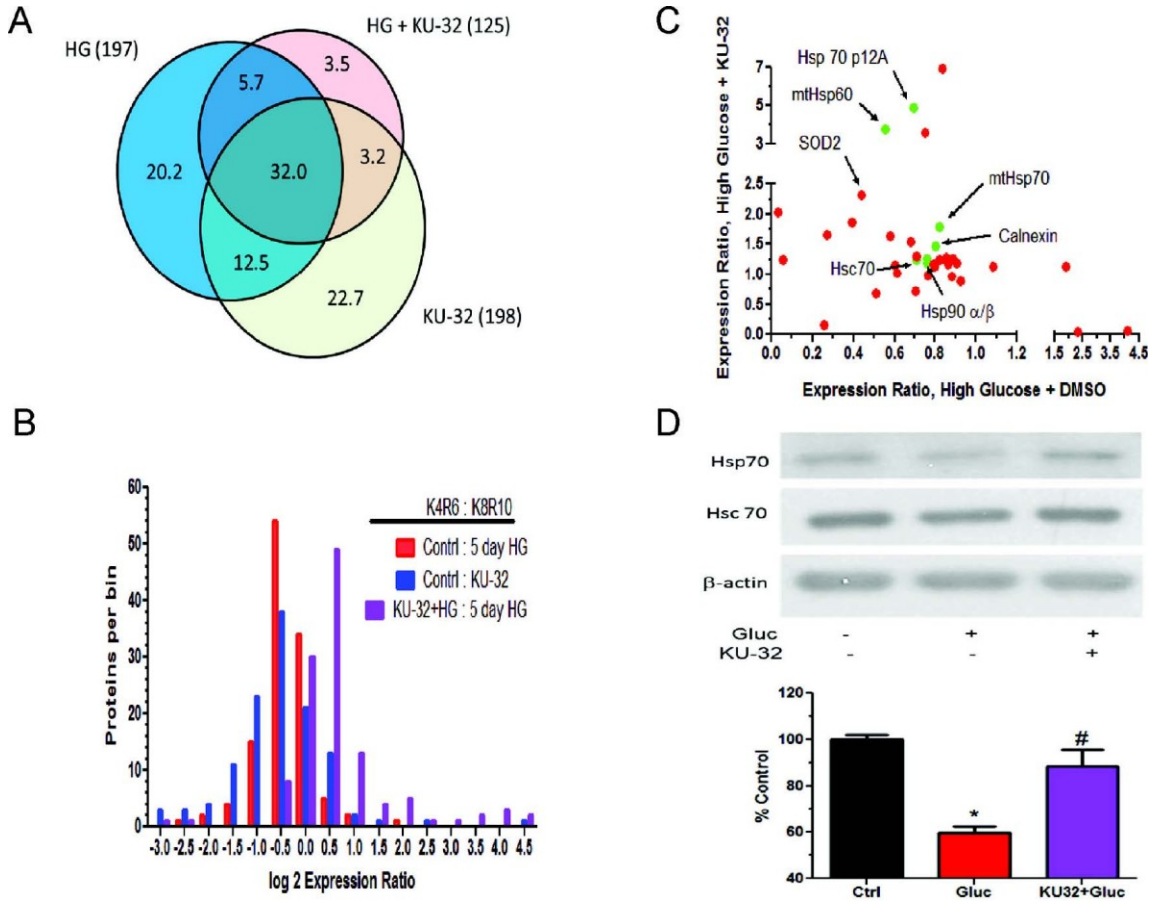

Figure 3-3. Distribution of translationally induced proteins. (A) Venn diagram of quantified proteins in each group. Numbers in parentheses are total number of quantified proteins per treatment. Percent of unique and overlapping proteins are shown within the colored sections of the diagram. (B) Non-normalized protein expression ratios provided by MaxQuant were log 2 transformed, binned into 0.5 units and the total proteins per bin counted. (C) Expression ratios of all quantified chaperones (green) and mitochondrial proteins (red) detected in both the high glucose and high glucose + KU-32 treatments were plotted against each other. (D) Representative immunoblot and quantitation of Hsp70 levels from three separate neuronal cultures. *, $p < 0.05$ compared to control; #, $p < 0.05$ compared to glucose minus KU-32.

Mortalin/Grp75/stress-70 protein is a mitochondrial Hsp70 (mtHsp70) family member that is a component of the presequence translocase-associated motor complex[39] and its translation was modestly decreased by hyperglycemia. Similar to Hsp60, the identification of mtHsp70 was by numerous peptides in each treatment. Figure 3-4B shows the MS/MS spectra of a peptide that was identified by seven sequential y-and b-ions that were increased about 1.8-fold by KU-32 in cells subjected to hyperglycemic stress (Figure 3-4C). Importantly, immunoblot analysis from 3 separate neuronal cultures further verified this finding (Figure 3-4C). In contrast to Hsp60, mtHsp70 is not induced as part of the classic heat shock response, however, it is upregulated in response to other forms of cell stress and its overexpression can improve mitochondrial function during focal ischemia[40]. Additionally, about 99% of mitochondrial proteins are nuclear encoded and require translocation and import into the organelle[39]. Although little is known on the effect of diabetes on mitochondrial protein import in sensory neurons, diabetes decreased the rate of protein import into interfibrillar, but not subsarcolemmal cardiac mitochondria[7]. Since mtHsp70 and Hsp60 are respectively involved in the import and folding of proteins into the mitochondrial matrix[38], these data suggest that KU-32 may affect mitochondrial function by facilitating protein import and maturation.

KU-32 also promoted a 4.9-fold increase in the expression of another Hsp70 paralog, Hsp70 protein 12A (Hsp70 p12A), and this was verified by immunoblot analysis of separate neuronal cultures (Figure 3-4D). Hsp70 p12A is an atypical member of the Hsp70 family and despite the fact that HSPA12 genes evolved early in the evolution of vertebrates[41], the protein's localization and function remain poorly characterized. Recent reports have provided descriptions that Hsp70 p12A expression is decreased in prefrontal

cortex of schizophrenic brain[42] and increased in artherosclerotic lesions[43], but no functional properties were ascribed to these observations. Since Hsp70 p12A contains atypical ATPase and substrate binding domains[41], it may function as a co-chaperone.

Neither Hsp90α nor Hsp90β were significantly altered by KU-32 in the hyperglycemic neurons. Curiously, KU-32 induced a 1.5-fold increase in calnexin translation, which is a chaperone involved in protein quality control in the endoplasmic reticulum (ER). However, other ER chaperones such as Grp78 and Grp94 were readily identified by numerous peptides but not quantified, suggesting that they were not undergoing substantial changes in translation. Together, these data support that in hyperglycemically stressed neurons, inhibiting the C-terminus of Hsp90 is sufficient to increase several Hsp70 family members and other mitochondrial chaperones.

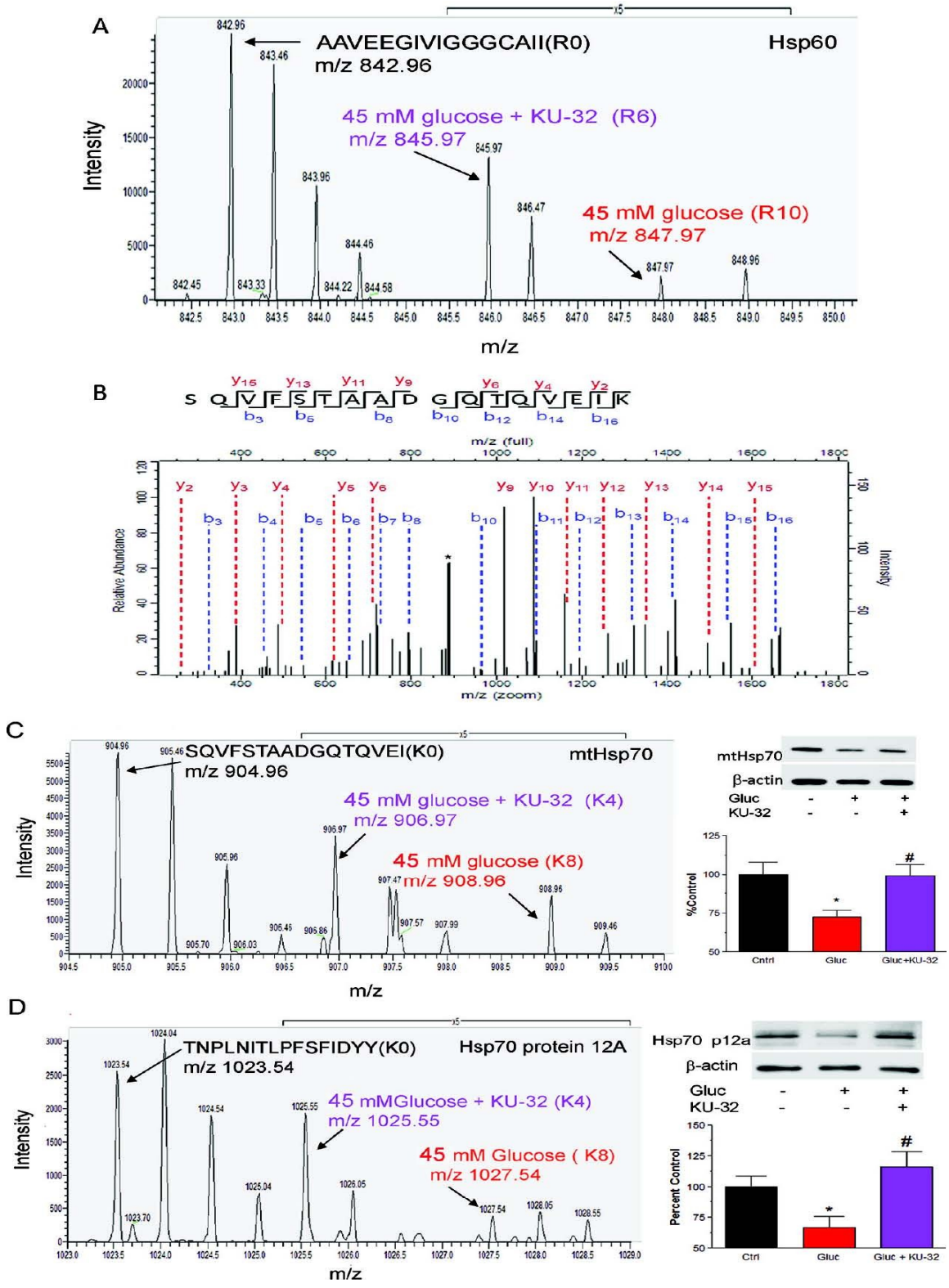

Figure 3-4. KU-32 induces the translation of Hsp60 and Hsp70 family members in hyperglycemic neurons. Primary neurons were incubated in medium containing 45 mM glucose

for 3 days and pulsed with either K4R6 or K8R10 Lys/Arg for an additional 48 h. The cultures were treated with 1 μM KU-32 (K4R6) or DMSO (K8R10) for the final 24 h of the incubation. Cell lysates were prepared, mixed in a 1:1 ratio and the samples processed for MS/MS analysis. (A) Representative MS scan showing an increase in Hsp60 in hyperglycemic neurons treated with KU-32 (R6 peptide) compared to glucose only (R10 peptide). Note the 5× scale amplification to demonstrate the increase in the R6 peptide compared to the R10 peptide. (B) MS/MS spectrum of the SQVFSTAADGQTQVEIK peptide of mtHsp70. The majority of the unannotated peaks arise from the loss of water and ammonia ion but their labeling was omitted for clarity. The asterisk indicates a peak that was unassigned. (C) Representative MS scan showing an increase in mtHsp70 in hyperglycemic neurons treated with KU-32 (K4 peptide) compared to glucose only (K8 peptide); 5× scale amplification as discussed above. A representative immunoblot and quantitation (n = 3) of the effect of hyperglycemia and KU-32 on mtHsp70 expression is shown to the right of the spectrum. (D) Representative MS scan showing an increase in Hsp70 p12A in hyperglycemic neurons treated with KU-32 (K4 peptide) compared to glucose only (K8 peptide); 5× scale amplification as discussed above. A representative immunoblot and quantitation (n = 3) of the effect of hyperglycemia and KU-32 on Hsp70 p12A expression is shown to the right of the spectrum. *, $p < 0.05$ compared to control; #, $p < 0.05$ compared to glucose minus KU-32.

KU-32 Increased MnSOD Translation and Decreased Glucose-induced Superoxide Production

An established hallmark of mitochondrial dysfunction in DPN is the induction of oxidative stress, due in part to an increase in mitochondrial superoxide production[4]. Consistent with these data and our previous results[18], translation of MnSOD in hyperglycemically stressed neurons was about 50% less than that measured in control neurons (3 peptides quantified) and KU-32 promoted a 2.3 fold increase in the translation of MnSOD (Figure 3-5A) in the hyperglycemically stressed cells. Although only quantified by 2 peptides, the identification of this doubly charged peptide was substantiated by a sequential series of 10 b-ions and 11 y-ions (Figure 3-5B). Moreover, immunoblot analysis of separate neuronal cultures verified that hyperglycemia decreased MnSOD and that KU-32 treatment significantly increased its expression (Figure 3-5A).

To determine if the increase in MnSOD by KU-32 corresponded to a decrease in superoxide production, the ratio of ethidium/dihydroethidium was used as a nonorganelle selective measure of superoxide. Neurons were pretreated with vehicle or KU-32 and exposed to 45 mM glucose for 6 h to acutely increase superoxide levels[22]. Hyperglycemia increased superoxide levels and KU-32 significantly blocked this effect (Figure 3-5C). To determine if KU-32 prevented superoxide production within mitochondria in neurons subjected to the more chronic hyperglycemic stress that was used in the proteomic analyses, we used MitoSox red and the mitochondrial marker, MitoTracker Green. Five days of hyperglycemia increased mitochondrial superoxide levels and treating the cells with KU-32 for the final 24 h significantly decreased this response (Figure 3-5D & E). As a positive control, some neurons were treated with

antimycin A prior to the addition of the dyes. These data support that modulating the activity of Hsp90 with KU-32 is sufficient to increase MnSOD and decrease glucose-induced mitochondrial oxidative stress.

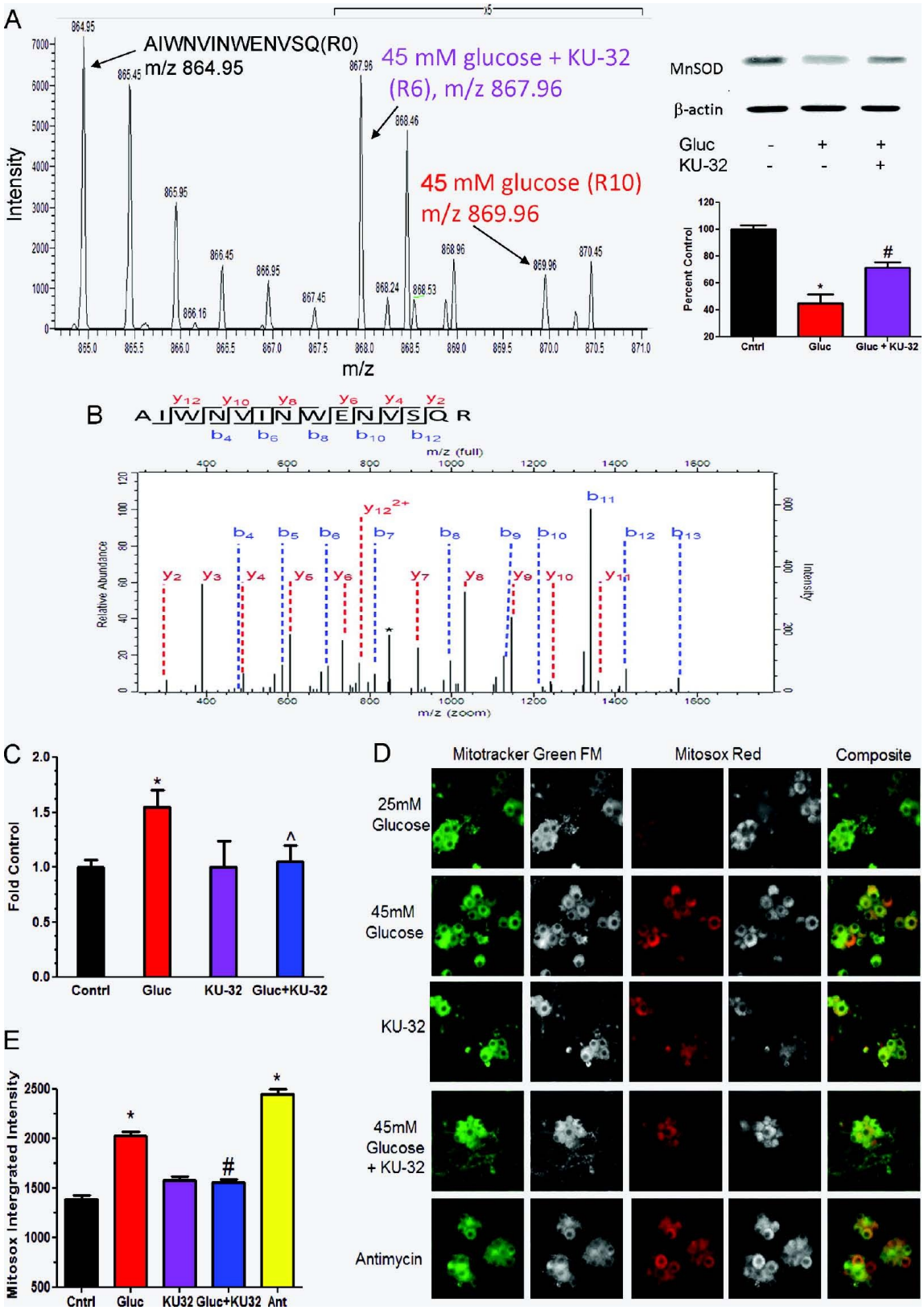

Figure 3-5. KU-32 induces the translation of MnSOD and decreases mitochondrial

superoxide in hyperglycemic neurons. Primary neurons were incubated in medium containing 45 mM glucose for 3 days and pulsed with either K4R6 or K8R10 Lys/Arg for an additional 48 h. The cultures were treated with 1 μM KU-32 (K4R6) or DMSO (K8R10) for the final 24 h of the incubation. Cell lysates were prepared, mixed in a 1:1 ratio and the samples processed for MS/MS analysis. (A) Representative MS scan showing an increase in MnSOD in hyperglycemic neurons treated with KU-32 (R6) compared to glucose only (R10). Note the 5× scale amplification to demonstrate the increase in the R6 relative to R10 peptide. A representative immunoblot and quantitation (n = 3) of the effect of hyperglycemia and KU-32 on MnSOD expression is shown to the right of the spectrum. (B) MS/MS spectrum of the AIWNVINWENVSQR peptide. The majority of the unannotated peaks arise from the loss of water and ammonia ion but their labeling were omitted for clarity. The asterisk indicates a peak that was unassigned. (C) Effect of KU-32 on decreasing glucose-induced superoxide production as measured using the ratio of ethidium/dihyroethidine. Results are expressed as a fold control and are the mean ± SEM from three separate cultures. Gluc; 45 mM glucose. (D) Representative images showing that KU-32 decreased glucose-induced mitochondrial superoxide production as visualized using MitoSox Red. Neurons were costained with Mitotracker Green to localize mitochondria. Gray panels show raw gray scale images that were exported prior to being colorized in Image J. Cells treated with antimycin A (Ant) served as a positive control for superoxide generation. (E) Quantitative image analysis from three separate neuron cultures. *, $p < 0.05$ compared to control; #, $p < 0.05$ compared glucose minus KU-32.

Increased Translation of Mitochondrial Chaperones and MnSOD by KU-32 Correlates with an Improved Bioenergetic Profile

Hyperglycemia-induced oxidative stress renders mitochondrial proteins more susceptible to oxidative damage. Relative to their rate of production, a slower rate of repair by mitochondrial chaperones favors accumulation of oxidatively damaged proteins in the organelle[44]. Thus, the ability of KU-32 to increase mitochondrial chaperones and decrease oxidative stress suggests that the bioenergetic profile of the organelle may also be enhanced. To this end, we used a XF96 Extracellular Flux Analyzer to assess the effect of hyperglycemia and KU-32 treatment on oxygen consumption rat (OCR). The XF96 analyzer measures OCR in real time using intact cells and results in Figure 3-6A show a typical mitochondrial function experiment from ~5000 sensory neurons per well (n =4) respiring in DMEM containing 5.5 mM glucose. The first four rates represent basal OCR (light blue shading) and each rate measure was normalized to the total amount of protein per well and expressed as a percent of the final basal OCR (rate 4). Measuring OCR in intact cells in the absence and presence of respiratory chain poisons is the single most useful test to stringently assess mitochondrial dysfunction[36]. Oligomycin is an ATP synthase inhibitor and its injection decreases the basal OCR. The magnitude of this decrease is indicative of the percent of the basal OCR that is coupled to ATP synthesis (dark blue shading) and the residual OCR is due to proton leak (uncoupled respiration). FCCP is a protonophore whose addition provides a measure of maximal respiratory capacity (MRC, red shading). MRC assesses the functional integrity of the respiratory chain since electron transfer is no longer rate limited by the proton gradient across the inner mitochondrial membrane[36]. Nicholls has defined spare respiratory capacity (SRC)

as the arithmetic difference between MRC and the basal OCR (pink shading)[45]. SRC provides a functional indication of how close to its bioenergetic limit a cell is respiring[36]. A loss of SRC, especially in neurons that have variable ATP demands, limits their ability to match energetic needs to environmental demands and renders the cells more susceptible to secondary stressors[46-47]. Thus, treatment-induced differences in MRC and SRC are indicative of mitochondrial dysfunction affecting the bioenergetic limits and reserve capacity of the neurons. Although not measured in the current experiment, the green shading is representative of non-mitochondrial OCR values obtained the presence of rotenone and antimycin A to inhibit complexes I and III, respectively.

Neurons were incubated in medium containing 25 or 45 mM glucose for 5 days and treated with KU-32 for the final 24 h. To assess respiration under a standard glucose concentration, the cells were placed in serum-free DMEM containing 5.0 mM glucose and 1 mM pyruvate at 37 °C for 1 h prior to measuring OCR. After measuring basal OCR, the cells were exposed to oligomycin and no significant differences were observed in the magnitude of ATP-coupled OCR and proton leak (Figure 3-6B). In contrast, though FCCP stimulated MRC above basal OCR in all treatments, neurons exposed to hyperglycemic stress exhibited a significantly blunted MRC relative to control cells (Figure 3-6B). Similarly, SRC was also significantly decreased in the glycemically stressed cells compared to control (Figure 3-6C, solid bars).

In cells maintained in 25 mM glucose and treated with KU-32, the average MRC and SRC was slightly decreased but this was not significantly different from control. Consistent with the efficacy of KU-32 in decreasing mitochondrial superoxide levels, glycemically stressed cells treated with the drug showed a significant improvement in

both MRC (Figure 3-6B) and SRC (Figure 3-6C, solid bars) compared to the neurons incubated in high glucose alone. The blunted MRC and SRC apparent in the hyperglycemically stressed cells supports that they are energetically stressed and that mitochondrial workload is increased.

The respiratory state apparent ($State_{app}$) provides a quantitative indication of mitochondrial workload and can be estimated from these data[47]. As mitochondrial workload decreases, $State_{app}$ approaches 4, a metabolic indicator that minimal ATP-coupled respiration is needed and OCR is primarily uncoupled[47]. On the other hand, high ATP demand requires state 3.0 respiration (comparable to that induced by FCCP, Figure 3-6B). The $State_{app}$ values were 3.5 ± 0.5 and 3.5 ± 0.3 in neurons treated with vehicle or KU-32, respectively, indicating the basal mitochondrial workload required to meet ATP needs. In contrast, hyperglycemia promoted a significant decrease in $State_{app}$ (3.3 ± 0.3, Figure 3-6C, striped bars), suggesting that ATP demand is depleting reserve capacity and that the organelles are approaching bioenergetic failure[37]. Importantly, KU-32 treatment significantly improved this decline. The ability of KU-32 to increase MRC, SRC and $State_{app}$ supports that the cells have recovered significant respiratory capacity that correlates with the induction of mitochondrial chaperones and a decrease in superoxide production. Although numerous factors contribute to OCR[37], hyperglycemia-induced damage to respiratory chain proteins may decrease the efficiency of electron transport to affect SRC and increase mitochondrial workload.

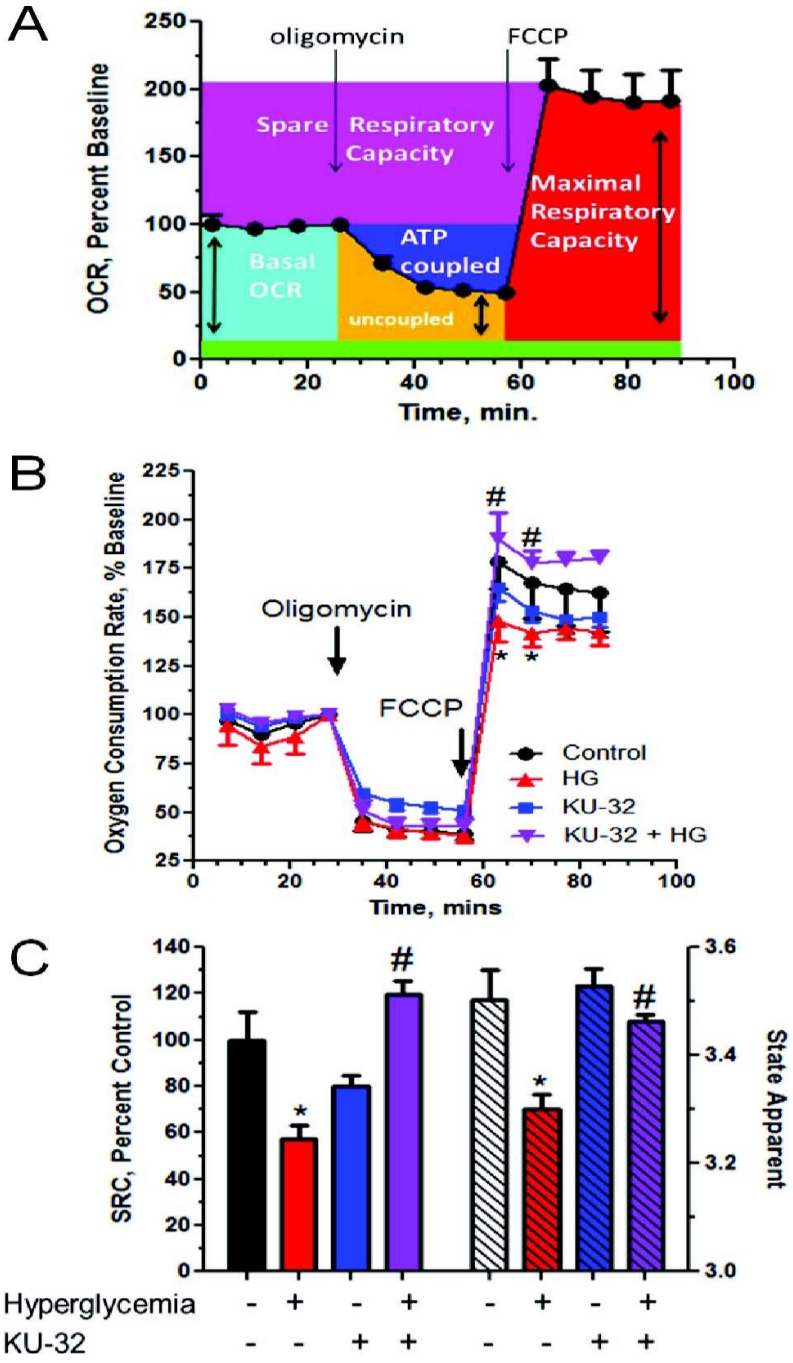

Figure 3-6. Hyperglycemia decreased mitochondrial bioenergetics which was reversed by KU-32 treatment. (A) Example of a mitochondrial function experiment in the XF96 extracellular flux analyzer. Basal OCR (light blue) is given by the first four rate measures. The addition of 1 µg/mL oligomycin inhibits ATP synthase and the decrease in OCR gives a measure of ATP-coupled respiration (dark blue). Residual OCR in the presence of oligomycin

provides a measure of proton leak (orange). The addition of 1 μM FCCP dissipates the proton gradient across the inner mitochondrial membrane and assesses maximal respiratory capacity (MRC, red). Spare respiratory capacity (SRC, pink) is assessed as the difference between MRC and the basal OCR. The green shading represents the estimated contribution of nonmitochondrial respiration to basal OCR but was not directly measured in the experiment shown. (B) Primary neurons were seeded into a 96 well plate and incubated in medium containing 25 or 45 mM glucose for 5 days and treated with 1 μM KU-32 or DMSO for the final 24 h. The cells were placed in medium containing 5 mM glucose and 1 mM pyruvate prior to the respiratory measures. Results shown are the mean ± SEM from 5 to 8 wells per treatment from one experiment repeated three times. Arrows indicate the injection of oligomycin and FCCP. Hyperglycemia induced a significant decrease in MRC relative to control neurons (*, $p < 0.05$) and KU-32 treatment significantly increased MRC compared to cells treated with high glucose only (#, $p < 0.001$). (C) Hyperglycemia significantly decreased SRC (*, $p < 0.05$, left axis and solid bars) and $State_{app}$ (*, $p < 0.01$, right axis and striped bars) compared to control cells. Both SRC ($^{\#}$, $p < 0.001$) and $State_{app}$ ($^{\#}$, $p < 0.05$) were significantly improved by KU-32 treatment compared to cells treated with high glucose alone.

3.4 Discussion

Our previous work on novobiocin-based C-terminal Hsp90 inhibitors has demonstrated that they induce Hsp70 and protect cortical and sensory neurons from toxicity induced by β-amyloid peptides and hyperglycemia, respectively[13,15]. Although the neuroprotective efficacy of KU-32 in reversing DPN required the presence of Hsp70, the current study sought to unbiasedly identify whether KU-32 promoted the translation of other proteins that may aid sensory neurons in tolerating glucotoxic stress[48]. Using pSILAC, we identify that mitochondrial chaperones and MnSOD are also increased by KU-32 treatment of hyperglycemically stressed cells. Consistent with the induction of MnSOD, KU-32 decreased mitochondrial superoxide levels in neurons subjected to 5 days of hyperglycemia. Similarly, hyperglycemia decreased various measures of mitochondrial respiratory capacity and treating the neurons with KU-32 significantly improved both maximum and spare respiratory capacity.

Previous investigators have shown that embryonic sensory neurons cultured in vitro for 3 days are susceptible to glucose-induced apoptosis[49-50]. However, 2−3 week old cultures of embryonic sensory neurons are resistant to glucose-induced cell death[11,17], similar to adult sensory neurons[51]. Although the more differentiated embryonic neurons can serve as a cell model to examine mechanisms of hyperglycemic stress unrelated to apoptosis, their response to hyperglycemia does not necessarily mimic that observed in adult neurons. For example, hyperglycemia induced a robust increase in superoxide in adult sensory neurons isolated from chronically diabetic mice but not from neurons obtained from control animals[18,52]. Thus, obtaining sensory neurons from adult diabetic animals that have received drug treatment will also be a beneficial approach toward

dissecting the mechanism of drug efficacy on improving mitochondrial function. Although correlative, since mitochondrial function is clearly compromised in the improved expression of mitochondrial chaperones and enhanced respiratory capacity may at least partially underlie the efficacy of KU-32 in reversing sensory hypoalgesia in diabetic mice[18,52-53]. We would like to emphasize that our approach in using the differentiated embryonic neurons has no implications on the role or relevance of glucose-induced apoptosis to DPN. The neuroprotective properties of KU-32 in ameliorating DPN are unlikely to center on preventing sensory neuron death since apoptosis has not been demonstrated as a key feature in the development of DPN[54-56].

It is important to note that Hsp70 is a necessary component of drug efficacy since gene deletion of inducible forms of Hsp70 ablated the ability of KU-32 therapy to reverse several indices of experimental DPN[11]. However, this does not rule out that the induction of mitochondrial chaperones and MnSOD are not a critical aspect of the effect of KU-32 on improving mitochondrial function, and by extension, DPN. Emerging data supports that diabetes increases oxidative stress and mitochondrial fission/fusion in sensory neurons[57-59]. Decreasing oxidative stress and maintaining the fidelity of protein import to support this turnover would be essential to maximizing the bioenergetic capacity of the organelle. As both Hsp70 and mtHsp70 aid mitochondrial protein import via separate import pathways[39], we hypothesize that these proteins may enhance mitochondrial bioenergetics by facilitating the import of respiratory and antioxidant proteins; MnSOD is likely to be imported into the mitochondrial matrix via mtHsp70. To this end, it will be critical to define whether the necessity of Hsp70 induction for drug efficacy is related to improved mitochondrial function and/or protein import. Similarly, the

sufficiency/necessity of mtHsp70 and MnSOD induction by KU-32 to improving mitochondrial function in response to hyperglycemic stress remains to be determined.

In conclusion, the salient findings of this study provide proof-of-principle that a novel C-terminal Hsp90 inhibitor can decrease mitochondrial superoxide levels and improve organellar bioenergetics in hyperglycemically stressed neurons. These functional improvements correlated with the translational induction of MnSOD and mitochondrial chaperones by KU-32. Thus, the reported efficacy of KU-32 therapy in ameliorating sensory hypoalgesia in DPN may relate to improved mitochondrial function.

References

1. Calcutt, N.A., Cooper, M.E., Kern, T.S. & Schmidt, A.M. Therapies for hyperglycaemia-induced diabetic complications: from animal models to clinical trials. *Nat Rev Drug Discov* **8**, 417-430 (2009).
2. Tomlinson, D.R. & Gardiner, N.J. Glucose neurotoxicity. *Nat Rev Neurosci* **9**, 36-45 (2008).
3. Muchowski, P.J. & Wacker, J.L. Modulation of neurodegeneration by molecular chaperones. *Nat Rev Neurosci* **6**, 11-22 (2005).
4. Pop-Busui, R., Sima, A. & Stevens, M. Diabetic neuropathy and oxidative stress. *Diabetes/Metabolism Research and Reviews* **22**, 257-273 (2006).
5. Obrosova, I.G. Diabetes and the peripheral nerve. *Biochimica et Biophysica Acta (BBA) - Molecular Basis of Disease* **1792**, 931-940 (2009).
6. Akude, E., Zherebitskaya, E., Roy Chowdhury, S., Girling, K. & Fernyhough, P. 4-Hydroxy-2-Nonenal Induces Mitochondrial Dysfunction and Aberrant Axonal Outgrowth in Adult Sensory Neurons that Mimics Features of Diabetic Neuropathy. *Neurotoxicity Research* **17**, 28-38 (2010).
7. Baseler, W.A.*, et al.* Proteomic alterations of distinct mitochondrial subpopulations in the type 1 diabetic heart: contribution of protein import dysfunction. *American Journal of Physiology - Regulatory, Integrative and Comparative Physiology* **300**, R186-R200 (2011).
8. Pratt, W.B., Morishima, Y., Peng, H.-M. & Osawa, Y. Proposal for a role of the Hsp90/Hsp70-based chaperone machinery in making triage decisions when proteins undergo oxidative and toxic damage. *Experimental Biology and Medicine* **235**, 278-289 (2010).
9. Bienemann, A.S., Lee, Y.B., Howarth, J. & Uney, J.B. Hsp70 suppresses apoptosis in sympathetic neurones by preventing the activation of c-Jun. *Journal of Neurochemistry* **104**, 271-278 (2008).
10. Chaudhury, S., Welch, T.R. & Blagg, B.S.J. Hsp90 as a Target for Drug Development. *ChemMedChem* **1**, 1331-1340 (2006).
11. Matts, R.L.*, et al.* A systematic protocol for the characterization of Hsp90 modulators. *Bioorganic & Medicinal Chemistry* **19**, 684-692 (2011).
12. Matts, R.L.*, et al.* Elucidation of the Hsp90 C-Terminal Inhibitor Binding Site. *ACS Chemical Biology* **6**, 800-807 (2011).
13. Ansar, S.*, et al.* A non-toxic Hsp90 inhibitor protects neurons from Aβ-induced toxicity. *Bioorganic & Medicinal Chemistry Letters* **17**, 1984-1990 (2007).
14. Lu, Y., Ansar, S., Michaelis, M.L. & Blagg, B.S.J. Neuroprotective activity and evaluation of Hsp90 inhibitors in an immortalized neuronal cell line. *Bioorganic & Medicinal Chemistry* **17**, 1709-1715 (2009).
15. Urban, M.J.*, et al.* Inhibiting heat-shock protein 90 reverses sensory hypoalgesia in diabetic mice. *Asn Neuro* **2**(2010).
16. Chowdhury, S.K.R., Dobrowsky, R.T. & Fernyhough, P. Nutrient excess and altered mitochondrial proteome and function contribute to neurodegeneration in diabetes. *Mitochondrion* **11**, 845-854 (2011).
17. Zhang, L.*, et al.* Hyperglycemia Alters the Schwann Cell Mitochondrial Proteome and Decreases Coupled Respiration in the Absence of Superoxide Production. *Journal of Proteome Research* **9**, 458-471 (2009).
18. Akude, E.*, et al.* Diminished Superoxide Generation Is Associated With Respiratory Chain Dysfunction and Changes in the Mitochondrial Proteome of Sensory Neurons From Diabetic Rats. *Diabetes* **60**, 288-297 (2011).

19. Schwanhäusser, B., Gossen, M., Dittmar, G. & Selbach, M. Global analysis of cellular protein translation by pulsed SILAC. *PROTEOMICS* **9**, 205-209 (2009).
20. Zanazzi, G.*, et al.* Glial Growth Factor/Neuregulin Inhibits Schwann Cell Myelination and Induces Demyelination. *The Journal of Cell Biology* **152**, 1289-1300 (2001).
21. Yu, C., Rouen, S. & Dobrowsky, R.T. Hyperglycemia and downregulation of caveolin-1 enhance neuregulin-induced demyelination. *Glia* **56**, 877-887 (2008).
22. Vincent, A.M., Kato, K., McLean, L.L., Soules, M.E. & Feldman, E.L. Sensory Neurons and Schwann Cells Respond to Oxidative Stress by Increasing Antioxidant Defense Mechanisms. *Antioxidants & Redox Signaling* **11**, 425-438 (2009).
23. Huang, Y.-T. & Blagg, B.S.J. A Library of Noviosylated Coumarin Analogues. *The Journal of Organic Chemistry* **72**, 3609-3613 (2007).
24. Okado-Matsumoto, A. & Fridovich, I. Subcellular Distribution of Superoxide Dismutases (SOD) in Rat Liver. *Journal of Biological Chemistry* **276**, 38388-38393 (2001).
25. Steen, H. & Mann, M. The abc's (and xyz's) of peptide sequencing. *Nat Rev Mol Cell Biol* **5**, 699-711 (2004).
26. Cox, J. & Mann, M. MaxQuant enables high peptide identification rates, individualized p.p.b.-range mass accuracies and proteome-wide protein quantification. *Nat Biotech* **26**, 1367-1372 (2008).
27. Cox, J.r.*, et al.* Andromeda: A Peptide Search Engine Integrated into the MaxQuant Environment. *Journal of Proteome Research* **10**, 1794-1805 (2011).
28. Cox, J.*, et al.* A practical guide to the MaxQuant computational platform for SILAC-based quantitative proteomics. *Nat. Protocols* **4**, 698-705 (2009).
29. Huang, D.W., Sherman, B.T. & Lempicki, R.A. Systematic and integrative analysis of large gene lists using DAVID bioinformatics resources. *Nat. Protocols* **4**, 44-57 (2008).
30. Maere, S., Heymans, K. & Kuiper, M. BiNGO: a Cytoscape plugin to assess overrepresentation of Gene Ontology categories in Biological Networks. *Bioinformatics* **21**, 3448-3449.
31. Shannon, P.*, et al.* Cytoscape: A Software Environment for Integrated Models of Biomolecular Interaction Networks. *Genome Research* **13**, 2498-2504 (2003).
32. Vincent, A.M., McLean, L.L., Backus, C. & Feldman, E.L. Short-term hyperglycemia produces oxidative damage and apoptosis in neurons. *The FASEB Journal* (2005).
33. Robinson, K.M., Janes, M.S. & Beckman, J.S. The selective detection of mitochondrial superoxide by live cell imaging. *Nat. Protocols* **3**, 941-947 (2008).
34. Mukhopadhyay, P.*, et al.* Simultaneous detection of apoptosis and mitochondrial superoxide production in live cells by flow cytometry and confocal microscopy. *Nat. Protocols* **2**, 2295-2301 (2007).
35. Wu, M.*, et al.* Multiparameter metabolic analysis reveals a close link between attenuated mitochondrial bioenergetic function and enhanced glycolysis dependency in human tumor cells. *American Journal of Physiology - Cell Physiology* **292**, C125-C136 (2007).
36. Brand, M.D. & Nicholls, D.G. Assessing mitochondrial dysfunction in cells (vol 435, pg 297, 2011). *Biochem. J.* **437**, 575-575 (2011).
37. Sansbury, B.E., Jones, S.P., Riggs, D.W., Darley-Usmar, V.M. & Hill, B.G. Bioenergetic function in cardiovascular cells: The importance of the reserve capacity and its biological regulation. *Chemico-Biological Interactions* **191**, 288-295 (2011).
38. Deocaris, C.C., Kaul, S.C. & Wadhwa, R. On the brotherhood of the mitochondrial chaperones mortalin and heat shock protein 60. *Cell Stress & Chaperones* **11**, 116-128 (2006).
39. Schmidt, O., Pfanner, N. & Meisinger, C. Mitochondrial protein import: from proteomics to functional mechanisms. *Nat Rev Mol Cell Biol* **11**, 655-667 (2010).

40. Xu, L., Voloboueva, L.A., Ouyang, Y., Emery, J.F. & Giffard, R.G. Overexpression of mitochondrial Hsp70/Hsp75 in rat brain protects mitochondria, reduces oxidative stress, and protects from focal ischemia. *J Cereb Blood Flow Metab* **29**, 365-374 (2008).
41. Brocchieri, L., de Macario, E.C. & Macario, A.J.L. hsp70 genes in the human genome: Conservation and differentiation patterns predict a wide array of overlapping and specialized functions. *Bmc Evolutionary Biology* **8**(2008).
42. Pongrac, J.L*., et al.* Heat shock protein 12A shows reduced expression in the prefrontal cortex of subjects with schizophrenia. *Biological Psychiatry* **56**, 943-950 (2004).
43. Han, Z., Truong, Q.A., Park, S. & Breslow, J.L. Two Hsp70 family members expressed in atherosclerotic lesions. *Proceedings of the National Academy of Sciences* **100**, 1256-1261 (2003).
44. Deocaris, C., Kaul, S. & Wadhwa, R. From proliferative to neurological role of an hsp70 stress chaperone, mortalin. *Biogerontology* **9**, 391-403 (2008).
45. Nicholls, D.G., Johnson-Cadwell, L., Vesce, S., Jekabsons, M. & Yadava, N. Bioenergetics of mitochondria in cultured neurons and their role in glutamate excitotoxicity. *Journal of Neuroscience Research* **85**, 3206-3212 (2007).
46. Choi, S.W., Gerencser, A.A. & Nicholls, D.G. Bioenergetic analysis of isolated cerebrocortical nerve terminals on a microgram scale: spare respiratory capacity and stochastic mitochondrial failure. *Journal of Neurochemistry* **109**, 1179-1191 (2009).
47. Dranka, B.P., Hill, B.G. & Darley-Usmar, V.M. Mitochondrial reserve capacity in endothelial cells: The impact of nitric oxide and reactive oxygen species. *Free Radical Biology and Medicine* **48**, 905-914 (2010).
48. Calcutt, N.A. Tolerating diabetes: an alternative therapeutic approach for diabetic neuropathy. *Asn Neuro* **2**(2010).
49. Russell, J.W., Sullivan, K.A., Windebank, A.J., Herrmann, D.N. & Feldman, E.L. Neurons Undergo Apoptosis in Animal and Cell Culture Models of Diabetes. *Neurobiology of Disease* **6**, 347-363 (1999).
50. RUSSELL, J.W*., et al.* High glucose-induced oxidative stress and mitochondrial dysfunction in neurons. *The FASEB Journal* **16**, 1738-1748 (2002).
51. Fernyhought, P., Roy Chowdhury, S.K. & Schmidt, R.E. Mitochondrial stress and the pathogenesis of diabetic neuropathy. *Expert Review of Endocrinology & Metabolism* **5**, 39+ (2010).
52. Zherebitskaya, E., Akude, E., Smith, D.R. & Fernyhough, P. Development of Selective Axonopathy in Adult Sensory Neurons Isolated From Diabetic Rats. *Diabetes* **58**, 1356-1364 (2009).
53. Chowdhury, S.K.R*., et al.* Mitochondrial Respiratory Chain Dysfunction in Dorsal Root Ganglia of Streptozotocin-Induced Diabetic Rats and Its Correction by Insulin Treatment. *Diabetes* **59**, 1082-1091 (2010).
54. Kishi, M., Tanabe, J., Schmelzer, J.D. & Low, P.A. Morphometry of Dorsal Root Ganglion in Chronic Experimental Diabetic Neuropathy. *Diabetes* **51**, 819-824 (2002).
55. Zochodne, D.W., Verge, V.M.K., Cheng, C., Sun, H. & Johnston, J. Does diabetes target ganglion neurones? Progressive sensory neurone involvement in long-term experimental diabetes. *Brain* **124**, 2319-2334 (2001).
56. Cheng, C. & Zochodne, D.W. Sensory Neurons With Activated Caspase-3 Survive Long-Term Experimental Diabetes. *Diabetes* **52**, 2363-2371 (2003).
57. Figueroa-Romero, C*., et al.* SUMOylation of the mitochondrial fission protein Drp1 occurs at multiple nonconsensus sites within the B domain and is linked to its activity cycle. *The FASEB Journal* **23**, 3917-3927 (2009).
58. Edwards, J*., et al.* Diabetes regulates mitochondrial biogenesis and fission in mouse neurons. *Diabetologia* **53**, 160-169 (2010).

59. Vincent, A., *et al*. Mitochondrial biogenesis and fission in axons in cell culture and animal models of diabetic neuropathy. *Acta Neuropathologica* **120**, 477-489 (2010).

Chapter 4: Synthesis and Evaluation of Novologues as C-Terminal Hsp90 Inhibitors with Cytoprotective Activity against Sensory Neuron Glucotoxicity

(Kusuma, B.R., Zhang, L., Sundstrom, T., Peterson, L.B., Dobrowsky, R.T. and Blagg, B.S.J. (2012) Synthesis and Evaluation of Novologues as C-Terminal Hsp90 Inhibitors with Cytoprotective Activity against Sensory Neuron Glucotoxicity. J. Med. Chem. **55**, 5797-5812)

Abstract

KU-32 is a first-generation novologue (a novobiocin-based, C-terminal, heat shock protein 90 (Hsp90) inhibitor), that decreases glucose-induced death of primary sensory neurons and reverses numerous clinical indices of diabetic peripheral neuropathy in mice. The current study sought to exploit the C-terminal binding site of Hsp90 to determine whether the optimization of hydrogen bonding and hydrophobic interactions of second generation novologues could enhance neuroprotective activity. Using a series of substituted phenylboronic acids to replace the coumarin lactone of KU-32, we identified electronegative atoms placed at the *meta*-position of the B-ring exhibit improved cytoprotective activity, which is believed to result from favorable interactions with Lys539 in the Hsp90 C-terminal binding pocket. Consistent with these results, a *meta*-3-fluorophenyl substituted novologue **(11b)** exhibited a 14-fold lower ED_{50} compared to KU-32 for protection against glucose-induced toxicity of primary sensory neurons.

4.1 Introduction

Approximately 26 million Americans are afflicted with either Type 1 or Type 2 diabetes. Despite the use of insulin and oral anti-diabetic medications to help maintain euglycemia, about 60-70% of these individuals develop diabetic peripheral neuropathy (DPN)[1]. To date, approaches toward the treatment of DPN have centered on pathways/targets directly limited to hyperglycemia (i.e., polyol & hexosamine pathways, advanced glycation end products (AGEs), enhanced oxidative stress, PKC activation)[2]. Unfortunately, the contribution of these targets/pathways to the progression of DPN differs between individuals and does not occur with biochemical uniformity. Consequently, these approaches have resulted in little success for the management of DPN. As an alternative approach, we have explored the pharmacologic modulation of molecular chaperones to promote a broad cytoprotective response that may enhance a patient's ability to tolerate hyperglycemic insults and improve the symptoms of DPN.

Molecular chaperones, such as heat shock proteins 90 and 70 (Hsp90, Hsp70), are essential for folding nascent polypeptides into their biologically active structures and for the refolding of aggregated and denatured proteins that occur upon cellular stress.[3,4] Numerous conditions that cause cell stress can also induce the "heat shock response" (HSR); the transcriptional upregulation of antioxidant genes and chaperones such as Hsp70. Importantly, small molecule inhibition of Hsp90 is sufficient to induce the HSR. KU-32 is a small molecule Hsp90 C-terminal inhibitor that is based on novobiocin, a naturally occurring antimicrobial agent that inhibits DNA gyrase (Figure 4-1)[5,6-7]. Although the etiology of DPN is unrelated to the accumulation of one specific mis-folded or aggregated protein, hyperglycemia is the central mechanism which increase oxidative

stress and the oxidative modification of amino acids[8-9] that impair protein folding[10], decrease mitochondrial protein import[11] and promote mitochondrial dysfunction[2,8]. In the absence of single, disease-specific protein aggregate, pharmacologic induction of cytoprotective molecular chaperones had been shown to improve myelinated and unmyelinated fiber function in cellular models of glucotoxic stress and animal models of DPN[12]. Mechanistically, KU-32 is ineffective at preventing neuregulin-induced demyelination of myelinated cultures of sensory neurons prepared from Hsp70.1 and 70.3 double knockout mice, indicating that Hsp70 is necessary for the neuroprotective activity manifested by KU-32. Similarly, weekly treatment with KU-32 restored normal sensory and motor nerve function in diabetic wild type mice, but was unable to reverse multiple clinical indices of DPN in the diabetic Hsp70 knockout mice[12]. Collectively, these studies provide the biological and clinical rationale to support the modulation of molecular chaperones as a viable approach toward the treatment of DPN.

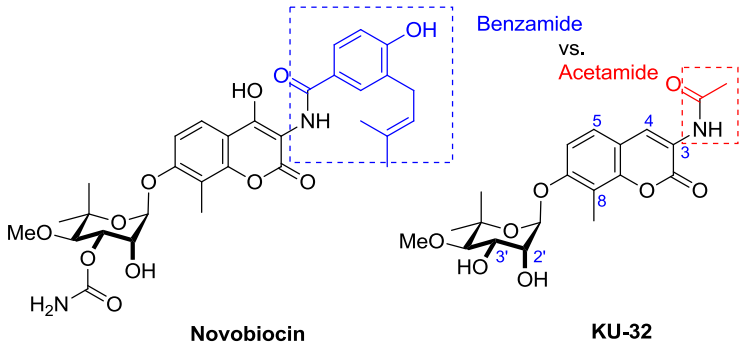

Figure 4-1. Chemical structures of novobiocin and KU-32.

An enviable aspect of KU-32 is that it induces Hsp70 at concentrations well below those needed to inhibit Hsp90's protein folding ability[12]. Thus, KU-32 possesses a rather broad therapeutic window that dissociates cytoprotective properties from

potentially cytotoxic effects resulting from the degradation of Hsp90-dependent client proteins[13]. Previous studies have shown that molecules like KU-32, which contain an acetamide, manifest neuroprotective properties. However, specific chemical attributes that enhance the neuroprotective properties of novobiocin-based analogs were not explored[14-15]. Therefore, we assessed the neuroprotective efficacy of a series of rationally designed novologues in decreasing glucotoxicity induced in primary unmyelinated sensory neurons. .

4.2 Experimental Methods:

Preparation of Embryonic Dorsal Root Ganglion (DRG) Neuron Cultures

DRG from embryonic day 15-18 Sprague Dawley rat pups were harvested into Leibovitz's L15 medium (L15) and dissociated with 0.25% trypsin for 30 min at 37°C. The ganglia were sedimented at 1,000 x g for 5 min, resuspended in growth media [phenol red free Neurobasal medium (Gibco, Grand Island, NY) containing 25 mM glucose, 1X B-27 additive, 50 ng/ml NGF (Harlan Bioscience, Indianapolis, IN), 4 mM glutamine, 100 U/mL penicillin and 100 μg/mL streptomycin] and triturated with a fire-polished glass pipette. The cells were cultured on collagen-coated (0.1 mg/mL collagen followed by overnight air drying in a laminar flow hood) black-walled 96-well plates (Corning Incorporated Corning, NY) at a seeding density of 2-3 x 10^4 cells per well. DRG neurons were re-fed the next day with fresh growth media containing 40 μM fluorodeoxyuridine and 10 μM cytosine β-D-arabinoside (both from Sigma Aldrich, St. Louis, MO) for 2 days to remove proliferating cells. Experiments were performed on DRG neurons on the third day in culture after placing the cells in fresh growth medium.

Glucotoxicity Assay

As immature DRG are susceptible to hyperglycemia-induced death[16], an additional 20 mM glucose was added to the growth medium (yielding a total of 45mM glucose) for 4 hours. Preliminary experiments found that 20 mM excess glucose for 4 hrs was sufficient to induce a reproducible 40-50% loss in neuronal viability. As a result, the toxicity induced by the acute change in glucose concentration makes it a useful model for drug screening[12,17]. Given the short time frame that the neurons are grown in vitro,

they are not pure neuronal cultures but instead, highly enriched. Importantly, the contaminating SCs that remains in the culture are resistant to glucose-induced death as we and others have reported previously[16,18]. Unfortunately, the use of highly purified cultures is problematic since the cells extend neurites and establish connections with each other, thus becoming resistant to hyperglycemia-induced death[19].

DRG neurons were incubated overnight with the novologues in the presence of Neurobasal medium, 50 ng/ml NGF and antibiotics only. In order to monitor the efficiency of our the novologues in protecting DRG neurons against glucotoxicity, we made use of Calcein AM (Invitrogen, Carlsbad, CA) to measure cell viability. Hydrolysis of calcein AM to a fluorescent product can only occur in live cells. Excess glucose was added to the cultures for 4 hrs and cell viability was measured by incubating the cells with 2 μM calcein AM for 30 min in the dark at 37°C. Fluorescence was then measured using a plate reader with excitation and emission wavelengths set to 485nm and 520nm, respectively. The arbitrary fluorescence readings were normalized to the total amount of protein from each respective well of the neuronal cultures. The protein concentrations in each well were determined using the DC protein assay (Bio-Rad). Significant differences in the efficacy of the novologues for increasing cell viability were determined using a Kruskal-Wallis non-parametric ANOVA and Dunn's post-test.

Luciferase Reporter Assay and Client Protein Degradation

A 1.5 kb region upstream of the start codon of the human *HSPA1A* gene was synthesized by GeneArt (Life Technologies, Grand Island, NY) and a 5' Kpn I and 3' Sac I sites added to direct cloning into the pGL3 basic luciferase reporter plasmid. DNA sequencing verified the integrity of the promoter sequence and the presence of two heat

shock elements. 50B11 cells[20] were grown in 10 cm dishes in DMEM containing 25 mM glucose, 10% FCS and 5 μg/ml blasticidin. The cells were transfected using lipofectamine and after 24 hr, were re-seeded into 24 well plates at a density of 2 x 10^5 cells per well. The cells were permitted to attach to the plate for 6 hrs in growth medium and treated with the indicated concentrations of the various novologues for 16 hr. Luciferase activity was assessed and normalized to the total protein concentration of each well. Results shown are from triplicate wells obtained in at least three separate experiments. Preliminary experiments validated that the reporter was strongly activated as expected by either heat shock (~ 10 fold) or 250 nM geldanamycin (~4-5 fold). Client protein degradation in MCF7 cells was performed as we have previously described[12]. Immunoblot analysis was performed as described[12] and antibodies for Hsp70 and β-actin were from Stressgen-Enzo Life Sciences (Farmingdale, NY) and Santa Cruz Biotechnology (Santa Cruz, CA), respectively.

Chemistry General.

All chemical-related spectra and procedures were performed by the Blagg group and are reported in the published version of the manuscript[21].

4.3 Results & Discussion

Design Rational for Second Generation Novologues

The Blagg group used molecular modeling and azide-containing novobiocin derivatives as photoaffinity probes to elucidate the Hsp90 C-terminal binding site[22]. Like novobiocin, KU-32 (Figure 4-2A) appears in the same docking region and exhibits similar binding interactions with both the protein backbone and the amino acid side chains of the Hsp90 C-terminal binding site. However, the coumarin lactone ring of KU-32 appears too distant from the Lys539 residue to provide any complementary interactions and there is a large hydrophobic pocket that could accommodate more flexible linkers. Thus, the goals of our chemical-biology undertaking was to create structural variants that preserved the necessary attributes for neuroprotection, but add modifications that would explore whether increasing interactions with these regions of the protein may improve neuroprotective efficacy. Consequently, we designed a novel novologue scaffold (Figure 4-2B) where the 3'-carbamate on noviose, that is detrimental to Hsp90 inhibitory activity[23], is omitted while the 7-noviosyl linkage and the requisite 2',3'-diol was maintained. Functionalities were incorporated onto the 3-aryl substituent (B-ring) where it projects into the binding pocket and provides additional hydrophobic and hydrogen bonding interactions to complement the scaffold interactions with Lys539. A flexible projection of the 4-ethyl acetamide from the A-ring was included to better occupy the large hydrophobic pocket (Figure 4-2C) that remains vacant with the coumarin ring system of KU-32 (Figure 4-2D). Based on the novologue design, a library based on this generic scaffold was constructed to validate structure-activity relationships (SAR) that impart neuroprotection.

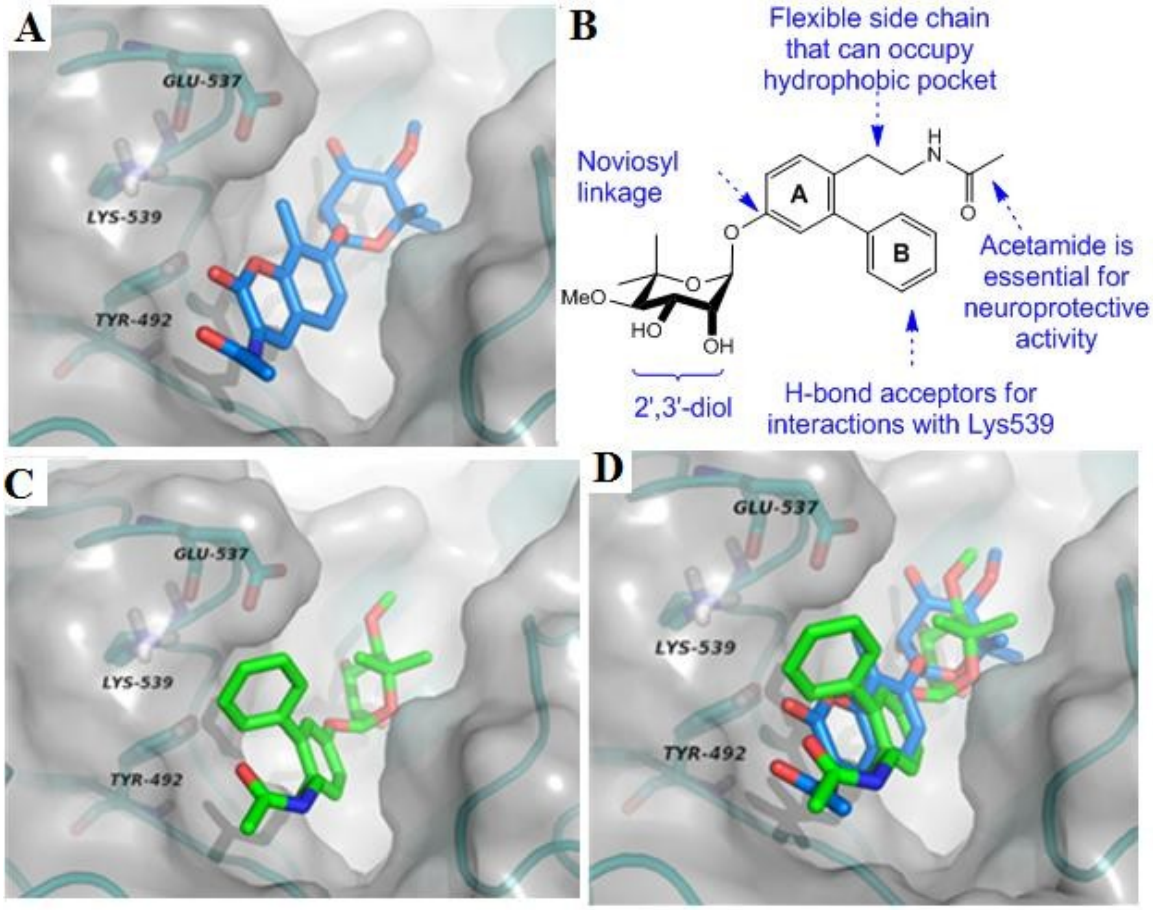

Figure 4-2. Hsp90 C-terminal binding site and proposed novologue design. **A)** KU-32 docked to Hsp90 C-terminal binding site. **B)** Structure of novologue and its attributes. **C)** Novologue docked to Hsp90 C-terminal binding site. **D)** Overlay of KU-32 and novologue docked to Hsp90 C-terminal binding site.

Based on prior work, phenyl boronic acids containing both electronic and steric moieties that could provide crucial interactions with Lys539 and the surrounding pocket were chosen for this study. Towards this goal, phenylboronic acids containing electronegative atoms at the *meta*- and *para*-positions were used to create a series of novologues (Figure 4-3). In addition, hydrogen bond acceptors were included at these locations to provide potential hydrogen bonding interactions with the protonated form of Lys539. To test the hypothesis regarding the region surrounding the flexible side chain, two cyclohexene analogues **20a–b** (Figure 4-4) were also synthesized. These analogues have the same linker length but contain a bulky cyclohexane tether between the biaryl ring system and the acetamide to explore interactions with the hydrophobic pocket of Hsp90. Detailed discussion of the novologues synthesis will not be included in this dissertation[21].

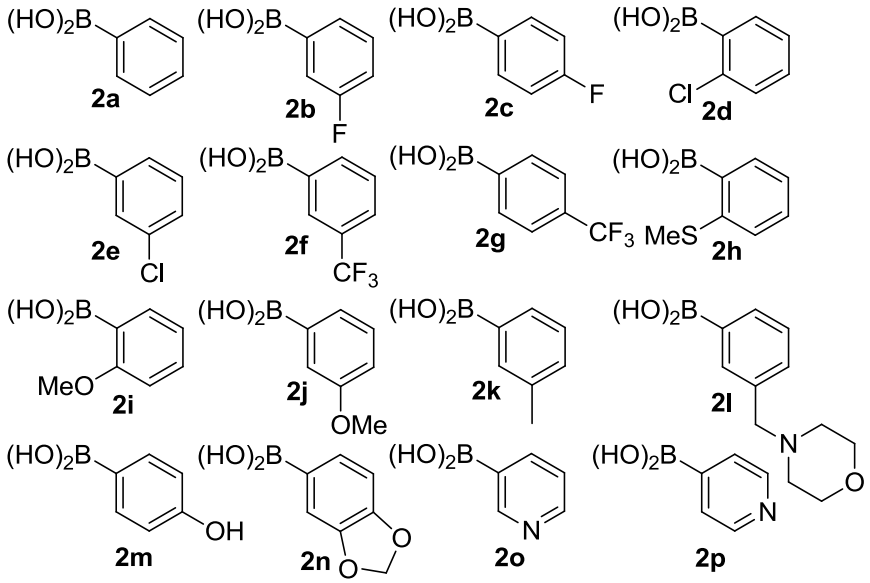

Figure 4-3. Boronic acids selected for incorporation into novologue X scaffold.

Hydrophobic groups (**2j**, **2k**) and a tertiary amine (**2l**) were included as control in this series.

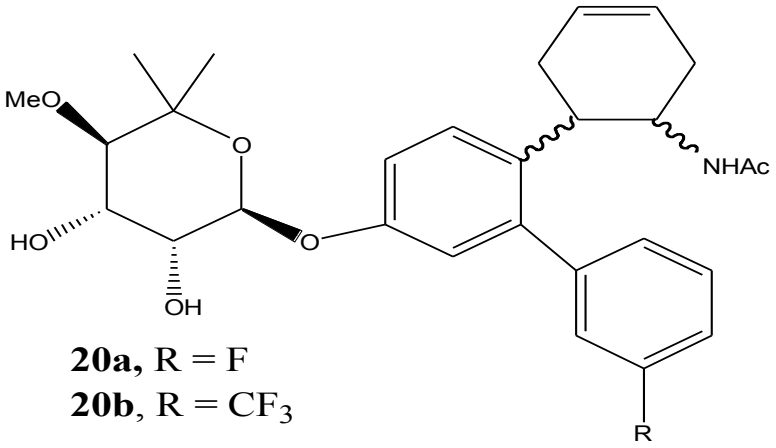

Figure 4-4. Cyclohexene containing novologues.

Evaluation of Neuroprotective Efficacy

Upon synthesis of ethyl acetamide side chain novologues **11a–p** that contain various substitutions on the B-ring (hydrogen bond acceptors, hydrogen bond donors, hydrophobic groups, and a tertiary amine), their neuroprotective efficacy against glucose-induced toxicity of embryonic dorsal root ganglion (DRG) sensory neuron cultures was evaluated. As shown in Table 4-1, *meta*-substituted acetamide novologues (**11b**, **11e** and **11f**) showed significant protection against glucotoxicity and were comparable to that observed with KU-32. Although the corresponding *ortho*- and *para*- substituted (**11c**, **11d** and **11g**) derivatives showed significant protection against glucose-induced cell death, they were modestly less effective than novologues **11b**, **11e** and **11f**. However in the case of analogues **11i** (*ortho*-OMe) and **11j** (*meta*-OMe) the opposite trend was observed. Electronegative atoms at the *meta*-position (F, Cl, CF_3) exhibited greater cytoprotective activity, which is believed to result from favorable interactions with Lys539 in the Hsp90 C-terminal binding pocket. Consistent with this hypothesis, increasing the size of the electronegative atom at the *meta*-position (F to Cl to CF3) resulted in a decrease in neuroprotective activity. Similarly, steric bulk was disfavored as well. Analogue **11b** (*meta*-F) was the most cytoprotective (95%±14) compound evaluated.

Electronegative atoms at the *ortho*- or *para*-position on ring B (**11c**, **11d** and **11g**) manifested activities comparable to the unsubstituted analogue (**11a**) and were less active than the corresponding *meta*-substituted analogues (**11b**, **11e** and **11f**). Although novologues **11d** and **11g** manifested protection against neuronal glucotoxicity, they were less effective than KU-32 and **11b**. Hydrogen bond donors at the *para*-position (**11m**)

appeared to be undesired as **11m** (*para*-OH) was unable to provide significant protection against glucotoxicity. It was also somewhat, but not significantly less protective than the unsubstituted analogue (**11a**).

Table 4-1. Cell viability data of ethyl acetamide side chain novologues.

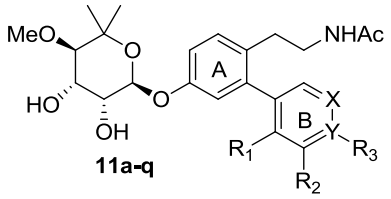

11a-q

Entry	R_1	R_2	R_3	X	Y	% of cell viability [a]
KU-32	-	-	-	-	-	86% ± 2
11a	H	H	H	C	C	76%±11[#]
11b	H	F	H	C	C	95%±14[#]
11c	H	H	F	C	C	75%±27[#]
11d	Cl	H	H	C	C	71%±21[#,*]
11e	H	Cl	H	C	C	90%±23[#]
11f	H	CF3	H	C	C	83%±16[#]
11g	H	H	CF3	C	C	74%±19[#,*]
11h	SMe	H	H	C	C	83%±40[#]
11i	OMe	H	H	C	C	92%±10[#]
11j	H	OMe	H	C	C	78%±34[#]
11k	H	Me	H	C	C	82%±30[#]
11l	H	CH_2-N-morpholine	H	C	C	83%±26[#]
11m	H	H	OH	C	C	67%±10[*]
11n	H	-OCH_2O-		C	C	83%±18[#]
11o	H	H	H	N	C	61%±7[*]
11p	H	H	H	C	N	81%±12[#]

[a]In the presence of 1 μM of each novologue + 20 mM excess glucose. Viability in the presence of 20mM excess glucose + DMSO was 54% ± 2. #, $p<0.05$ versus glucose + DMSO; * $p<0.05$ versus glucose + KU-32 (n=6-24) per novologue.

On the other hand, hydrogen bond acceptors at the *para*-position (**11c** and **11g**) protected against glucose-induced neuronal death but did not display significantly increased protection compared to the novologue containing a *para*-position hydrogen bond donor (**11m**).

Pyridine-containing analogues (**11o–p**) were also synthesized and evaluated for neuroprotective activity. The 3-pyridine analogue (**11o**) was unable to protect against glucose-induce toxicity and was also significantly less protective than the corresponding 4-pyridine analogue, **11p**, KU-32, and the unsubstituted phenyl analogue, **11a**. Although the 4-pyridine-containing analogue (**11p**) demonstrated a modestly improved neuroprotective activity when compared to the simple phenyl analogue **11a**, this difference in efficacy was not significant.

Neuroprotective activity was also determined for the cyclohexene-containing novologues (**20a–b**) that contain the fluoro or trifluoromethane substituent at the *meta*-position of ring B. In general, cyclohexene-containing analogues **20a-b** were less efficacious than the corresponding derivatives that contain a flexible side chain (**11b** versus **20a,** and **11f** versus **20b**). Although not statistically different, novologue **20a** (*meta*-F) exhibited slightly better cytoprotective activity than analogue **20b** (*meta*-CF_3), which follows the same trend observed for flexible acetamide-containing compounds (**11b** versus **11f**). Although these data are inconsistent with our hypothesis that accommodation of the hydrophobic pocket would improve efficacy, the cyclohexene ring may exceed the space allowed in this binding cleft.

Table 4-2. Cell viability data of cyclohexene analogues.

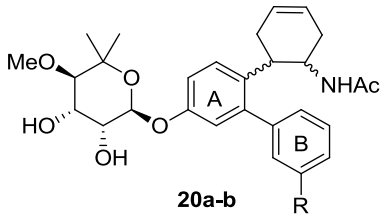

20a-b

Entry	R	% of cell viability [a]
KU-32	-	86% ± 2
20a	F	78%±18%[#]
20b	CF3	69%±15% [#,*]

[a]In the presence of 1 μM novologue + 20 mM excess glucose. Viability in the presence of 20mM excess glucose + DMSO was 54% ± 2. #, $p<0.05$ versus glucose + DMSO; * $p<0.05$ versus glucose + KU-32 (n=8) per novologue.

Neuroprotective Activity of Novologues is Dose Dependent

The data in Table 4-1 clearly support that the majority of novologues synthesized decrease neuronal toxicity induced by hyperglycemic stress. Although some of these compounds appear more effective than KU-32 at 1 M, the differences were relatively minor. Therefore, to further scrutinize their efficacy, compounds exhibiting high neuroprotective activity were further evaluated for determination of EC_{50} values. Since the difference in efficacy for novologues with *meta*-F and *meta*-CF3 substitutions on **11b** and **11f** were not significantly different from KU-32 or each other at 1 μM, the EC_{50} values for these compounds were determined alongside **11h**, **11l**, **11n**, and **11o**. As shown in Figures 4-5A and 5B, EC_{50} values were significantly improved upon closer inspection and clear distinctions were obtained. Novologue **11b** yielded an EC_{50} value (13.0 ± 3.6 nM) that was approximately 14-fold lower than KU-32 (240.2 ± 42.5 nM) or **11f** (187.7 ± 43.5 nM). Similar results were also observed for novologue **11n**, which exhibited an EC_{50} value of 18.4 ± 3.2 nM**.** In contrast, novologue **11h** which manifested similar efficacy to KU-32 at 1 μM, exhibited an EC_{50} of 384 ± 108 nM, approximately 1.6-fold greater than KU-32.

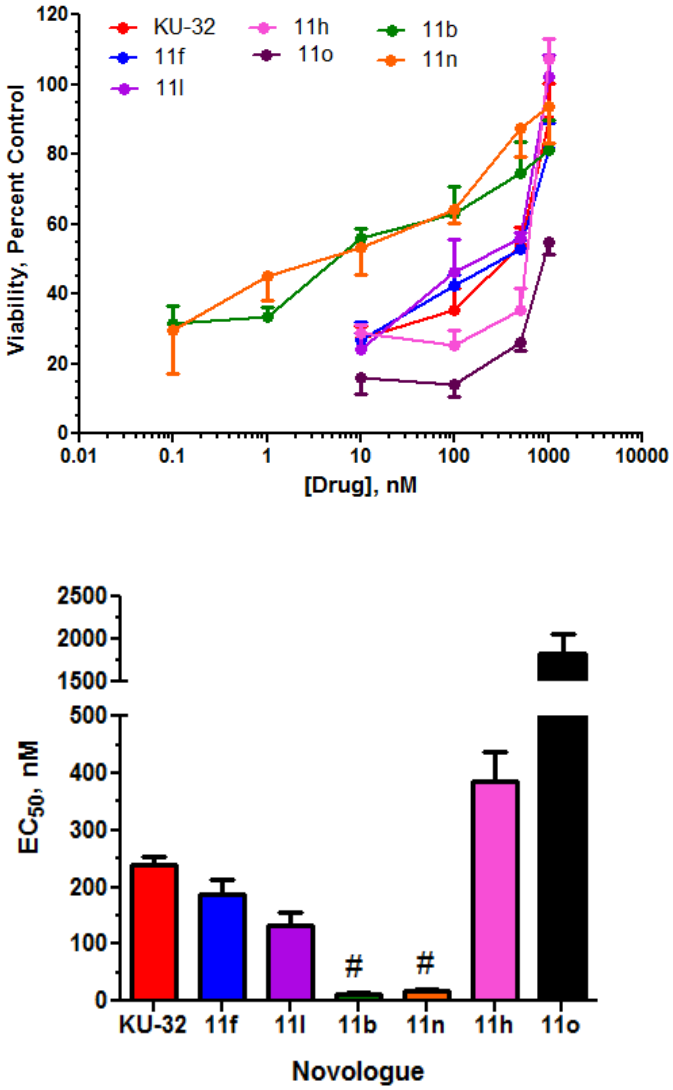

Figure 4-5. Determination of EC_{50} of select novologues. A) DRG sensory neurons were incubated in the absence or presence of 0.1-1000 nM of the indicated novologue overnight and then subjected to 4 hrs of hyperglycemia. Cell viability was measured as described in Experimental Methods and the data expressed as percent of normoglycemic controls. Under hyperglycemic conditions and in the absence of any novologues, cell viability was 20% ± 7. **B)** The EC_{50} was determined using the $EC_{anything}$ function of GraphPad Prism 5.0 and the mean ± SEM (n=3-8) is shown. #, $p < 0.05$ versus KU-32.

Novologues Protect Sensory Neurons with Induction of Hsp70

The data in Figure 4-5 demonstrate that novologues **11b, 11i** and **11n** are more cytoprotective than the initial lead compound, KU-32. Since we have previously shown that the cytoprotective activity manifested by KU-32 requires Hsp70[12], we determined the ability of the novologues to induce Hsp70, relative to KU-32. To this end, a luciferase reporter assay was developed in which the expression of luciferase is driven by the human Hsp70 promoter containing two heat shock binding elements[24]. Since primary sensory neurons transfect poorly, an immortalized sensory neuron cell line (50B11 cells) was used for transfection[20]. Importantly, 50B11 cells have a very low basal level of Hsp70 expression, similar to primary sensory neurons[7]. Twenty-four hours after transfection with the reporter, cells were re-seeded into 12 well plates and incubated for an additional 24 hr. The cells were then treated for 16 hr with 10–1000 nM of the indicated novologues, cell lysates were prepared, luciferase activity assessed and luminescence normalized to total protein per well. Consistent with its increased efficacy in protecting against glucotoxicity, **11b** was more effective than KU-32 at activation of the Hsp70 promoter (Figure 4-6A) and also increased expression of Hsp70 protein at lower concentrations relative to KU-32 (Figure 4-6B). Although **11i** had a similar EC_{50} as **11b** in preventing glucotoxicity, it only activated the Hsp70 promoter at 1 μM and the magnitude of this effect was no better than either KU-32 or **11b**. However, it was surprising that despite the low EC_{50} of **11n** in protecting against glucotoxicity, **11n** did not increase luciferase activity at any concentration tested nor did it increase Hsp70 protein expression as effectively as KU-32 or **11b.** These results suggest that **11n** likely

affects Hsp70 levels indirectly and that the mechanism for neuroprotection may be distinct from that of related novologues.

Lastly, we mentioned that an attractive property of the modified novobiocin scaffold of KU-32 is that it induces Hsp70 at concentrations well below those needed to inhibit Hsp90's protein folding ability[12]. Therefore, to confirm that this new scaffold manifests similar activity, **11b** was evaluated against MCF-7 breast cancer cells that are highly reliant upon the Hsp90 protein folding machinery. As can be observed, no client protein degradation occurred at concentrations up to 5 μM, indicating the potential for a large therapeutic window for this scaffold as well.

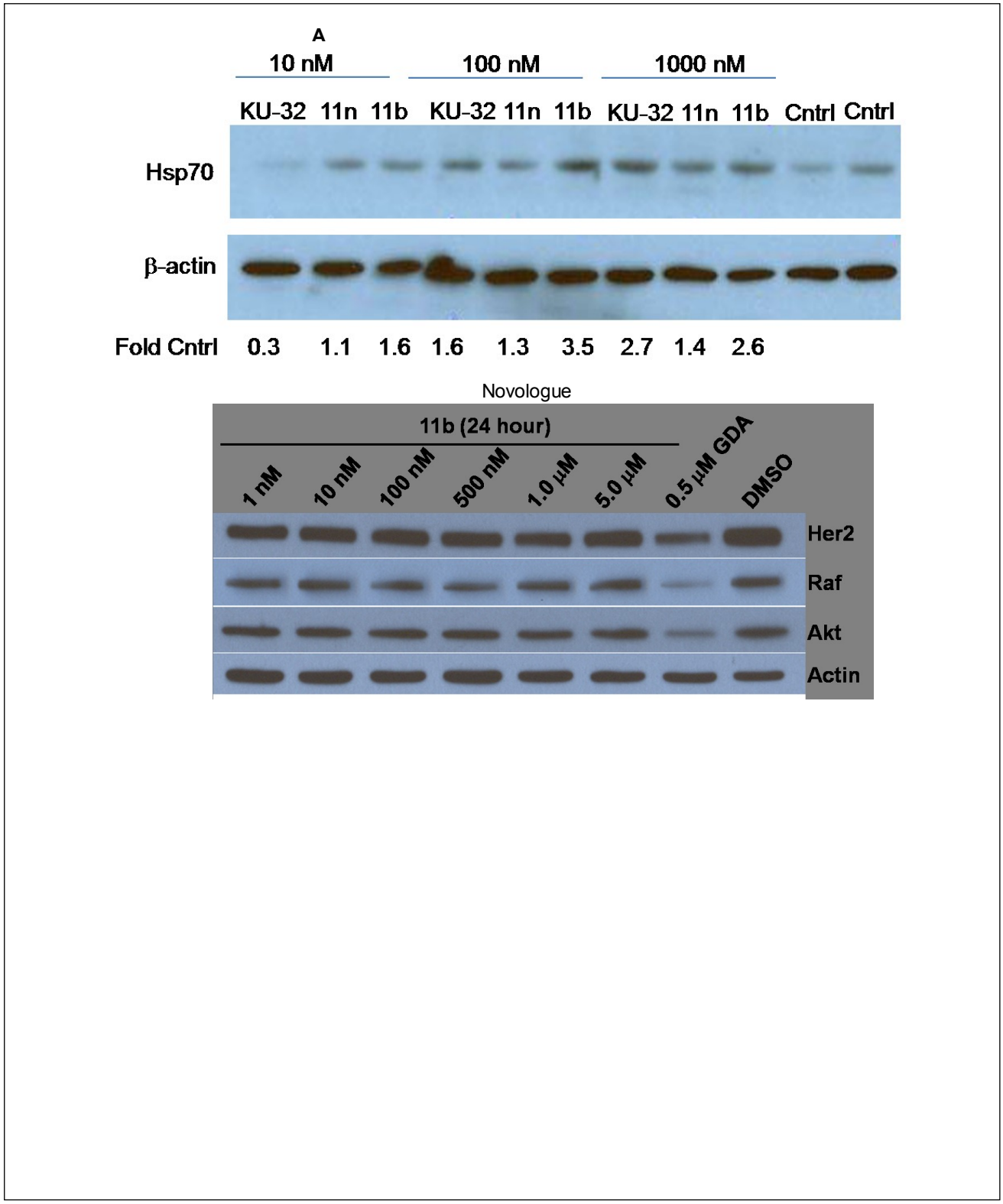

Figure. 4-6. Induction of Hsp70 by select novologues in the absence of client protein degradation. A) 50B11 cells were transfected with a luciferase reporter whose expression was

drive by the human Hsp70 promoter. The cells were treated with the indicated concentration of select novologues for 16 hr and luciferase activity assessed. **, $p < 0.01$ and ***, $p < 0.001$ versus control; ^, $p < 0.05$ and ^^^, $p < 0.001$ versus KU-32 at same concentration. B) DRG sensory neurons were incubated in the presence of DMSO (Cntrl) or 10-1000 nM of the indicated novologue overnight and then subjected to 4 hrs of hyperglycemia. The neurons were harvested and Hsp70 and β-actin levels were determined by immunoblot analysis. Band intensity was quantified using Image J, Hsp70 expression was normalized to the level of β-actin and expressed as a fold control. C) MCF7 cells were treated with the indicated concentrations of 11b for 24 hr, cell lysates were prepared and the levels of the Hsp90 client proteins, Her2, Raf, and Akt determined by immunoblot analysis. As a positive control, some cells were treated with 500 nM geldanamycin (GDA) to induce client protein degradation. The level of β-actin verified equivalent protein loading.

4.4 Conclusion

Using the recently reported model for the Hsp90 C-terminal binding site, a novologue scaffold was designed to afford putative interactions with previously unoccupied regions of the binding pocket, including Lys539. Through systematic replacement of substituents on the novologue B-ring (see Table 4-2), compound **11b** was identified as a neuroprotective agent that exhibited ~14-fold greater efficacy against glucose-induced toxicity than the lead compound, KU-32. The concentration of **11b** needed to manifest neuroprotective activity correlated well with its ability to induce Hsp70 levels, and therefore linking cytoprotection to Hsp70 induction. When combined, these data demonstrate the rationally-designed novologue scaffold provides a promising platform on which diversification of the B-ring can lead to compounds that exhibit better neuroprotective activities.

References

1. Veves, A., Backonja, M. & Malik, R.A. Painful Diabetic Neuropathy: Epidemiology, Natural History, Early Diagnosis, and Treatment Options. *Pain Medicine* **9**, 660-674 (2008).
2. Tomlinson, D.R. & Gardiner, N.J. Glucose neurotoxicity. *Nat Rev Neurosci* **9**, 36-45 (2008).
3. Mayer, M.P. & Bukau, B. Hsp70 chaperones: Cellular functions and molecular mechanism. *Cellular and Molecular Life Sciences* **62**, 670-684 (2005).
4. Peterson, L.B. & Blagg, B.S. To fold or not to fold: modulation and consequences of Hsp90 inhibition. *Future Med Chem* **1**, 267-283 (2009).
5. Burlison, J.A., Neckers, L., Smith, A.B., Maxwell, A. & Blagg, B.S.J. Novobiocin: Redesigning a DNA Gyrase Inhibitor for Selective Inhibition of Hsp90. *Journal of the American Chemical Society* **128**, 15529-15536 (2006).
6. Zhang, L.*, et al.* Hyperglycemia alters the schwann cell mitochondrial proteome and decreases coupled respiration in the absence of superoxide production. *J Proteome Res* **9**, 458-471 (2010).
7. Zhang, L., Zhao, H., Blagg, B.S.J. & Dobrowsky, R.T. C-Terminal Heat Shock Protein 90 Inhibitor Decreases Hyperglycemia-induced Oxidative Stress and Improves Mitochondrial Bioenergetics in Sensory Neurons. *Journal of Proteome Research* **11**, 2581-2593 (2012).
8. Obrosova, I.G. Diabetes and the peripheral nerve. *Biochimica et Biophysica Acta (BBA) - Molecular Basis of Disease* **1792**, 931-940 (2009).
9. Akude, E., Zherebitskaya, E., Roy Chowdhury, S., Girling, K. & Fernyhough, P. 4-Hydroxy-2-Nonenal Induces Mitochondrial Dysfunction and Aberrant Axonal Outgrowth in Adult Sensory Neurons that Mimics Features of Diabetic Neuropathy. *Neurotoxicity Research* **17**, 28-38 (2010).
10. Muchowski, P.J. & Wacker, J.L. Modulation of neurodegeneration by molecular chaperones. *Nat Rev Neurosci* **6**, 11-22 (2005).
11. Baseler, W.A.*, et al.* Proteomic alterations of distinct mitochondrial subpopulations in the type 1 diabetic heart: contribution of protein import dysfunction. *American Journal of Physiology - Regulatory, Integrative and Comparative Physiology* **300**, R186-R200 (2011).
12. Urban, M.J.*, et al.* Inhibiting heat-shock protein 90 reverses sensory hypoalgesia in diabetic mice. *Asn Neuro* **2**(2010).
13. Peterson, L.B. & Blagg, B.S.J. To fold or not to fold: modulation and consequences of Hsp90 inhibition. *Future Medicinal Chemistry* **1**, 267-283 (2009).
14. Burlison, J.A.*, et al.* Development of Novobiocin Analogues That Manifest Anti-proliferative Activity against Several Cancer Cell Lines. *The Journal of Organic Chemistry* **73**, 2130-2137 (2008).
15. Donnelly, A.C.*, et al.* The Design, Synthesis, and Evaluation of Coumarin Ring Derivatives of the Novobiocin Scaffold that Exhibit Antiproliferative Activity. *The Journal of Organic Chemistry* **73**, 8901-8920 (2008).
16. Vincent, A.M., Kato, K., McLean, L.L., Soules, M.E. & Feldman, E.L. Sensory Neurons and Schwann Cells Respond to Oxidative Stress by Increasing Antioxidant Defense Mechanisms. *Antioxidants & Redox Signaling* **11**, 425-438 (2009).
17. Vincent, A.M., Stevens, M.J., Backus, C., McLean, L.L. & Feldman, E.L. Cell culture modeling to test therapies against hyperglycemia-mediated oxidative stress and injury. *Antioxidants & Redox Signaling* **7**, 1494-1506 (2005).

18. Zhang, L., *et al.* Hyperglycemia Alters the Schwann Cell Mitochondrial Proteome and Decreases Coupled Respiration in the Absence of Superoxide Production. *Journal of Proteome Research* **9**, 458-471 (2009).
19. Yu, C., Rouen, S. & Dobrowsky, R.T. Hyperglycemia and downregulation of caveolin-1 enhance neuregulin-induced demyelination. *Glia* **56**, 877-887 (2008).
20. Chen, W., Mi, R., Haughey, N., Oz, M. & Höke, A. Immortalization and characterization of a nociceptive dorsal root ganglion sensory neuronal line. *Journal of the Peripheral Nervous System* **12**, 121-130 (2007).
21. Kusuma, B.R., *et al.* Synthesis and Evaluation of Novologues as C-Terminal Hsp90 Inhibitors with Cytoprotective Activity against Sensory Neuron Glucotoxicity. *Journal of Medicinal Chemistry* **55**, 5797-5812 (2012).
22. Matts, R.L., *et al.* Elucidation of the Hsp90 C-Terminal Inhibitor Binding Site. *ACS Chemical Biology* **6**, 800-807 (2011).
23. Burlison, J.A., Neckers, L., Smith, A.B., Maxwell, A. & Blagg, B.S.J. Novobiocin: Redesigning a DNA Gyrase Inhibitor for Selective Inhibition of Hsp90. *Journal of the American Chemical Society* **128**, 15529-15536 (2006).
24. Calamini, B., *et al.* Small-molecule proteostasis regulators for protein conformational diseases. *Nat Chem Biol* **8**, 185-196 (2012).

Chapter 5: Future Outlooks & Conclusion

5.1 Hsp70 Family & Mitochondrial Import

Mitochondria consist of two membranes, the outer and the inner membrane, and two aqueous compartments, the intermembrane space and the matrix. Although mitochondria have their own genome (mtDNA) in the matrix, 99% of all mitochondrial proteins are encoded in the nucleus and cytoplasmically synthesized[1]. Thus, mitochondria require specific mechanisms (translocases) for precise recognition, translocation, and insertion of preproteins both across and into the mitochondrial membranes[2]. Preproteins are usually immature, loosely folded proteins which may lose their translocation competence and undergo aggregation or be degraded by cellular proteases before import. To prevent these adverse reactions, preproteins destined for mitochondria are guided by molecular chaperones that recognize an N-terminal cleavable targeting sequence necessary to direct the proteins to mitochondria[3-5]. Cytosolic Hsp70 is one of the chaperones that binds to the targeting sequences, thereby promoting protein recognition and binding onto the mitochondria[6-7]. Deletion of *SSA* genes, which encode cytosolic Hsp70 in yeast, demonstrated impaired protein translocation into mitochondria and preprotein accumulation in the cytosol of the mutant cells[8]. Translocation of the preprotein into the mitochondrial matrix requires two driving forces: the mitochondrial membrane potential ($\Delta\Psi_m$) and an ATP-dependent import motor, consisting of mitochondrial Hsp70 (mtHsp70), the translocase subunit Tim44, and the co-chaperone Mge1[9].

MtHsp70 is another member of the Hsp70 family and has been identified as the only ATPase component of the mitochondrial inner membrane import complex[10]. Therefore, mtHsp70 is an essential core chaperone for facilitating import, folding assembly and degradation of proteins in the mitochondria matrix[2]. Interestingly, mtHsp70 primarily localizes to neurons in the brain, but is observed in glial cells upon pathological activation[11]. Tim44 functions as a membrane anchor for mtHsp70, whereas Mge1 is a nucleotide exchange factor that promotes ADP/ATP binding and release in mtHsp70[2]. Knockdown of mtHsp70 in HeLa cells leads to a collapse of $\Delta\Psi_m$, accumulation of ROS, decrease of mtDNA copy numbers and alterations in mitochondrial morphology under H_2O_2 stress[12]. Similar observations were made by Baseler *et al* where cardiac interfibrillar mitochondria isolated from the diabetic animals showed decreased $\Delta\Psi_m$ and mtHsp70 expression along with impaired mitochondrial import[13]. In contrast, i*n vivo* gene delivery of Tim44, the essential binding partner of mtHsp70, showed attenuated oxidative stress and inflammatory responses in diabetic rats with increased import of antioxidants such as MnSOD, suggesting that mtHsp70 stability is crucial for mitochondria import efficiency[14].

5.2 MtHsp70 & Other Cellular Responses

Besides performing in mitochondrial import, mtHsp70 is also involved in a variety of biological functions involved with stress. Overexpression of mtHsp70 in PC12 cells lowered ROS production and its accumulation under glucose deprivation suggests that mtHsp70 is directly involved in decreasing oxidative stress[15]. In fact, evidence shows mtHsp70 directly interact with the tumor suppressor p53 and the adaptor protein p66Shc, both of which are involved in the propagation of pro-apoptotic oxidative stress

signals[16]. P66Shc is a cytoplasmic signal transducer, however, a fraction of p66Shc was found localized within the mitochondria where it forms a complex with mtHsp70. More importantly, UV-induced oxidative stress abrogated the mtHsp70-p66Shc interactions, leading to a collapse of $\Delta\Psi_m$ and cellular apoptosis[17]. Recruitment of p53 by mtHsp70 promoted an anti-apoptotic effect in ouabain treated vascular smooth muscle cells by deactivating p53 activity[18]. Moreover, a recent study showed that RelA, a NF-κB family member, can translocate into the mitochondria where it interacts with mtHsp70 and repress mitochondrial gene expression, oxygen consumption and cellular ATP levels, thereby, promoting glycolysis in cancer cells[19]. This observation may be analogous to DPN where activation of PKC induces NF-κB and not only promotes an inflammatory response but also contributes to mitochondria energy failure by interacting with mtHsp70. Overall, the above studies show that mtHsp70 can serve as a potential, novel therapeutic target in the study of hyperglycemia-induced mitochondria dysfunction.

5.3 Regulation of mtHsp70 by KU-32 & Its Impact on Mitochondrial Function

In chapter 3, we showed that KU-32 protects neurons from glucotoxicity by improving mitochondrial function and decreasing oxidative stress. Mechanistically, the drug efficacy of KU-32 is correlated to cytosolic Hsp70 expression *in vivo,* however increased expression of mtHsp70 has also been reported in hyperglycemically-stressed sensory neurons treated with KU-32[20-21]. Therefore, it is critical to define whether functional expression of mtHsp70 is necessary for KU-32-enhanced mitochondrial function in sensory neurons under hyperglycemic stress.

Functional mtHsp70 & Regulation of Mitochondrial Function by KU-32

In order to study the functional contribution of mtHsp70 to mitochondria activity, MKT-077, a rhodacyanine dye that inhibits mtHsp70 by modifying its secondary and tertiary structure, was used in preliminary studies[22]. MKT-077 can impair mitochondrial electron transport chain activity in isolated intact mitochondria in a dose dependent manner[23]. Thus, to determine the effect of mtHsp70 inhibition on neuronal mitochondria respiration, DRG neurons were cultured in media containing a dose titration of 0.1μM, 1μM or 3μM of MKT-077 for 48 hours and 1μM KU-32 was given in the final 24 hours. Oxygen consumption was assessed using conditions similar to those described in Chapter 3. As we reported in Chapter 3, KU-32 increased maximal respiratory capacity (MRC) (Figure 5-1A) and MKT-077 concentrations significantly decreased MRC in a dose dependent manner. More importantly, KU-32 may require functional mtHsp70 for its neuroprotective efficacy against hyperglycemia-induced mitochondrial dysfunction since

MKT-077 blunted the KU-32-induced increase in MRC (Figure 5-1B). In contrast, neurons showed no significant difference in non-mitochondrial respiration when treated with rotenone/antimycin cocktail. These results suggest that functional mtHsp70 is vital to mitochondrial but not non-mitochondrial respiration.

Protein abundance is regulated via modulation of transcription, mRNA stability, post-translational modification and turnover. Control of the timing, location, and amount of gene expression can have a profound effect on individual organelle function. A rigorous yet fundamental approach to study transcriptional regulation of mtHsp70 by KU-32 is to identify the promoter region which is usually located in the immediate vicinity of transcription start site. KU-32 has been shown to activate the human Hsp70 promoter which contains two heat shock elements (HSE), which is characterized by an array of inverted repeats of the motif nGAAn[24]. Even though mtHsp70 is uninducible by heat, KU-32 may still activate mtHsp70 through the HSE sequence or other previously unidentified regulatory regions that may be identified by truncating the promoter sequences[15]. In addition, functional expression of mtHsp70 may also be related to an increase mRNA stability or production. Thus, quantitative measures of the mtHsp70 mRNA level across treatments may serve as another indicator to study the effect of KU-32 on mtHsp70 gene expression.

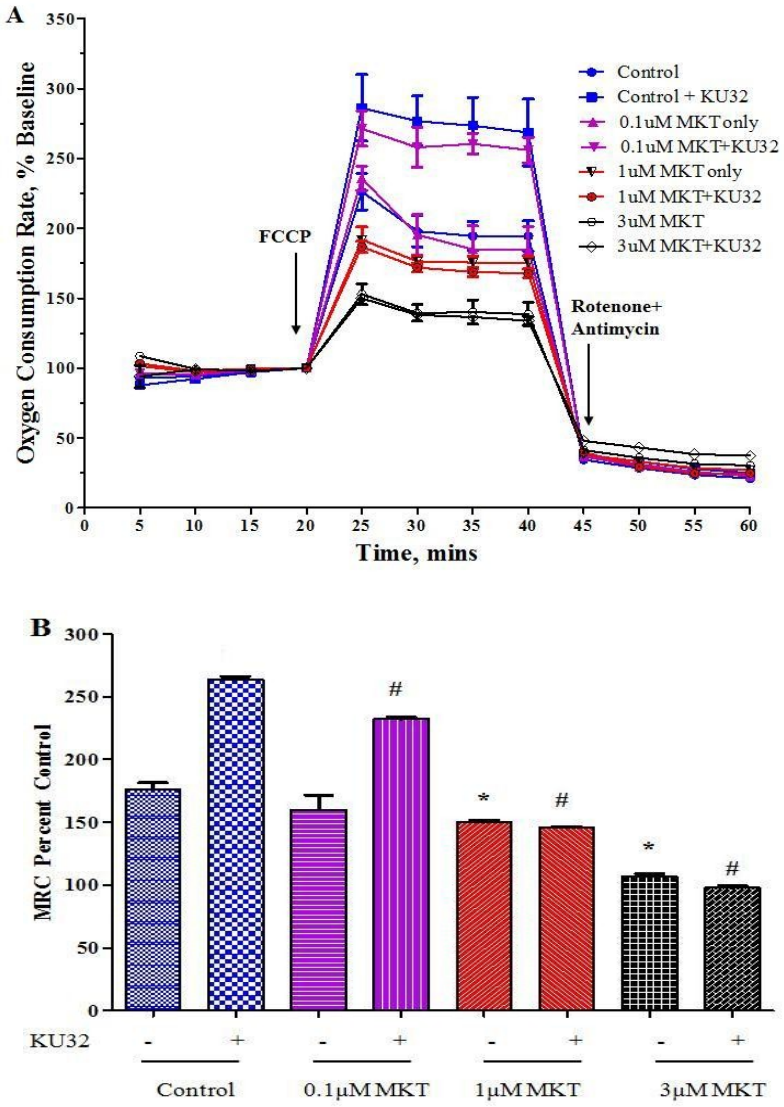

Figure 5-1. MKT-077 impairs mitochondrial respiration in a dose dependent manner. Primary DRG neurons were seeded into a 96 well plate and incubated in medium containing 25 mM glucose. The DRG neurons were incubated with MKT-077 at different concentration for 48 h and 1 μM KU-32 or DMSO were treated to neurons at the final 24 h. The cells were placed in medium containing 5 mM glucose and 1 mM pyruvate prior to the respiratory measures. (A) Results shown are the mean ± SEM from 3 to 4 wells per treatment from one experiment. Arrows indicate the injection of FCCP and rotenone/ antimycin cocktail. (B) While MKT-077 alone did not induce significant change in MRC at 0.1μM (*, $p < 0.01$) relative to

control neurons, the MRC with KU-32 treatment showed a significant dose-response decrease with increased concentration of MKT-077 ($^{\#}$, $p < 0.001$).

MKT-077 is a lipophilic cation and this aspect of its structure aids its accumulation in mitochondria[24]. However, despite its efficacy in decreasing mitochondrial respiration, it may not necessarily be specific for inhibiting mtHsp70. Therefore, lentivirus-mediated RNA interference (RNAi) which exerts a powerful and unitary knockdown of a target protein was employed. Preliminary studies using lentivirus-mediated knockdown of mtHsp70 expression showed decreased mtHsp70 expression with an increasing multiplicity of infection (MOI) in primary DRG neurons (Figure 5-2). However, mtHsp70 expression was not affected following non-targeting shRNA infection or polybrene treatment. This suggests that RNAi could be employed as a target-specific approach to study of the role of mtHsp70 in contributing to the ability of KU-32 to improve mitochondrial function. Given that knockdown of mtHsp70 collapses $\Delta\Psi_m$ and impairs mitochondrial import, treatment of KU-32 should presumably have no impact on either of the indices if KU-32 manifest its efficacy with functional expression of mtHsp70[12-13]. Otherwise, KU-32 may be improving mitochondrial function through other regulatory pathways.

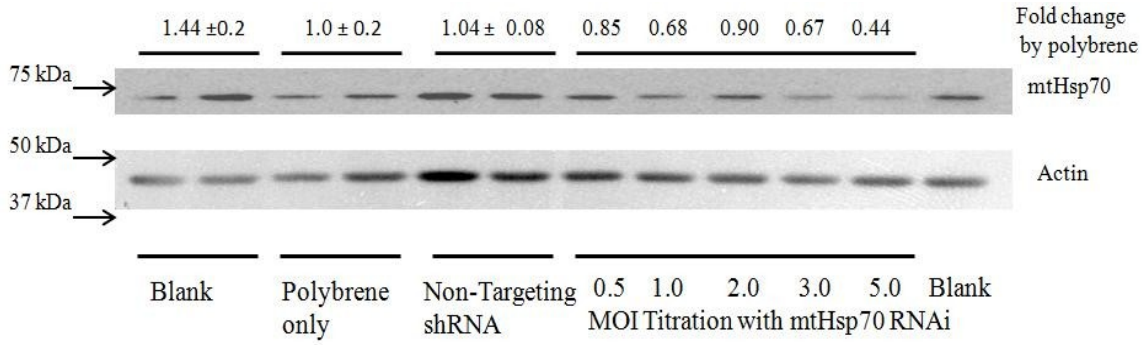

Figure 5-2. Targeted knockdown of mtHsp70 using lentivirus-mediate RNA interference. Expression of mtHsp70 in primary DRG neurons was decrease with increased MOI titration of lentivrial particles.

5.4 Conclusions

In summary, this dissertation systematically explored two aspects of mitochondrial dysfunction in glycemically stress sensory neurons and SCs using an unbiased proteomic approach. First, hyperglycemia alters mitochondrial function and these changes are consistent with a potential role of altered bioenergetics in contributing to the progression of sensory neuropathy. Specifically, hyperglycemia decreased the level of translation and protein expression of antioxidants and mitochondrial chaperones concurrent with an increase in oxidative stress in DRG sensory neurons. More importantly, these are accompanied by a compromised in mitochondrial bioenergetic efficiency, a sign of energy failure in DPN. Of note, despite the lack of superoxide production in SCs, its mitochondria bioenergetics are compromised as demonstrated with decreased ATP-coupled respiration and increased proton leak. However, SCs may have countered the hyperglycemic stress by increasing its overall mitochondrial protein expression including the antioxidant, MnSOD, and shifting the need for ATP production from mitochondrial respiration to glycolysis.

Given that hyperglycemia mediates mitochondrial dysfunction, a second focus of this dissertation explored the mechanism of neuroprotection via pharmacological induction of molecular chaperones. As shown in Chapters 3, short term treatment of KU-32, the novobiocin-derived Hsp90 inhibitor, significantly improved mitochondrial function in DRG sensory neurons under hyperglycemic stress by increasing chaperone and antioxidant translation, enhancing mitochondrial bioenergetics and decreasing superoxide production. In addition, this dissertation also demonstrates that the

neuroprotective efficacy of KU-32 can be enhanced through systematic structural modification of its interaction with the Hsp90 C-terminal binding site.

In the future, it will be important to explore the possibility that molecular chaperones may mediate neuronal protection by improving mitochondrial import. As 99% of mitochondrial proteins originate from transcription of nuclear genes, their transport and import into mitochondria requires both cytosolic and mitochondrial Hsp70 paralogs. Emerging data supports that diabetes increases oxidative stress and mitochondrial fission/fusion in sensory neurons. Decreasing oxidative stress and maintaining the fidelity of protein import to support this turnover would be essential to maximizing the bioenergetic capacity of the organelle. The ability of KU-32 to increase Hsp70 isoforms, decrease oxidative stress and improve mitochondrial bioenergetics provides solid rationale that multiple Hsp70 paralogs may improve DPN by functioning as chaperones to improve protein import and aid the repair/removal of oxidatively damaged proteins within mitochondria.

References

1. Wiedemann, N., Frazier, A.E. & Pfanner, N. The Protein Import Machinery of Mitochondria. *Journal of Biological Chemistry* **279**, 14473-14476 (2004).
2. Neupert, W. Protein import into mitochondria. *Annual Review of Biochemistry* **66**, 863-917 (1997).
3. Schatz, G. & Dobberstein, B. Common Principles of Protein Translocation Across Membranes. *Science* **271**, 1519-1526 (1996).
4. Koehler, C.M., Merchant, S. & Schatz, G. How membrane proteins travel across the mitochondrial intermembrane space. *Trends in Biochemical Sciences* **24**, 428-432 (1999).
5. Jensen, R.E. & Johnson, A.E. Opening the door to mitochondrial protein import. *Nat Struct Mol Biol* **8**, 1008-1010 (2001).
6. Chirico, W.J., Waters, M.G. & Blobel, G. 70K heat shock related proteins stimulate protein translocation into microsomes. *Nature* **332**, 805-810 (1988).
7. Deshaies, R.J., Koch, B.D., Werner-Washburne, M., Craig, E.A. & Schekman, R. A subfamily of stress proteins facilitates translocation of secretory and mitochondrial precursor polypeptides. *Nature* **332**, 800-805 (1988).
8. Murakami, H., Pain, D. & Blobel, G. 70-kD heat shock-related protein is one of at least two distinct cytosolic factors stimulating protein import into mitochondria. *The Journal of Cell Biology* **107**, 2051-2057 (1988).
9. Voos, W. & Rottgers, K. Molecular chaperones as essential mediators of mitochondrial biogenesis. *Biochimica Et Biophysica Acta-Molecular Cell Research* **1592**, 51-62 (2002).
10. Yaguchi, T., Aida, S., Kaul, S.C. & Wadhwa, R. Involvement of mortalin in cellular senescence from the perspective of its mitochondrial import, chaperone, and oxidative stress management functions. in *Biogerontology: Mechanisms and Interventions*, Vol. 1100 (eds. Rattan, S.I.S. & Akman, S.) 306-311 (2007).
11. Burbulla, L.F.*, et al.* Dissecting the role of the mitochondrial chaperone mortalin in Parkinson's disease: functional impact of disease-related variants on mitochondrial homeostasis. *Human Molecular Genetics* **19**, 4437-4452 (2010).
12. Yang, H.*, et al.* Mitochondrial dysfunction induced by knockdown of mortalin is rescued by Parkin. *Biochemical and Biophysical Research Communications* **410**, 114-120 (2011).
13. Baseler, W.A.*, et al.* Proteomic alterations of distinct mitochondrial subpopulations in the type 1 diabetic heart: contribution of protein import dysfunction. *American Journal of Physiology-Regulatory Integrative and Comparative Physiology* **300**, R186-R200 (2011).
14. Matsuoka, T.*, et al.* Gene delivery of Tim44 reduces mitochondrial superoxide production and ameliorates neointimal proliferation of injured carotid artery in diabetic rats. *Diabetes* **54**, 2882-2890 (2005).
15. Liu, Y., Liu, W., Song, X.D. & Zuo, J. Effect of GRP75/mthsp70/PBP74/mortalin overexpression on intracellular ATP level, mitochondrial membrane potential and ROS accumulation following glucose deprivation in PC12 cells. *Molecular and Cellular Biochemistry* **268**, 45-51 (2005).
16. Kaul, S.C., Deocaris, C.C. & Wadhwa, R. Three faces of mortalin: A housekeeper, guardian and killer. *Experimental Gerontology* **42**, 263-274 (2007).
17. Orsini, F.*, et al.* The Life Span Determinant p66Shc Localizes to Mitochondria Where It Associates with Mitochondrial Heat Shock Protein 70 and Regulates Trans-membrane Potential. *Journal of Biological Chemistry* **279**, 25689-25695 (2004).
18. Taurin, S.*, et al.* Proteome analysis and functional expression identify mortalin as an antiapoptotic gene induced by elevation of Na+ (i)/ K+ (i) ratio in cultured vascular smooth muscle cells. *Circulation Research* **91**, 915-922 (2002).

19. Johnson, R.F., Witzel, I.-I. & Perkins, N.D. p53-Dependent Regulation of Mitochondrial Energy Production by the RelA Subunit of NF-κB. *Cancer Research* **71**, 5588-5597 (2011).
20. Urban, M.J.*, et al.* Inhibiting heat-shock protein 90 reverses sensory hypoalgesia in diabetic mice. *Asn Neuro* **2**(2010).
21. Zhang, L., Zhao, H., Blagg, B.S.J. & Dobrowsky, R.T. C-Terminal Heat Shock Protein 90 Inhibitor Decreases Hyperglycemia-induced Oxidative Stress and Improves Mitochondrial Bioenergetics in Sensory Neurons. *Journal of Proteome Research* **11**, 2581-2593 (2012).
22. Wadhwa, R.*, et al.* Selective toxicity of MKT-077 to cancer cells is mediated by its binding to the hsp70 family protein mot-2 and reactivation of p53 function. *Cancer Research* **60**, 6818-6821 (2000).
23. ModicaNapolitano, J.S.*, et al.* Selective damage to carcinoma mitochondria by the rhodacyanine MKT-077. *Cancer Research* **56**, 544-550 (1996).
24. Modica-Napolitano, J.S.*, et al.* Selective Damage to Carcinoma Mitochondria by the Rhodacyanine MKT-077. *Cancer Research* **56**, 544-550 (1996).